Interpretation of oceanic magnetic anomalies using a linear inverse technique

Michael Alexander Hutton

INTERPRETATION OF OCEANIC MAGNETIC ANOMALIES USING A LINEAR INVERSE TECHNIQUE

A Thesis submitted for the Degree of
Doctor of Philosophy
in the
University of Durham

by
Michael Alexander Hutton

Graduate Society

October, 1970

ACKNOWLEDGEMENTS

I wish to thank Professor G.M. Brown for providing the facilities for this research and Professor M.H.P. Bott for his supervision and encouragement throughout this work.

I am grateful to the following individuals and institutions for generously providing original magnetic, bathymetric and seismic data: Dr. B.D. Loncarevic and Dr. D.I. Ross, Atlantic Oceanographic Laboratory, Canada; Dr. M.T. Jones, National Institute of Oceanography, England; Dr. E.M. Herron, Lamont Geological Observatory, U.S.A.; Dr. D.C. Krause, University of Rhode Island, U.S.A.

I would particularly like to thank Dr. B.D. Loncarevic of the Atlantic Oceanographic Laboratory for the opportunity of participating in the C.S.S. HUDSON cruise to the Mid-Atlantic Ridge in 1968.

This work has been financed by a Natural Environment Research Council Research Studentship for three years.

ABSTRACT

A direct magnetic interpretational technique has been developed and applied to oceanic magnetic anomalies. The method of interpretation computes a distribution of magnetization, within a specified two-dimensional model - given the direction of magnetization, from the observed magnetic anomalies. The technique is based on the numerical solution of a linear integral equation which is approximated by a finite set of linear algebraic equations. These equations relate (n) observed magnetic anomaly field points to (m) unknown magnetization values. Solution of this system of equations is carried out by computer, using matrix operations. The programming procedure allows model elements of irregular cross-section to be incorporated within the magnetic layer and provides a solution to both the completely determined and overdetermined problem (i.e. $n \geq m$). Details of this procedure are presented together with an evaluation of methods of application.

Interpretations of magnetic profiles in the North Atlantic Ocean, the Gulf of Aden and the Pacific Ocean are presented in terms of computed distributions of magnetization confined to Layer 2. Results are discussed in terms of the Vine-Matthews hypothesis of sea-floor spreading and certain apparent differences in the bulk magnetization of the oceanic crust.

Model studies confirm the feasibility of a thin magnetic layer (0.5 km), situated just below the sea-floor. The approximate shape of this magnetic layer is deduced from known magnetization values obtained from dredged rock samples.

Interpretation of magnetic data from the Pacific Ocean indicates that both vertical and inclined source bodies, within Layer 2, represent plausible models, although extensive subhorizontal bodies (dipping at 10^{o} and less) are unlikely.

CONTENTS

LIST OF FIGURES

LIST OF TABLES

CHAPTER 1

INTRODUCTION

1.1 Oceanic Magnetic Anomalies

Oceanic magnetic anomalies are distinctive, short wavelength disturbances of the earth's total magnetic field. These magnetic anomalies are almost entirely caused by local variations in the magnetic properties of the earth's crust. There are three principal types of magnetic anomalies observed over the oceans of the world. These are the anomalies associated with the mid-ocean ridge system, magnetic anomalies of great linearity and continuity extending for hundreds of kilometres, and the magnetic anomalies associated with the isolated bathymetric high or seamount.

Systematic marine magnetic observations only really began to be carried out in the late 1950's. This advance stemmed mainly from the successful application of the fluxgate magnetometer, developed originally as an airborne instrument for the detection of submarines, to the task of measuring magnetic field intensity at sea (Heezen et al 1953). More recent work (Hill 1959) has developed the use of a proton precession magnetometer suitable for towing behind a ship. This instrument has largely superseded the fluxgate magnetometer, for shipboard use, in that it gives an absolute measurement of the earth's magnetic field and requires no orientation of the measuring head.

Magnetic anomalies associated with the mid-ocean ridge system - a continuous submarine mountain chain extending for 70-80,000 kilometres throughout the ocean basins of the world - were first recorded and described by Heezen et al (1953), whilst later Ewing et al (1957) noted the characteristic association of a large magnetic anomaly with

the mid-Atlantic rift valley. However, information in general was necessarily limited as profiles were very widely spaced and often merely represented reconnaissance traverses made en route.

Mason (1958) published the results of a detailed marine magnetometer survey off the west coast of the U.S.A. near California. The magnetic contour maps revealed a strikingly linear pattern of positive and negative magnetic anomalies of about 400 gamma amplitude, trending north-south for over 460 kilometres. Mason & Raff (1961) and Raff & Mason (1961) and Raff (1966) published the results of further survey work extending the mapped area and confirming the basic pattern. Vacquier et al (1961) concluded from this work that certain large offsets observed in the magnetic anomaly pattern could be interpreted in terms of extensive transcurrent faulting, although later to be understood in terms of transform faulting (Wilson 1965).

Due to the absence, at that time, of any comparable marine magnetic survey the exact implications of the magnetic anomalies observed in the north-east Pacific were not realized. However, as more data accumulated, the origin and significance of such magnetic lineations rapidly became more apparent (Vine & Matthews 1963; Heirtzler & Le Pichon 1965; Vine 1966; Pitman & Heirtzler 1966). Recent extensive areal surveys in the North Atlantic (Heirtzler et al 1966; Avery et al 1968; Avery et al 1969) have convincingly demonstrated the now familiar pattern of these anomalies. Strips of positive and negative magnetic anomalies, about 30 kilometres wide, are now known to strike approximately parallel to the local mid-ocean ridge crest for many hundreds of kilometres. Numerous widely spaced shipboard and airborne magnetic profiles, perpendicular to the axis of the ridge system, have confirmed a rough bilateral symmetry in the

(1 gamma = 10^{-5} oersted)

observed pattern about the ridge centre.

Magnetic anomalies associated with seamounts have a much less extensive distribution than those associated with the mid-ocean ridge system. Typical anomalies are lenticular in plan, having dimensions of tens of kilometres, and are generally of the order of a few hundred gamma in amplitude. Often such anomalies may be simply related to a comparatively isolated local structure whose geometry is reasonably well defined.

1.2 Oceanic Magnetic Anomalies and Sea-Floor Spreading

Oceanic magnetic anomalies recorded on long profiles approximately perpendicular to the local ridge axis have been shown to have an essentially two-dimensional form. These magnetic anomalies may therefore be satisfactorily interpreted in terms of a magnetic body infinitely elongated parallel to the strike of the ridge axis.

It was relatively quickly established that such oceanic magnetic anomalies were not caused by the sharply dissected relief of the mid-ocean floor or a relatively uniform magnetic basement, but rather by a magnetic inhomogeneity of the rocks within the oceanic crust. The Curie isotherm, at about 15-20 kilometres below sea-level, controls the lower limit of permanently magnetized rocks whilst bathymetric and seismic evidence suggests that near the axial zone of mid-ocean ridges the upper surface of the basaltic layer, i.e. Layer 2, crops out very close to or at the sea bed. The task of interpreting oceanic magnetic anomalies is therefore that of determining the required distribution of magnetization within the oceanic crust as defined by Layers 2 and 3. As magnetic measurements alone cannot always differentiate between a relatively thin body that is strongly

magnetized and a thick body which is weakly magnetized - the exact vertical extent of any magnetic body is generally unknown.

The first detailed model simulations attempted for oceanic magnetic anomalies were carried out by Mason (1958) and Mason & Raff (1961) for the magnetic lineations observed in the north-east Pacific. These authors presented a number of possible two-dimensional solutions, each an isolated body of magnetically anomalous material capable of explaining almost exactly individual features of the magnetic anomaly. Mason & Raff (1961) suggested that the various models obtained could be grouped into three possible geological categories:

(i) isolated sheets of basic lava within Layer 2;

(ii) elevated folds or fault blocks from Layer 3 reaching the sea bed;

(iii) mantle intrusives, extending throughout the oceanic crust.

Whilst these interpretations adequately explained individual features of the observed magnetic pattern, they did not really provide a satisfactory explanation of the systematic lateral change in the magnetic anomalies, particularly with respect to the petrology of the underlying crust. The lack of topographic and seismic expression for these structures, noted by Mason & Raff (1961), has also provided a serious objection to all three possibilities. The significant conclusion of Mason (1958) and Mason & Raff (1961) was that the magnetic anomalies originated from a source body whose upper surface lay within the 'volcanic' layer of the oceanic crust, close to the sea bed.

This work was closely followed by Dietz's presentation of the hypothesis of sea-floor spreading (Dietz 1961; Hess 1962). This hypothesis employed a large scale convection current mechanism directly

concerned with the creation of oceanic crust and upper mantle at mid-ocean ridges. The oceanic crust and lithosphere are directly coupled with the convective overturn of the mantle. The sea-floor therefore represents the uppermost part of the mantle convection cell spreading away from the axis of the mid-ocean ridge system at a rate of a few cm/year. Dietz drew attention to the magnetic lineations in the north-east Pacific; concluding that they fitted into the concept of a spreading sea-floor, with the lineations developing normal to the direction of creep, but did not suggest a causal relationship.

Vine & Matthews (1963) suggested a completely different form of crustal model, to that of Mason & Raff (1961), to account for the oceanic magnetic anomalies observed in the north-east Pacific and over mid-ocean ridges in general. These authors linked the theory of sea-floor spreading (Dietz 1961; Hess 1962) with the palaeomagnetic results of Cox et al (1963) who had begun to assemble a provisional radiometric time scale for polarity reversals in the earth's magnetic field during the Pleistocene and late Pliocene. Vine & Matthews suggested that the characteristic positive and negative magnetic lineations observed over mid-ocean ridges could be interpreted in terms of material of alternately normal and reversed magnetic polarity. They envisaged mantle material being emplaced at the ridge crest from a convective up-current. Then as the injected material cooled through its Curie point it acquired a significant component of thermo-remanent magnetization parallel to the ambient geomagnetic field. Assuming a continuous process of sea-floor spreading at the ridge crest, successive polarity reversals of the earth's dipole field would result in strips of oceanic crust, magnetized alternately in a parallel and anti-parallel sense, moving symmetrically away from the ridge axis. Magnetic

anomalies observed across mid-ocean ridges should therefore reflect a symmetrical distribution of magnetization which in turn represents a symmetrical record of the geomagnetic time scale as a function of the local spreading rate.

The Vine-Matthews hypothesis successfully overcame the necessity of an extensive discontinuous structure with unusually large variations in magnetization implied by Mason & Raff's interpretation, and provided strong support for the theories of continental drift and sea-floor spreading. Using the Vine-Matthews hypothesis, Vine & Wilson (1965) successfully related the magnetic pattern observed across the Juan de Fuca ridge, off the British Columbian coast, to the revised geomagnetic polarity time scale of Cox et al (1964). They showed that the magnetic anomalies could be interpreted in terms of a symmetrical distribution of magnetization within the oceanic crust. This model represented the known reversal history of the earth's magnetic field for the last 3.4 million years, assuming an average spreading rate of about 1.5 cm/yr/limb for material injected at the ridge axis. This work was the first experimental attempt to relate observed magnetic data to an absolute time scale.

Subsequent similar model studies by Vine (1966); Pitman & Heirtzler (1966); Heirtzler et al (1968) and others have satisfactorily explained observed oceanic magnetic anomalies on a world-wide scale. The models used are often several hundreds of kilometres in length and are formed from a series of two-dimensional rectangular blocks, of alternating magnetic polarity, which are symmetrical about the ridge crest. The model blocks nominally represent Layer 2 of the oceanic crust, this is about two kilometres thick on average. Layer 2, the basaltic or 'volcanic' layer, is generally thought to be the main source of the

magnetic anomalies (Vine & Wilson 1965; Bott 1967) although the exact contribution and composition of Layer 3, the main crustal layer, is not known.

The general mechanism of sea-floor spreading is thought to involve the continued injection of basaltic feeder dykes along the median line of the mid-ocean ridge system. Whilst in nature one might expect material to be injected with an irregular distribution, statistical work by Matthews & Bath (1967) and Harrison (1968) applied to the observed magnetic anomalies has supported a localized origin. Computations by Matthews & Bath (1967) have indicated that the majority of dyke-like material should be emplaced within a band approximately 10 km wide - roughly corresponding to the median valley width in the mid-Atlantic ridge at 45^{o}N. Similar work by Harrison (1968) has suggested that for areas where magnetic lineations are well developed such as the Reykjanes Ridge and the East Pacific Rise then the majority of dykes are injected in a band approximately 6 km wide.

Criticism of the Vine-Matthews hypothesis was initially expressed by Heirtzler & Le Pichon (1965) and Talwani et al (1965) with regard to the nature of oceanic magnetic anomalies recorded across the mid-Atlantic ridge. These authors claimed that the transition, from low-amplitude short wavelength anomalies over the axial zone of the ridge to higher-amplitude, long wavelength anomalies over the more distant flanks, was not compatible with the Vine-Matthews hypothesis of a common origin. However, Vine (1966) has suggested that a possible explanation for this phenomenon may be that the frequency of reversals was higher in more recent times, combined with a possible change in field intensity. Hence the often rather abrupt boundary between flank and axial zone magnetic anomalies would simply reflect the time of this change.

The essential conclusion of Vine & Matthews was that the regular magnetic pattern is due to systematic polarity changes in the remanent magnetization of rocks within the oceanic crust. This idea has been challenged by certain authors (Luyendyk & Melson 1967; Ozima, Ozima & Kaneoka 1968), who suggest that regular fissure line eruptions may produce comparable magnetic patterns. Van Andel (1968) has suggested that possible alternatives to the straightforward structural development of mid-oceanic ridges (Dietz 1961; Hess 1962) may also exist. The geological models of Van Andel generally accept dyke injection in some form as responsible for the production of symmetric patterns of positive and negative magnetic anomalies.

However, it may be stated that no theory comparable to that of Vine & Matthews has yet been proposed to explain oceanic magnetic anomalies satisfactorily and still remain consistent with other geophysical evidence. Today, almost all methods of interpretation rely on relating patterns of alternate positive and negative peaks, rather than attempting exact interpretations of individual anomalies. Evidence summarized in the following section gives strong support to this type of interpretational approach and confirms its general world-wide applicability.

1.3 The Geomagnetic Time Scale

During the past few years it has proved possible to establish a radiometric time scale for reversals in the earth's magnetic field by combining palaeomagnetic research with age dating using the potassium-argon method (Cox et al 1968, in summary). Successive work over the last decade has now defined a quantitative reversal time scale for the period up to 4.5 million years B.P. (Cox 1969). Cox and others note that at the present time this time scale probably

cannot be extended in detail much beyond 5 or 6 million years because the errors in the radiometric ages of the older rocks are too large. However, this would not preclude the possibility of dating certain distinctive polarity transitions or defining longer periods of uniform polarity.

Vine & Wilson (1965) and Vine (1966) used the radiometric time scales of Cox et al (1964) and Doell & Dalrymple (1966) to directly date oceanic magnetic anomalies observed across mid-ocean ridge crests in terms of the Vine-Matthews hypothesis. Magnetic profiles lack an absolute time base in themselves and must be calibrated against known points. By extrapolation it is then possible to establish considerable details of the reversal time scale, beyond that of the radiometric time scale, from the magnetic anomaly profile (Vine 1966).

Pitman & Heirtzler (1966) published the results of four magnetic profiles recorded across the Pacific-Antarctic ridge. The characteristics of these profiles, a linear magnetic trend parallel to the ridge axis and classic symmetry about the ridge centre (e.g. Eltanin - 19 traverse) completely supported the Vine-Matthews hypothesis. The interpretation of these profiles by Pitman & Heirtzler, using the known radiometric time scale (Cox et al 1964; Doell & Dalrymple 1966), in terms of a sea-floor spreading model with a constant rate of spreading, allowed the definition of major polarity epochs during the last 10 million years. The application of this deduced sequence of polarity reversals, using a reduced spreading rate, to magnetic profiles observed over the Reykjanes Ridge produced equally acceptable simulation profiles.

A similar extrapolated time scale was deduced independently by Vine (1966) from the East Pacific data.

The validity of the radiometric time scale established by Cox et al (1964) has received impressive confirmation from the work of Opdyke et al (1966) on deep-sea sedimentary cores. Piston cores from the Antarctic (Opdyke et al 1966) and Indian Ocean (Opdyke & Glass 1969) have revealed a unique form of magnetic stratigraphy based on systematic changes in inclination of the direction of remanent magnetization. The sequence of normally and reversely magnetized sections determined from top to bottom of such cores have compared extremely well with the magnetic stratigraphy worked out on lava flows by Cox et al (1964) using K-Ar dating. The possibility of any large gaps in the core records was precluded by the continuous nature of the known palaeontological stratigraphy.

The technique established by Opdyke et al (1966), in principle, permits the resolution of core specimens down to a cubic centimetre - depending on the rate of sedimentation this would represent a period from one thousand to ten thousand years. This potential precision is very much finer than that which could be hoped from radiometric methods or oceanic magnetic anomalies. The technical problem of retrieving a long, continuous deep-sea core at present limits the method to sampling, at best, the top sixteen metres of sediment. This represents a time span of about 4-5 million years, depending on local conditions.

Recently extensive magnetic profile data from the Pacific, Atlantic and Indian oceans have now been interpreted in terms of the Vine-Matthews hypothesis of sea-floor spreading (Pitman et al 1968; Dickson et al 1968; Le Pichon & Heirtzler 1968). Heirtzler et al (1968) in summary, have shown that by assuming that all these magnetic profiles are caused by a common sequence of normally and reversely magnetized bodies, modified slightly in each case to allow for different

rates of spreading; then it is possible to deduce a revised geomagnetic time scale extending over the last 80 million years. The actual time scale was established using the Vema 20 magnetic profile from the South Atlantic as a standard and assuming a constant rate of ocean floor spreading for the entire period of the time scale. This geomagnetic time scale is now used as a standard interpretational reference scheme to calibrate contemporary magnetic data across mid-ocean ridges in terms of the Vine-Matthews hypothesis of sea-floor spreading.

The possible errors inherent in this twenty-fold extrapolation, from the known radiometric time scale clearly present a serious problem in the application of this chronology. However, strong support has been given to the later part of this time scale by the good correlation of the magnetic stratigraphies independently established by Hays & Opdyke (1967) from the study of deep-sea cores; and by Dalrymple et al (1967) from 45 Pliocene rock samples in the Western U.S.A. Heirtzler et al (1968) have commented on certain observations that conflict with the proposed time scale, whilst Ozima, Ozima and Kanoeka (1968) and Loncarevic et al (in press) have discussed radiometric dates disagreeing with ages predicted from identified magnetic patterns. These difficulties are not yet resolved, being further complicated by the uncertainties in obtaining good K-Ar dates for young rocks.

Perhaps the most striking support of the Heirtzler et al time scale has been provided by the results of Leg 3 of the JOIDES deep sea drilling programme (Maxwell et al 1970). If the time scale is correct in an absolute sense, drilling at any point away from the axis of the ridge should show sediments no older than that predicted

from the magnetic anomaly pattern. Eight holes were drilled across the flanks of the mid-Atlantic ridge at about 30° South. This is approximately the same vicinity as the standard Vema 20 magnetic anomaly profile. When the distances from the ridge axis are plotted against the estimated age of the sediment/basement contact the eight sites nearly fall on a straight line suggesting that the rate of spreading has been roughly constant for 70 million years in the South Atlantic. The good agreement of these palaeontological age dates with the magnetic ages predicted from the Heirtzler et al time scale may be seen in Table I.

In general therefore, data from magnetic anomalies and deep sea drill holes support the absolute time scale of Heirtzler et al (1968) and suggest a steady-state spreading history throughout the ocean basins of the world. This opposes the view of Ewing and Ewing (1967) and Le Pichon (1968) and others who have postulated an episodic spreading history, principally involving a discontinuity at about 10 million years B.P. The balance of this, and other evidence reviewed by Schneider & Vogt (1968), seems to suggest that the creation of oceanic crust is a pulsating process - though remaining essentially continuous. This and examples of variable spreading rates (Vine 1966; Phillips 1967) emphasize the importance of maintaining a critical interpretation of oceanic magnetic anomalies.

1.4 Plate Tectonics

The regular magnetic anomaly patterns observed over large areas of the oceans have strongly suggested that such areas exist as rigid crustal units. This is particularly emphasized by the simple truncation and apparent displacement of the magnetic pattern by such features as the Murray, Mendocino and Pioneer fracture zones in the East Pacific.

TABLE I

SOUTH MID-ATLANTIC RIDGE DRILLING SITES

Site No.	Magnetic anomaly age (m.y.)	Palaeontological age sediment above basement (m.y.)	Distance from ridge axis (km)	
			Linear	Rotation at 62°N, 36°W
16	9	11 ± 1	191 ± 5	221 ± 20
15	21	24 ± 1	380 ± 10	422 ± 20
18	..*	26 ± 1	506 ± 20	506 ± 20
17	34-38*	33 ± 2	643 ± 20	718 ± 20
14	38-39	40 ± 1.5	727 ± 10	745 ± 10
19	53	49 ± 1	990 ± 10	1010 ± 10
20	70-72	67 ± 1	1270 ± 20	1303 ± 10
21	--	>76 **	1617 ± 20	1686 ± 10

* Location of these sites within the characteristic magnetic anomaly pattern is uncertain.

** Basement rock not reached at site 21. (Maxwell et al 1970)

Wilson (1965) suggested that the mobile belts of the Earth's crust i.e. active mountain chains and island arcs, major faults and mid-ocean ridges represented a continuous boundary feature which divided the surface of the Earth into several large rigid plates. Wilson proposed that many of these boundary structures were inter-connected by a new class of fault known as a transform fault. This concept has provided important support for the theory of sea-floor spreading (Dietz 1961; Hess 1962). When oceanic crust is being created an apparent transcurrent fault, against which a mid-ocean ridge impinged on each side, would be active or seismic but would not lead to greater offsets of the ridge. The motion of the crust between the two ridge intersections with the fault would be opposite to that expected from an active transcurrent fault. This is the fundamental difference between transform and transcurrent faulting.

Sykes (1967) used the first motions of earthquakes from fracture zones on the mid-Atlantic ridge and East Pacific Rise to show that assuming a fault plane solution, the inferred sense of displacement was in agreement with that predicted for transform faults. Also the seismic activity was confined almost exclusively to the region between the two crests of the ridge, i.e. within the zone of differential shear assuming sea-floor spreading. Thus this evidence supported Wilson's hypothesis of transform faults (Wilson 1965) and the idea of ocean floor spreading away from the axis of the ridge.

Bullard et al (1965) demonstrated geometrically, with a computer technique, that individual areas on the surface of the earth could move as rigid blocks and remain compatible with the theories of sea-floor spreading and continental drift. This work was the first rigorous application of the concept of a pole of rotation to the problem of displacement on a spherical surface.

The extension of these basic ideas of Wilson (1965) and Bullard et al (1965) by Mckenzie & Parker (1967) introduced the general concept of individual aseismic areas moving as rigid plates on the surface of the earth. McKenzie & Parker successfully used this idea to explain the inferred motion of the oceanic Pacific-plate relative to the plate containing North America and Kamchatcka. Independent work by Morgan (1968) presented a similar hypothesis in which the entire earth's surface was described in terms of a number of rigid crustal blocks, whose boundaries were defined by the mid-ocean ridge system, trenches or young fold mountains and faults. The interaction and resulting modifications at the boundaries of these blocks were then described in terms of present day large scale extensional and compressional structures. This framework then explains in a global sense the relationship of the mid-oceanic ridge system, as an extensional feature involved in the creation of oceanic crust, and the trench system as a compressional feature concerned with the loss of crustal material due to thrusting and sinking of the lithosphere. These geometrical ideas of Morgan (1968) were then adopted by Le Pichon (1968) who further demonstrated the consistent nature of the overall pattern of sea-floor spreading, involving six large crustal blocks on the surface of the earth. Le Pichon particularly showed that evidence, from sea-floor spreading rates determined from oceanic magnetic anomalies, and the azimuth of transform faults at their intersections with the ridge axis, independently supported the relative motion of adjacent blocks.

Global earthquake studies by Isacks et al (1968) and others have significantly contributed towards refining and supporting the general ideas of plate tectonics. The world wide distribution of all known

earthquake epicentres, since 1961, clearly outlines the boundaries of the individual crustal plates, and shows that most include both continental and oceanic areas. The analysis of earthquake focal mechanisms by Isacks et al (1968) has confirmed the predicted relative motion of the major plates (Le Pichon 1968). Evidence presented by Sykes (1966) detailing deep and shallow earthquakes in the vicinity of island arc structures has clearly defined an inclined seismic zone compatible with a downgoing slab of lithosphere.

A significant problem in plate theory is the driving mechanism (Mckenzie 1969). Thermal convection in some form appears to be the only source of sufficient energy, but agreement goes no further. The oldest theory describing plate motion depends on large scale convection throughout at least the upper mantle. Viscous forces are then required to couple the plates to the moving mantle below (Holmes 1965). Elsasser (1967) has suggested that the motions of the plates themselves are not caused by viscous coupling to the mantle beneath, but that the lithosphere acts as a stress guide and that the surface motions of the plates are maintained by cold slabs of lithosphere sinking beneath island arcs and pulling the rest of the plates with them. Isacks & Molnar (1969) have inferred from their stress analysis of mantle earthquake mechanisms that such a downgoing slab of lithosphere could exert a pull on the surface portion of the slab, although this motion may be discontinuous.

The general ideas of plate tectonics now provide a valuable reference framework in which the integrated theories of continental drift, sea-floor spreading and transform faults successfully describe and relate the major surface features of the earth. Oceanic magnetic anomalies associated with the mid-ocean ridge system are particularly important in this respect since their interpretation in terms of the

Vine-Matthews hypothesis may not only reveal in detail the reversal history of the earth's magnetic field, but will also trace the evolution and relationships of the major plates of lithosphere.

CHAPTER 2

INTERPRETATIONAL PROCEDURE

2.1 Introduction

The task of interpreting any magnetic anomaly is that of estimating possible source bodies capable of explaining the observed anomaly. The acceptance of any such model as a solution depends on its geological feasibility and its compatibility with any other relevant geological or geophysical evidence available. However, the solution of this inverse problem is subject to a fundamental ambiguity inherent in potential field analysis. Any magnetic anomaly component in a two-dimensional Cartesian co-ordinate system must satisfy Laplace's equation. From the equivalent layer theorem given by Bott (1967) any such harmonic function may also be explained exactly by a suitable distribution of dipoles over a given horizontal plane. Since the choice of this surface is somewhat arbitrary there clearly exists an effectively infinite number of possible distributions capable of explaining a given anomaly. Because of this lack of uniqueness magnetic interpretation depends on the availability of further information against which working hypotheses may be tested. However, when it is possible to make certain assumptions about the anomalous magnetic source (Smith 1960, 1961; Roy 1962; Al-Chalabi 1970) then for a particular problem a unique solution may exist.

Standard magnetic interpretational procedures employ the visual comparison of observed anomaly profiles with theoretical curves computed for bodies of relatively simple geometry (e.g. Gay 1963). Other methods derive various numerical quantities such as gradients and half-widths from the anomaly profile. These are then used to

estimate information describing possible source bodies in terms of such factors as depth-to-width and limiting depth (egs. Smith 1961; Bruckshaw & Kunaratnam 1963).

Computer techniques, however, designed to evaluate magnetic anomalies caused by two and three-dimensional structures have provided by far the most flexible and efficient interpretational methods available (egs. Bott 1963, 1969a; Talwani & Heirtzler 1964). Using such schemes the model parameters necessary to define a given magnetic anomaly may be determined either by an 'indirect' approach, that is essentially trial and error, or more effectively by using a 'direct' procedure.

In the 'indirect method', theoretical anomalies are computed for 'trial' bodies and then compared with the observed anomalies. Any significant misfit noted then serves as a basis for modification of the source body. The procedure is then repeated, the parameters of the trial body being successively modified until a satisfactory fit of the computed anomaly with the observed one is obtained. The final model resulting from this 'trial and error' process is then considered to be a possible solution to the interpretational problem.

Indirect methods are generally time consuming from the point of view of number of computer runs required and the subjective nature of the modification procedure involved. However, the introduction of completely automated, iterative modification procedures, has significantly improved the ~~reliability~~ effectiveness of such interpretations (Butler 1968; Al-Chalabi 1970).

The 'direct methods' by definition operate directly on the observed magnetic anomaly in an attempt to derive optimum parameter

values defining the magnetic source. Their application to oceanic magnetic anomalies, associated with the mid-ocean ridge system, has been particularly successful due to the linear nature of the problem involved and the restrictive assumptions that may be made concerning the magnetic source (Bott 1967; Luyendyk 1969; Emilia & Bodvarsson 1969; Johnson 1969; Bott & Hutton 1970b).

2.2 The Linear Inverse Problem

The essential problem in interpreting oceanic magnetic anomalies is the determination of a suitable distribution of magnetization, within the oceanic crust, that will satisfactorily explain the observed anomalies. Bott (1967) formulated a linear inverse procedure directly applicable to this problem. The procedure is based on an integral equation relating the observed magnetic anomaly to a distribution of magnetization, varying only in the horizontal direction, within a two-dimensional source layer of specified shape and direction of magnetization. The numerical solution of this equation then determines the unknown distribution of magnetization directly from the magnetic anomalies which are observed.

The values of intensity of magnetization computed with this procedure (hereafter called the Linear Inverse technique) are 'effective' quantities and take into account both remanent and induced contributions, assumed to be in the same direction. The direction and magnitude of the anomalous magnetization vector is strictly given by the vector relation:

$$\underline{J} = k\,\underline{H} + \underline{Jr}$$

where

$\underline{H}$ = Earth's present magnetic field vector,

$\underline{Jr}$ = remanent magnetization vector,

k = susceptibility.

The direction of resultant magnetization is generally assumed to be parallel to the average geocentric dipole field. This is the assumption normally made in palaeomagnetic work. A suitable technique, such as that given by Bott (1969b), permits both the direction of magnetization and the direction in which the observed magnetic anomaly component is measured to be resolved into the plane perpendicular to the strike of the magnetic source body.

The basic integral equation formulated by Bott (1967, Fig.1) is as follows:

$$A(x) = \int_{-\infty}^{+\infty} J(\xi)\, K(n_1, n_2, B, (x-\xi))\, d\xi \qquad (1)$$

where

$A(x)$ is the observed magnetic anomaly at (x,o);

$J(\xi)$ is the intensity of magnetization as a function of the source body x co-ordinate;

K is a Kernel function defining the resulting magnetic contribution from the source bodies assuming unit magnetization.

Bott approximated (1) to a finite set of linear equations by the following procedure. The magnetic anomaly is digitized at suitable intervals to yield (n) values, while the magnetic layer is subdivided into (m) two-dimensional blocks ($n \geq m$) (Fig. 2.1), each assumed to be uniformly magnetized.

Equation (1) may then be written:

$$A_i = \sum_{j=1}^{m} K_{ij}\, J_j \qquad (i = 1,2,.....n) \qquad (2)$$

where

A_i represents the i^{th} digitized magnetic anomaly value;

K_{ij} is the magnetic anomaly at the i^{th} point caused by the j^{th} block, for an intensity of magnetization of one;

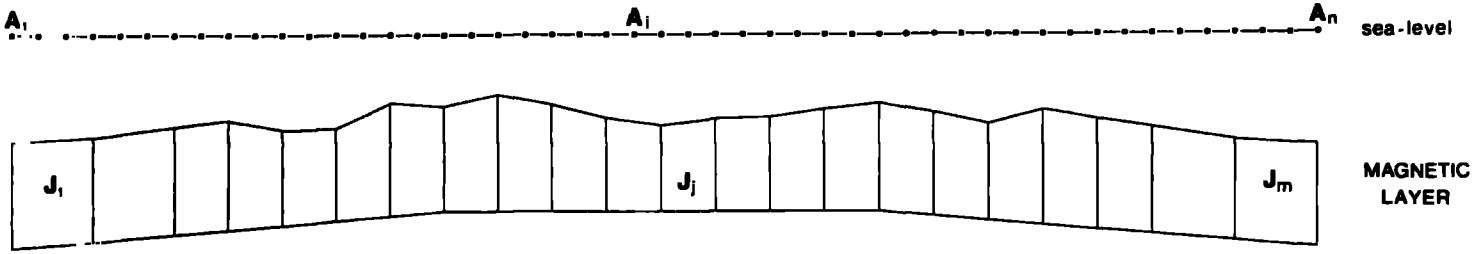

$$\begin{bmatrix} A_1 \\ \vdots \\ A_i \\ \vdots \\ \vdots \\ \vdots \\ A_n \end{bmatrix} = \begin{bmatrix} K_{11} & K_{12} & \cdots & \cdots & K_{1m} \\ K_{21} & K_{22} & \cdots & \cdots & K_{2m} \\ \cdots & \cdots & \cdots & \cdots & \cdots \\ \cdots & \cdots & \cdots & \cdots & \cdots \\ & & & & \\ & & & & \\ K_{n1} & \cdots & \cdots & \cdots & K_{nm} \end{bmatrix} \begin{bmatrix} J_1 \\ \vdots \\ J_j \\ \vdots \\ J_m \end{bmatrix}$$

J_j is the intensity of magnetization of the j^{th} block.

Equation (2) may be written more compactly in matrix form:

$$A = K\,J \qquad (3)$$

for a regular system of equations (m=n) then (3) has a formal solution given by

$$J = K^{-1}A \qquad (4)$$

When the system of equations is overdetermined, i.e. there are more equations than unknowns (n>m), equation (2) may be written in the form:

$$A_i - \sum_{j=1}^{m} K_{ij}\,J_j = e_i \qquad (i = 1,2.....n) \qquad (5)$$

The quantities e_i are 'residuals', which for a perfect fit would all be zero. As we are dealing with a practical system within which certain errors are unavoidable the residuals will not be exactly zero. We therefore look for the values of J_1, J_2 .... J_m which will minimize some function of these residual values. The minimization procedure carried out in the present work is the normal method of least-squares (Golub 1965). This requires that the function

$$\sum_{i=1}^{n} (e_i)^2 \qquad \text{be minimized.}$$

A formal solution for (5) in matrix notation is given by

$$J = (K^T K)^{-1}\,K^T\,A \qquad (6)$$

where K^T is the transpose of K (Tanner 1967; Bott 1967).

The solution according to equation (4) or (6) specifies a system of two-dimensional model blocks of variable magnetization which can give rise to the observed anomaly.

When compared with 'indirect' methods of interpretation used for simulating oceanic magnetic anomalies the Linear Inverse technique enjoys three main advantages:

(a) the procedure is more accurate and ~~entirely~~ objective. With the indirect approach theoretical magnetic profiles are only matched by eye against the observed profile. This involves the manual adjustment of the model parameters - generally the horizontal scale.

(b) the magnetization distribution is explicitly computed from the observed data. Indirect model work generally assumes the absence of any lateral variation in intensity of magnetization and employs a relatively simple, assumed magnetization pattern of alternating polarity across vertical boundaries.

(c) the computational procedure is completely automatic and carried out as a single computer operation.

The present study further develops the original work by Bott (1967) in which the technique was used to interpret a magnetic profile recorded across the Juan de Fuca ridge, in terms of an underlying distribution of magnetization within a horizontal Layer 2. Bott also showed that in attempting to match the high frequency content of the magnetic profile using Layer 3 (5-11 km) as the magnetic layer, unrealistic magnetization values resulted. This implied that Layer 3 was not causing the bulk of the observed anomalies. Emilia & Bodvarsson (1969) have presented a modified version of this 'direct' technique in which horizontal rectangular blocks are used to approximate to a sloping magnetic layer. Bott & Hutton (1970b) have described a further refinement of Bott's original method in which an irregular variation of the upper and lower surfaces defining the magnetic layer is permitted. The latest version of the Linear Inverse technique (section 2.3.2) is readily applicable to block shapes of irregular cross-section incorporated within a continuous magnetic layer. Other direct techniques applied to the problem

of interpreting oceanic magnetic anomalies have been presented by Johnson (1969) and Luyendyk (1969). The technique of Luyendyk is very similar to that of Bott & Hutton (1970b) whilst that of Johnson employs a 'non-linear' inverse method to compute magnetization values and certain optimum body co-ordinates for the magnetic layer.

2.3 The Computer Programme

This section describes two computer programmes which have been written to solve the Linear Inverse problem of interpreting two-dimensional oceanic magnetic anomalies. The programmes have been developed from earlier versions designed to solve the same problem (Bott 1967; Stacey 1968) - the original programme name 'MXOCEAN', now MK.III (A) and (B), has been retained for continuity. The new programmes have been written in PL/1 computer language for an I.B.M. 360/67 machine and improve on previous versions for the following reasons:

(a) the procedure is capable of incorporating irregular variation of the upper and lower surfaces of the magnetic layer;

(b) a least squares facility has been added permitting the solution of an overdetermined problem;

(c) the magnetic layer may be formed from model blocks of irregular cross-section.

These developments have resulted primarily from the availability of powerful computer facilities (N.U.M.A.C. I.B.M. 360/67). This has permitted the elimination of previous approximations in method and has facilitated a straightforward approach to the problem.

Much of the present work was carried out with programme 'MXOCEAN' III (A), this programme uses a vertical trapezium as the basic model unit. At a later stage the potential of a programme capable of incorporating a more flexible model unit was realized. This was achieved by transplanting a standard Durham University geophysical computer programme, 'MAGN' (Bott 1969a) as a subroutine, into the programme 'MXOCEAN' III (A). This resulted in the creation of programme 'MXOCEAN' III (B), providing a useful generalization of the technique. The essential difference between Programme (A) and (B) is within the computational technique used to evaluate the total field magnetic anomalies caused by the two-domensional model blocks forming the magnetic layer. The next two sections describe these alternative procedures.

2.3.1 The 'Vertical-Dyke' Method

This procedure is employed in Programme (A) and was developed primarily to allow the use of irregular topography at the top of the magnetic layer and a varying depth to the base. In order to carry this out the magnetic layer is formed from a series of adjacent two-dimensional trapezoidal blocks with vertical sides, Fig. 2.1. The non-parallel sides then permit a close representation to be made of any variation in relief.

It is supposed that the trapezoid shown in Fig. 2.2(a) is the j^{th} block of the magnetic layer and the field point O is the position at which the i^{th} observed anomaly value is recorded. The x-axis points in the direction of the magnetometer profile, perpendicular to the strike of the model, and the z-axis points vertically downwards. The block is assumed to possess unit magnetization with a dip of I_m and azimuth α_m measured from the strike towards the positive

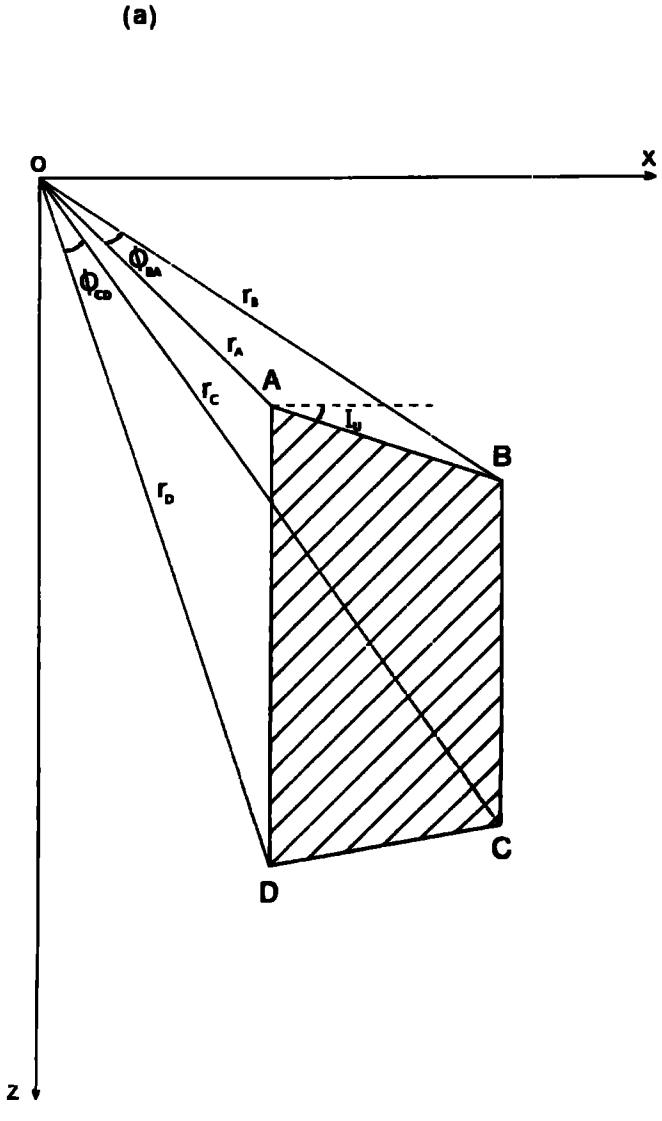

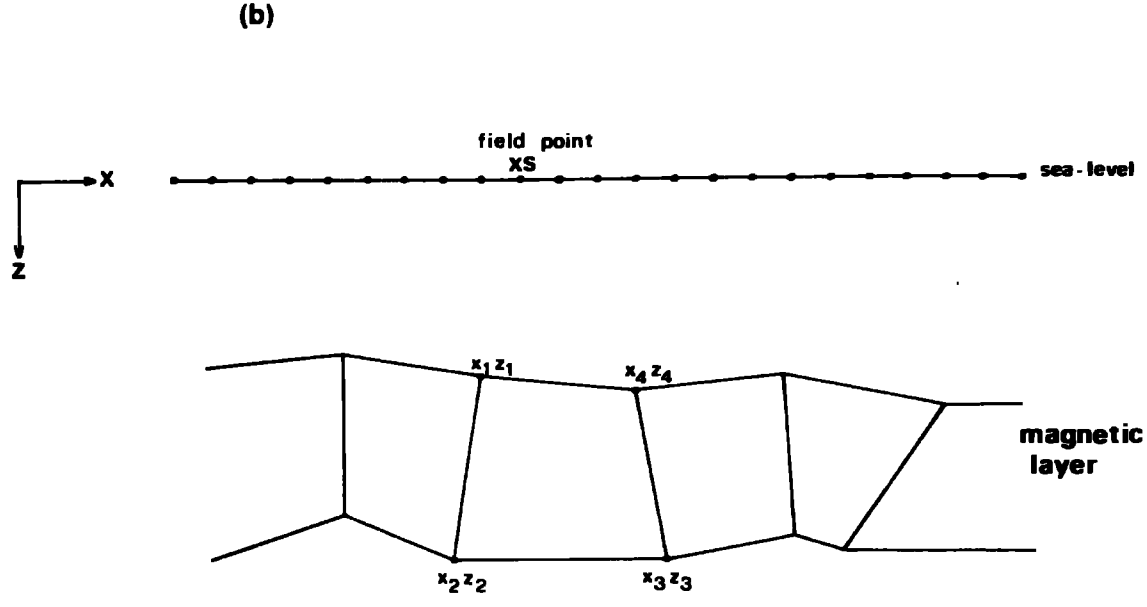

Fig. 2.2 (a) Geometry of the basic two-dimensional model unit (ABCD) in relation to the field point O.

(b) Illustration of an irregular model element (x_1 z_1 .. x_4 z_4) within the magnetic layer.

x-axis. The measured magnetic anomaly component at O has a dip of I_e and azimuth α_e measured as α_m. Using the notation of equation (2), K_{ij} is the magnetic anomaly at O caused by the j^{th} block. If the dip of the upper surface of the block is I_u and that of the lower surface I_l, both measured downwards from the positive x-axis, it may be shown that:

$$K_{ij} = 2F \cos I_u (\sin (I_u + B) \ln ({}^{r_B}/_{r_A}) - \phi_{BA} \cos (I_u + B))$$

$$- 2F \cos I_l (\sin (I_l + B) \ln ({}^{r_C}/_{r_D}) - \phi_{CD} \cos (I_l + B)).$$

where $B = \arctan (\tan I_m / \sin \alpha_m) + \arctan (\tan I_e / \cos \alpha_e)$

$$F = (\cos^2 I_e \sin^2 \alpha_e + \sin^2 I_e)^{\frac{1}{2}} \ (\cos^2 I_m \sin^2 \alpha_m + \sin^2 I_m)^{\frac{1}{2}}$$

r_A, r_B, r_C, r_D, ϕ_{BA} & ϕ_{CD} are defined in Fig. 2.2(a).

(Bott 1969b; Bott & Hutton 1970b)

This expression for K_{ij} is derived as follows:

(a) the co-ordinates of the upper non-parallel side, for any trapezoid, are used to define a vertical semi-infinite dyke with a sloping top. The magnetic anomaly due to this dyke, at a specified field point, is then computed assuming unit magnetization;

(b) a similar procedure is carried out for the lower non-parallel side of the trapezoid;

(c) the magnetic effect due to the trapezoid alone is the difference of these two quantities.

This sequence of operations is performed with two computer subroutines ('TOP' and 'MAGSDYKE' - Bott, private communication). The subroutine 'MAGSDYKE' has been restructured within the programme in

order to reduce execution time. Further details of these two subroutines are given by Stacey (1968).

2.3.2 The 'MAGN' Method

This procedure is used in Programme (B) and provides the increased facility, compared with the 'Vertical Dyke' Method in that any model block within the magnetic layer may be represented by a polygon rather than a vertical trapezium. The method is largely based on the computer programme 'MAGN' (Bott 1969a). This programme evaluates the magnetic anomaly components caused by two-dimensional bodies of specified shape and magnetization at field points above the level of the topmost part of the bodies. The computational procedure is based on the repeated use of formulae expressing the magnetic effect of a semi-infinite horizontal slab bounded by a plane sloping surface. The method used is similar in principle to that described by Talwani & Heirtzler (1964), further details and formulae are given by Stacey (1965) and Bott (1969a).

Within Programme (B) the essential part of the 'MAGN' programme has been re-structured to form a subroutine ('NGAM'). This procedure is capable of sequentially computing the magnetic anomaly, assuming unit magnetization, due to the various model blocks forming the magnetic layer. Fig. 2.2(b) shows an example of possible polygonal model elements incorporated within the magnetic layer.

The present version of Programme (B) has been written for use with model elements of quadrilateral shape. However, no difficulty is envisaged in increasing the number of sides to be considered if the need arises. Model elements of complex shape may always be formed from a number of simpler bodies - the important advantage of this procedure is the facility to consider lateral boundaries which are inclined rather than vertical.

2.3.3 Main Programme Structure

The following discussion refers to both Programmes (A) and (B) unless otherwise indicated. The Flow Chart shown in Fig. 2.3 illustrates the essential sequence of operations performed within these programmes.

Initially the programme requires the total number of digitized magnetic anomaly points and co-ordinate points defining the upper surface of the magnetic layer, to be used in the interpretation. These variables are then used within the main programme-block to control the extent of 'do-loops' and the bounds of declared arrays. This variable dimensioning capability permits efficient use of the available core store and facilitates data input. The inclination and azimuth of the earth's magnetic field and magnetization of the source body are also included at this point. Programmes (A) and (B) both follow the convention of Bott (1969a) with respect to the specification of these quantities. These directions are then transformed to represent components within the x-z plane, i.e. perpendicular to the strike of the body.

The next section of the programme lies within the main programme-block, and reads in information describing the shape of the magnetic layer to be used and the specified values of the observed magnetic anomaly. Within this section use is made of 'programme control data' to provide alternative forms of data input. Also Programme (A) can accept information allowing the regular successive combination of several prespecified model blocks within the magnetic layer. The actual combination is performed in the next stage of Programme (A). This facility permits maximum advantage, with respect to topographic contribution, from any closely profiled magnetic surface layer.

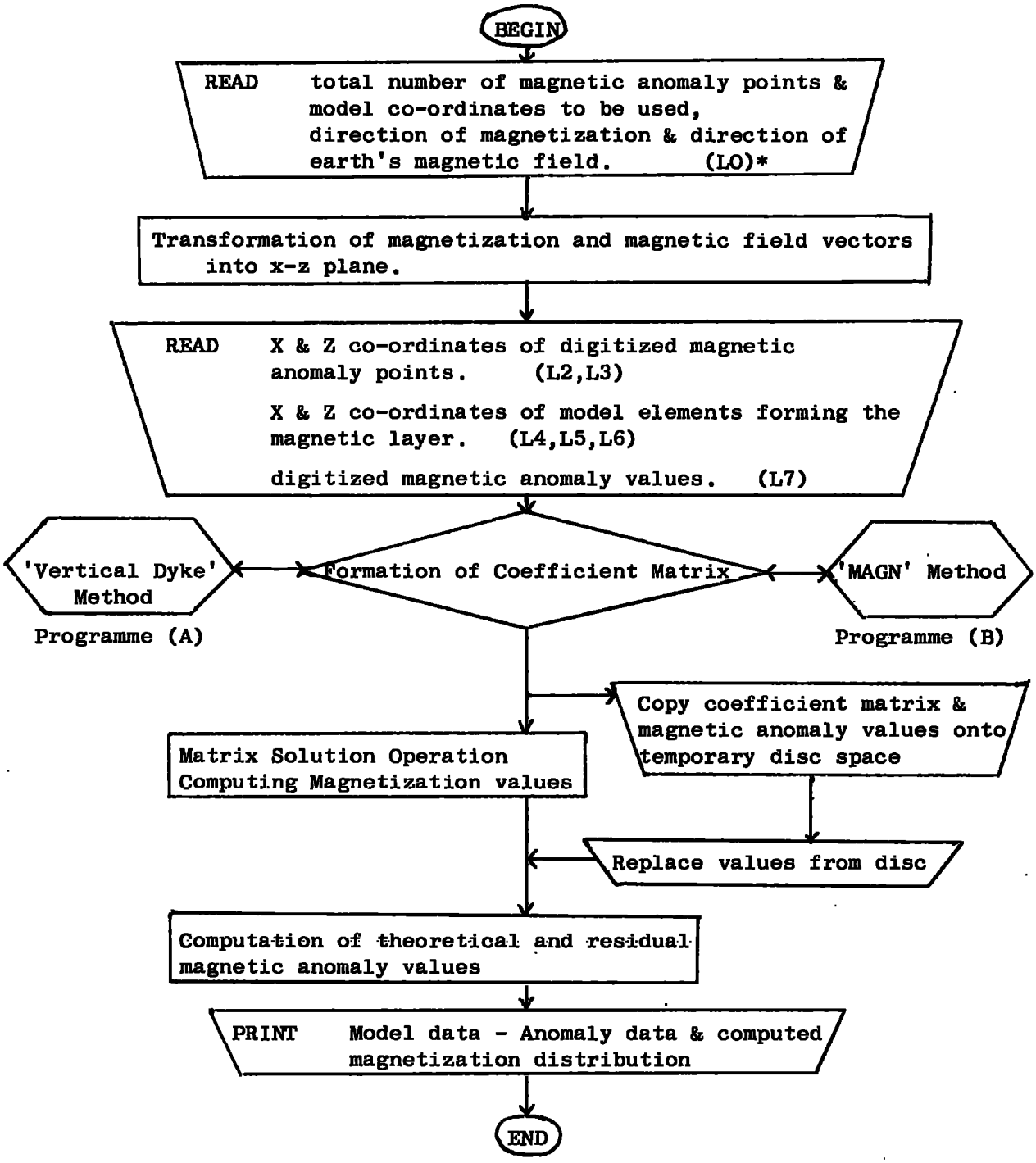

(* bracket labels correspond to statement labels in the programme 'print out', see Appendices 1 & 2)

Fig. 2.3 Flow diagram of the main programme

Stage I: The main programme then begins the major computational operation of forming the two-dimensional coefficient matrix. The elements of the coefficient matrix (K_{ij}) are established by considering each model block of the magnetic layer in turn and computing its magnetic effect, assuming unit magnetization, at all the field points specified for the observed anomaly profile. Individual row elements within the coefficient matrix then represent the sequential magnetic contribution of all the model blocks at one particular anomaly point (Fig. 2.1).

In Programme (A) the individual elements of the coefficient matrix are accessed and their values computed within a double 'do-loop', establishing the matrix row by row. A similar computational step, using the 'Vertical Dyke Method', is performed for each element. The subroutine 'TOP' permits a certain reduction in arithmetic, after the first outer loop, by storing constant parameters and re-supplying them to the later stages of the procedure.

In Programme (B) the coefficient matrix is formed inside a single 'do-loop'. Each loop passes the co-ordinates of one model block to the subroutine 'NGAM'. This procedure then evaluates the magnetic anomaly due to this block, at every field point specified for the observed magnetic anomaly. These values are then returned to the statement calling the subroutine and stored directly as one complete column in the coefficient matrix. The repeated application of this procedure to each model block within the magnetic layer establishes the coefficient matrix column by column. This computational procedure is slower than the 'Vertical Dyke Method' by a factor of about 2.3.

The following section of the programme copies the formed coefficient matrix (row by row) and the magnetic anomaly values as a temporary, sequential data-set on to magnetic-disc. This output of data to an external storage medium is carried out because the matrix equation solution routine destroys these arrays, which are required in a later section of the programme. The copy-storage of large arrays within the programme is prohibited due to restrictions in available core store.

Stage II: The problem of determining the required distribution of magnetization consists of solving the established system of linear equations. There are two principal methods of solution applicable to the problem; one yields an approximate solution (iteration) and the other yields an exact solution (Gaussian elimination).

Iterative methods obtain a solution by a series of successive approximations from an estimated initial solution vector (Emilia & Bodvarsson 1969). Such a procedure may be used to advantage, with regard to time considerations, when dealing with special sparse types of large matrices or a well conditioned (nxn) system of equations. An iterative technique will permit termination of the solution process within known data errors and can introduce a smoothing action if so desired (Emilia & Bodvarsson 1970). A direct method of solution such as Gaussian elimination with 'pivoting' will provide an answer in finite time, and the accuracy of the computed answers will depend mainly on the degree of ill-conditioning of the problem. Ill-conditioning occurs when small changes in the coefficient values give rise to large changes in the solution values. In the present work the coefficient values can generally be well defined and computational instability results almost exclusively from the sensitivity of the solution values to errors within the magnetic anomaly values.

When dealing with a completely determined system of equations, conditioning of the problem is significantly improved by the dominant diagonal elements. These automatically result because of the way in which the problem is generated and difficulties in solution are generally not encountered either in iterative or direct methods. However, when dealing with the solution of an overdetermined system of linear equations, using a least squares method, problems of conditioning are more significant since an exact agreement can no longer be attained at all data points considered. It is therefore important to choose a computational procedure which optimizes the reliability of the resulting least squares solution. Theoretically this problem reduces to solving a system of normal equations whose solution is given by equation (6), (Bott 1967; Tanner 1967). However, Anderssen (1969) points out that the inverse matrix $(K^TK)^{-1}$ 'has a notorious reputation for being poorly conditioned if not ill-conditioned' and recommends that methods based on the direct inversion (e.g. Gaussian elimination) of these normal equations should not be used.

In the present work the solution of the matrix equation (3) is conveniently carried out by use of pre-written Fortran, matrix subroutines (I.B.M. 1968). These subroutines are capable of dealing with any size array, limited only by the available core storage and time considerations. Their implementation within a PL/1 programme requires that two-dimensional arrays are exchanged in a transposed form due to different storage modes. Hence, throughout the main programme the coefficient matrix is always formed and operated with its columns written as rows and its rows written as columns. A PL/1 coding of the matrix subroutines has recently become available (I.B.M. 1969).

The subroutines 'LLSQ' (Golub 1965; I.B.M. 1968) and 'SIMQ' (I.B.M. 1968) have been found to be most useful, the former has been employed extensively. The subroutine 'SIMQ' obtains the solution of a set of linear equations, with an (nxn) coefficient matrix, by a process of successive elimination. The subroutine 'LLSQ' obtains a least-squares solution to an overdetermined system of linear equations using a Householder transformation technique. The procedure decomposes the coefficient and anomaly matrices into upper triangular forms and then computes a solution by back substitution. This method has been found to be consistently satisfactory in the present work and is recommended by Anderssen (1969) for general linear least squares problems.

The advantages of solving an overdetermined system of equations may be appreciated from the following considerations. With a completely determined system of linear equations, normal Gaussian elimination techniques provide an exact answer in that, the observed digitized magnetic anomaly values are explained completely by the calculated magnetization distribution. However, at magnetic anomaly points intermediate to those actually considered in the calculation, there will be some discrepancy between the theoretical anomaly computed from the evaluated magnetization distribution and the observed anomaly (Bott 1967). Clearly the larger the width of block considered the larger the intervening residuals will be. It is not possible to improve the overall fit simply by increasing the number of magnetic anomaly points and model blocks considered for a given problem. This will not only increase the computational time required but reducing the block width beyond a certain limit will introduce an inherent instability into the results (section 3.4). To obtain the maximum amount of information from a given magnetic profile it is desirable to use a number of magnetic anomaly values in excess of the number of model blocks forming

the magnetic layer. This procedure significantly improves the overall agreement between the observed and calculated magnetic anomaly fields and provides a more valid estimate of the degree of misfit between these two quantities.

Stage III: Immediately after completing the solution routine a check of the resulting error parameter is made, within the main programme, to ensure that the procedure was successful. Non-solution may result from error in data input or ill-conditioning of the particular problem.

The coefficient matrix and magnetic anomaly values are then replaced from magnetic-disc by overwriting the original programme locations. The right-hand side of the matrix equation (2) is then evaluated, using the recently computed values of magnetization, to yield a theoretical magnetic anomaly. Subtracting these calculated values from the observed values produces residual values along the profile. These residuals are then used to provide an estimate of the 'degree of fit' by computing the R.M.S. error. Details of the magnetic layer used, the observed, calculated and residual magnetic anomalies and the calculated magnetization distribution are then printed out.

A 'print-out' of Programmes (A) and (B) appears in appendices (1 & 2) together with data specifications. Both programmes have been verified exactly against each other and against theoretical magnetic anomalies generated from test models by use of the programme 'MAGN' (Bott 1969a). Using an I.B.M. 360/67 computer, compilation and link-editing for both programmes, takes about 17 seconds. For an average calculation involving 311 magnetic anomaly values and 125 model blocks the execution time required using Programme (A) was 3 minutes 5 seconds and using Programme (B) 4 minutes 3 seconds. These times are roughly

proportional to the sum of the cube of the number of model blocks and a constant times the number of anomaly values.

As the interpretational technique only deals with a finite profile length, certain errors are introduced into those values of magnetization computed near the ends of the magnetic layer. Magnetic anomaly points situated at the ends of a given profile are required to be explained by an asymmetric source, no consideration is made for the possible contribution of adjoining magnetic material located just beyond the survey line.

When an infinite horizontal layer is used as the source model, in attempting to correct for this edge effect, the solution of the matrix equation (2) proves to be indeterminate, the coefficient matrix being singular. This problem may be overcome by specifying the value of magnetization for one of the model blocks (c.f. Johnson 1969). When topographic control was available, for the upper surface of the magnetic layer, the indeterminacy associated with the infinite slab was generally resolved, except when model block widths narrower than the depth to the upper surface of the magnetic layer were used. This second indeterminacy is thought to result from ill-conditioning of the system induced partly by data errors.

The infinite-slab 'end-correction' (Appendix 6) has not been adopted for standard use with the present version of the interpretational technique. Oscillation in computed values of magnetization, obtained at the ends of profiles, may be reduced by allowing one model block (width = depth to upper surface of model) to extend beyond the surveyed magnetic line.

During the course of this computer work an attempt was made to programme a version of the Linear Inverse technique capable of treating, in a limited way, a vertical distribution of magnetization. The method adopted was to consider a magnetic layer, subdivided into a number of blocks as before, which was then underlain by a second magnetic layer formed from an equivalent number of blocks. Using a slightly modified version of Programme (A) the procedure carried out was to consider that the second layer merely represented a continuation of the first. The i^{th} row in the coefficient matrix therefore represented the successive magnetic contributions of those model blocks within the first layer followed by those of the second layer, at the i^{th} anomaly point.

Whilst a programmed version of this procedure exactly explained a simple two-layer test model, inconclusive results were obtained for observed magnetic data. This lack of success may have resulted from the banded diagonal structure introduced to the coefficient matrix which then induced an unstable solution. An alternative approach may be to weight the coefficient elements for the second layer and hence obtain conditional solution values.

CHAPTER 3

LIMITATIONS OF THE METHOD

3.1 The Magnetic Model

Topographic profiles, seismic refraction and gravity measurements all indicate that the crustal structure of the mid-ocean ridge system is broadly two-dimensional and parallel to its local axis (Le Pichon et al 1965; Talwani et al 1965). Magnetic surveys (Raff 1966; Heirtzler et al 1966; Avery et al 1968) have also shown that magnetic anomalies associated with the ridge system have an essentially two-dimensional form in a direction perpendicular to the ridge axis.

The interpretation of these magnetic anomalies has almost exclusively been carried out using Indirect Methods of simulation, employing the concept of sea-floor spreading (Vine 1966; Pitman & Heirtzler 1966; Heirtzler et al 1968). These methods assume a simple magnetic source model, formed from a series of adjacent, two-dimensional blocks of uniform thickness, representing Layer 2. The upper and lower boundaries of this magnetic layer are commonly taken to be plane surfaces, either horizontal or slightly inclined away from the ridge crest. The depth to the upper surface is generally set by the average bathymetry whilst available refraction evidence controls the lower surface.

However, bathymetric profiles across the crestal provinces of the ridge system (Heezen et al 1959) clearly reveal a jagged 'volcanic' relief that is almost certainly the upper surface of Layer 2 or a reasonable approximation. Ewing & Ewing (1967) have shown from a number of seismic profiler traverses across the mid-ocean ridge system that, at and near the axis of the ridge, sediment accumulation

is remarkably small. Furthermore the acoustic basement (assumed to be Layer 2) on which the sediments rest is uniformly rough from the crest of the ridge out to the lower flanks and underneath the basin sediments. The range of this basement relief can often reach a kilometre or more; indeed the thickness of the second layer is notoriously difficult to measure in seismic refraction work because of the variability and relief of its upper surface.

Whilst oceanic magnetic anomalies are not caused simply by this rough basement relief the topography does contribute towards the observed magnetic anomalies. Fig. 3.1 shows sections of four magnetic and bathymetric profiles observed across mid-ocean ridgecrests. The dotted line in each case represents a computed magnetic anomaly from the assumed two-dimensional bathymetric model, with a uniform magnetization contrast. In each case the chosen value of magnetization represented a value determined from the direct interpretation of the complete magnetic profile. For profiles (a) and (b) the topographic contributions have wavelength and amplitude of similar magnitude to the observed anomalies. For profiles (c) and (d) there exists a 50-100 gamma 'noise-ripple' across the profile. The precise magnetic effect of the topography is inextricably bound up with anomalies due to magnetization contrasts within the magnetic layer and hence one cannot make a simple topographic correction by assuming a uniformly magnetized topography. However, Fig. 3.1 demonstrates that this 'topographic-noise' is significant and when comparable to the amplitude of the observed magnetic anomaly can confuse and complicate a relatively simple picture.

Clearly, the allowance for such irregular topography on the upper surface of the magnetic layer will considerably clarify and improve the reliability of the interpretation of oceanic magnetic anomalies

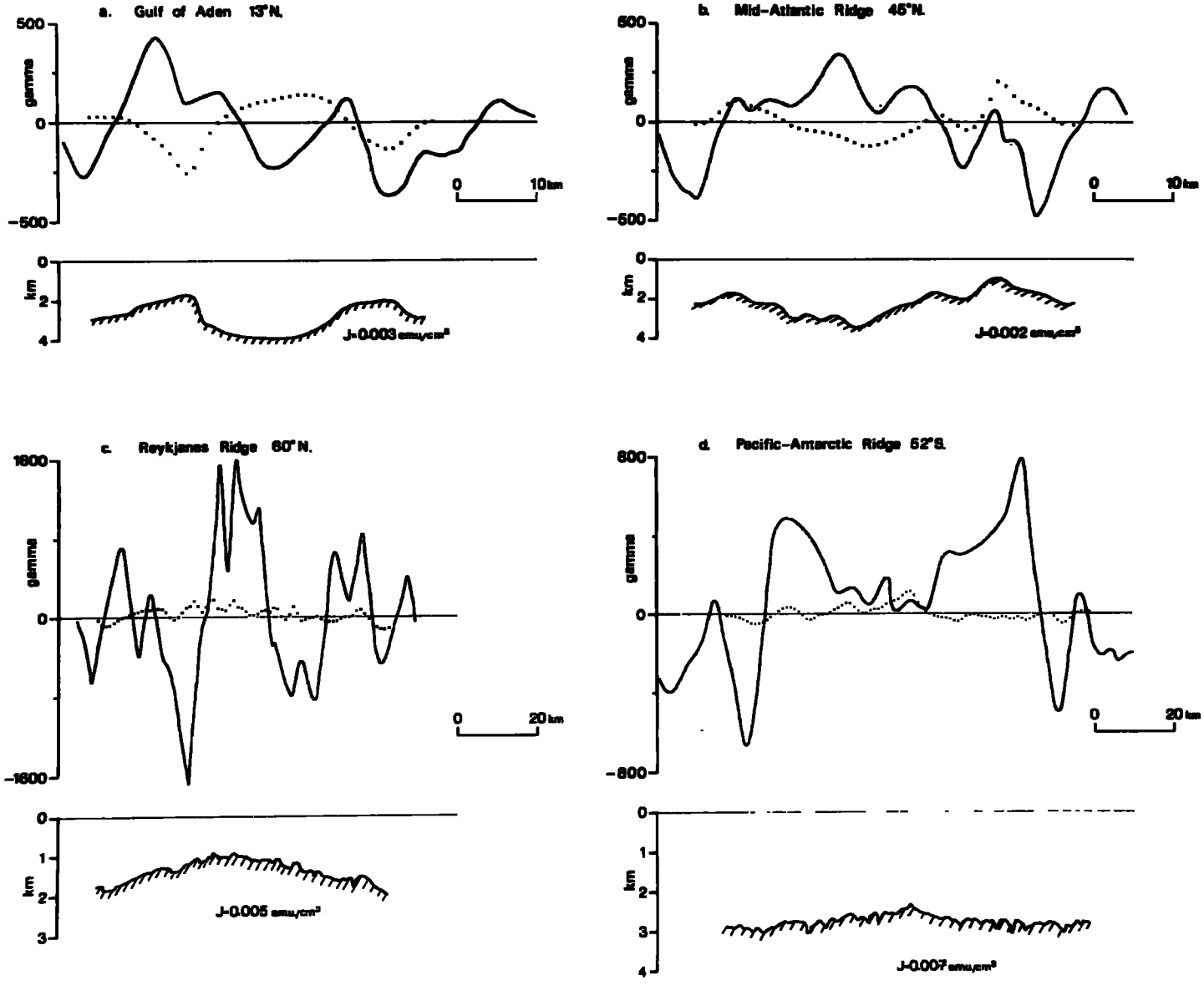
a. Gulf of Aden 13°N.
500
gamma
0
-500
0
10 km
0
km
2
4
J=0.003 emu/cm³
b. Mid-Atlantic Ridge 45°N.
500
gamma
0
-500
0
10 km
0
km
2
4
J=0.002 emu/cm³
c. Reykjanes Ridge 60°N.
1600
gamma
0
-1600
0
20 km
0
km
1
2
3
J=0.005 emu/cm³
d. Pacific-Antarctic Ridge 52°S.
800
gamma
0
-800
0
20 km
0
km
1
2
3
4
J=0.007 emu/cm³

(Vogt & Ostenso 1966; Luyendyk 1969; Bott & Hutton 1970b). Recent work (Talwani et al 1968; Irving et al 1970) suggests the existence of a thin (0.5 km) highly magnetic layer mantling the upper surface of Layer 2. Under these conditions a topographic correction is essential when attempting to accurately assess the distribution of magnetization within the oceanic crust.

However, the use of bathymetric or seismic profiler data in two-dimensional magnetic interpretation tacitly assumes that this data is also two-dimensional. Whilst this is not precisely true, reconnaissance and detailed surveys over sections of the crestal zone of the ridge system (Ulrich 1960, 1962; Loncarevic et al 1966), have shown that many topographic features on the sea-floor are significantly elongated parallel to the axis of the ridge crest. Such features generally have an elongation ratio greater than 4:1 which is the value usually accepted as adequate for two-dimensional interpretation. Errors in interpretation could result from the serious deviation of the bathymetric or profiler surface from a true two-dimensional structure although, in general, this is not considered to be a significant source of error.

3.2 Errors of Observation

All marine magnetic observations are subject to certain errors due to temporal disturbances of the earth's magnetic field and navigational problems. Shipboard magnetic measurements are generally made with proton precession magnetometers which record total magnetic intensity with an absolute accuracy of $\pm$1 gamma. Analyses of absolute errors arising from the motion of the towed sensor plus heading corrections (Bullard & Mason 1961; H. Neth. 1967; Barret 1967) indicate that under normal sea conditions the systematic error is generally less than $\pm$5 gamma for all courses.

The accuracy of any magnetic measurement is also limited by time-varying parts of the earth's magnetic field. These consist of the secular variation, the daily variation and irregular magnetic storm disturbances. Magnetic storm disturbances may easily reach hundreds of gamma and are practically impossible to correct for. The small errors introduced from secular changes in the earth's field are generally not important when considering individual survey lines. However, the influence of those oscillations in the earth's field which have a periodicity of about a day or less is more significant, particularly so for quantitative interpretation of magnetic data.

The 'quiet-day' daily variation (Chapman 1961) generally varies smoothly, mainly with local solar time, having an average 20-50 gamma amplitude extending over a period of 24 hours, with principal harmonics at 12, 8 and 6 hour periods (Bullard 1967). The effect of this variation on a recorded magnetic profile is to introduce corresponding low amplitude, long wavelength components into the observations. The 'disturbed-day' daily variation is thought to result from superimposed, short period oscillations associated with disturbances in the upper atmosphere. Such short period events have duration times ranging from a few minutes to an hour or so. The amplitude disturbances generally vary from a few gamma and less to 15-20 gamma (Jacobs & Westphal 1964; Rikitake 1966) and are responsible for local, short wavelength errors within magnetic observations.

A straightforward correction for the diurnal variation is generally not possible for deep sea survey work, unless a recording 'base', such as a moored buoy, is situated within the vicinity of the survey area (Cann & Vine 1966). A common practice is to show a

sequence of K-indices (Bartels 1957), from the nearest land station, alongside the recorded magnetic profiles, giving an indication of the uncertainty of the plotted magnetic field.

3.3 Long Wavelength Components within the Magnetic Anomaly and the Removal of a Regional Gradient

The influence of long wavelength components within the magnetic anomaly, on magnetization distributions resulting from the direct interpretation of oceanic magnetic profiles, may be shown by the following considerations (Bott - personal communication):

Consider a simple surface density distribution $\sigma(x)$ of sine waveform and wavelength λ given by:

$$\sigma(x) = \sigma_0 \sin \left(\frac{2\pi x}{\lambda} \right) \tag{7}$$

situated at an arbitrary depth, the z axis being directed vertically downwards. Then the gravitational anomaly produced at a height z above this plane follows from the appropriate particular solution of Laplace's equation:

$$\Delta g(x) = 2\pi G \sigma_0 \sin \left(\frac{2\pi x}{\lambda} \right) e^{\frac{-2\pi z}{\lambda}} \tag{8}$$

where G is the gravitational constant.

Using Poisson's relationship between gravity and magnetic potential and adopting the formulation of Bott (1969b) the magnetic anomaly (A) due to any two-dimensional body may be related to the derivatives of the corresponding gravity anomaly so

$$A = \frac{|J|}{G\sigma} \left(\sin B \frac{d}{dx} (\Delta g) - \cos B \frac{d}{dz} (\Delta g) \right) \tag{9}$$

The quantity B represents an angle which incorporates both the direction of magnetization and the direction in which the observed

magnetic anomaly is measured, within the x - z plane (Bott 1969b).

Applying (9) to the case of an infinite sheet (8) we obtain

$$A(x,0) = \frac{1}{\lambda} 4\pi^2 |J| e^{\frac{-2\pi z}{\lambda}} \sin\left(B + \frac{2\pi x}{\lambda} \right) \qquad (10)$$

This expression gives the magnetic anomaly caused by a two-dimensional sinusoidal distribution of magnetization at a depth z. The angle B represents a phase difference between the magnetic anomaly and the magnetization distribution. From (10) the amplitude of the magnetization distribution, required to cause a given fourier component of the magnetic anomaly, will be directly proportional to both the amplitude and wavelength of the anomaly component. Thus the influence on computed magnetization values becomes progressively more acute for longer wavelength components within the magnetic anomaly.

This may be demonstrated by considering the magnetization distributions required to explain two theoretical sinusoidal magnetic anomalies; one of short wavelength and the other of long wavelength, both of which have a 15 gamma amplitude (Fig. 3.2). The intensity values computed from these anomalies, using the Linear Inverse technique, for a horizontal source layer situated at unit depth, are shown in Fig. (3.2). The distribution of magnetization obtained from the short wavelength anomaly (Model 1), almost exactly explaining the observed values, shows that variations in intensity of the order of 0.0004 e.m.u./cm^3 are required. A more symmetrical pattern would perhaps be expected if truncation errors at the ends of the profile could be eliminated. The distribution of magnetization obtained from the long wavelength anomaly (Model 2), again almost exactly explaining the anomaly, reveals much larger variations ($\sim$ 0.002 e.m.u./cm^3). Clearly features of interest, over local sections of a given magnetic

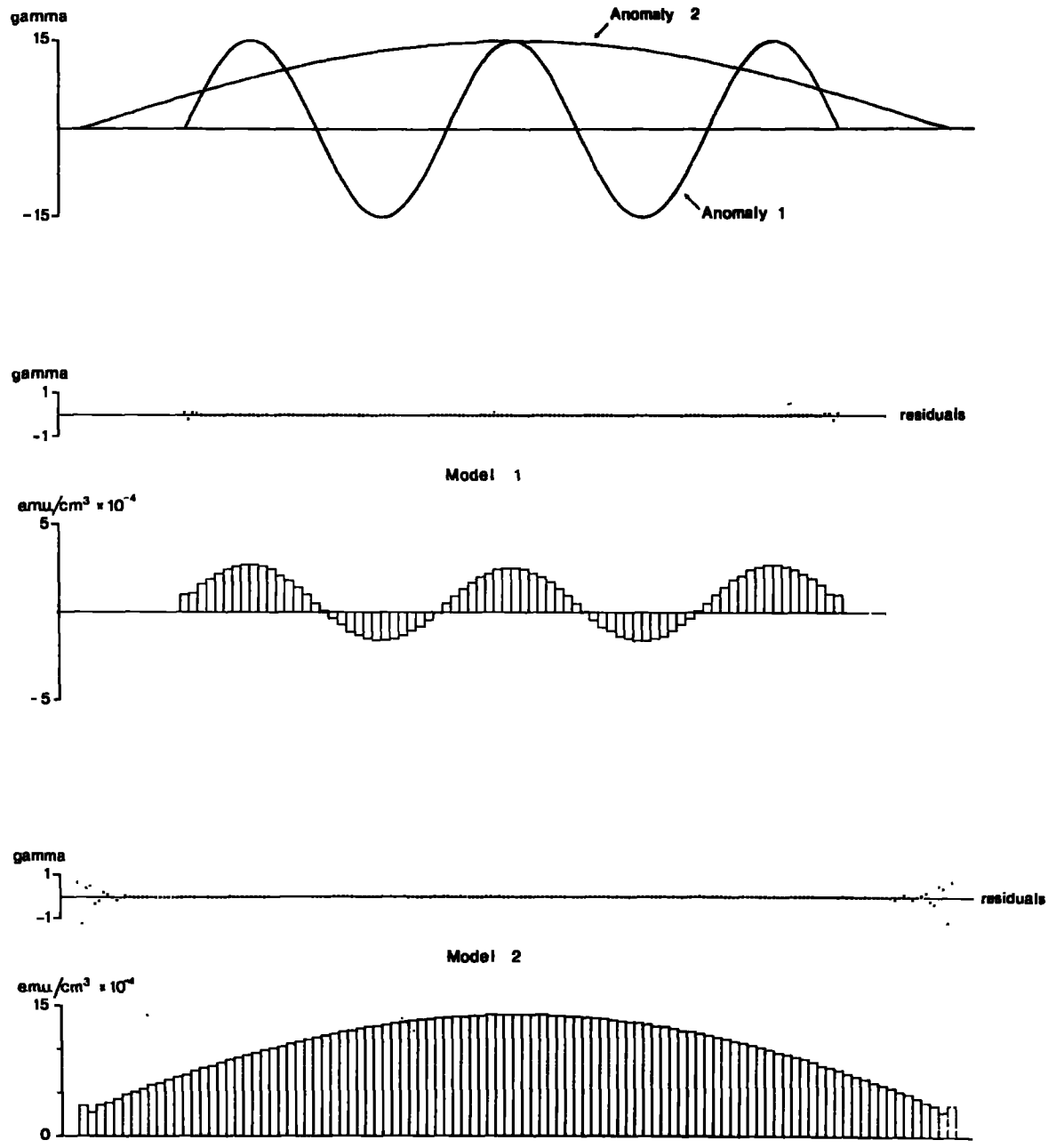

Fig. 3.2 Computed distributions of magnetization required to explain two theoretical sinusoidal magnetic anomalies, one of short wavelength (Model 1) and one of long wavelength (Model 2).

profile, may be seriously masked by the effects of such long wavelength components and some form of filtering will be desirable.

A practical example of the above situation may be seen from two possible interpretations of a magnetic profile observed in the Norwegian Sea (profile B-B, Fig. 5, Avery et al 1968). Initially a linear regional gradient, using the method of least squares, was subtracted from the total field values. The resulting anomaly values (Fig. 3.3) were then used to compute a magnetization distribution for a horizontal layer located between 4.2 and 7.2 km. These depths are based on seismic refraction measurements carried out in the Norwegian Sea by Ewing & Ewing (1959). The model blocks used are 3.2 km wide.

The magnetization values computed initially from the anomaly curve are shown in Model 1, Fig. 3.3. These results show a long wavelength component superimposed on the basic pattern. The principal long wavelength components within the magnetic profile were then determined by Fourier methods (Appendix 4) and the resulting trend is shown by a dotted line on the anomaly profile. This trend was then removed from the magnetic profile and a re-interpretation carried out. The magnetization distribution evaluated for this second case is shown in Model 2. The removal of these long wavelength components from the anomaly profile has clearly improved the overall definition of the short wavelength features within the magnetization distribution.

It is thought that such long wavelength fluctuations in magnetization are most probably not of crustal origin. These features would imply a systematic variation in crustal magnetization, extending over hundreds of kilometres, masking the record of polarity changes in the earth's magnetic field established through the process of sea-floor spreading. A suitable process capable of forming such broad scale

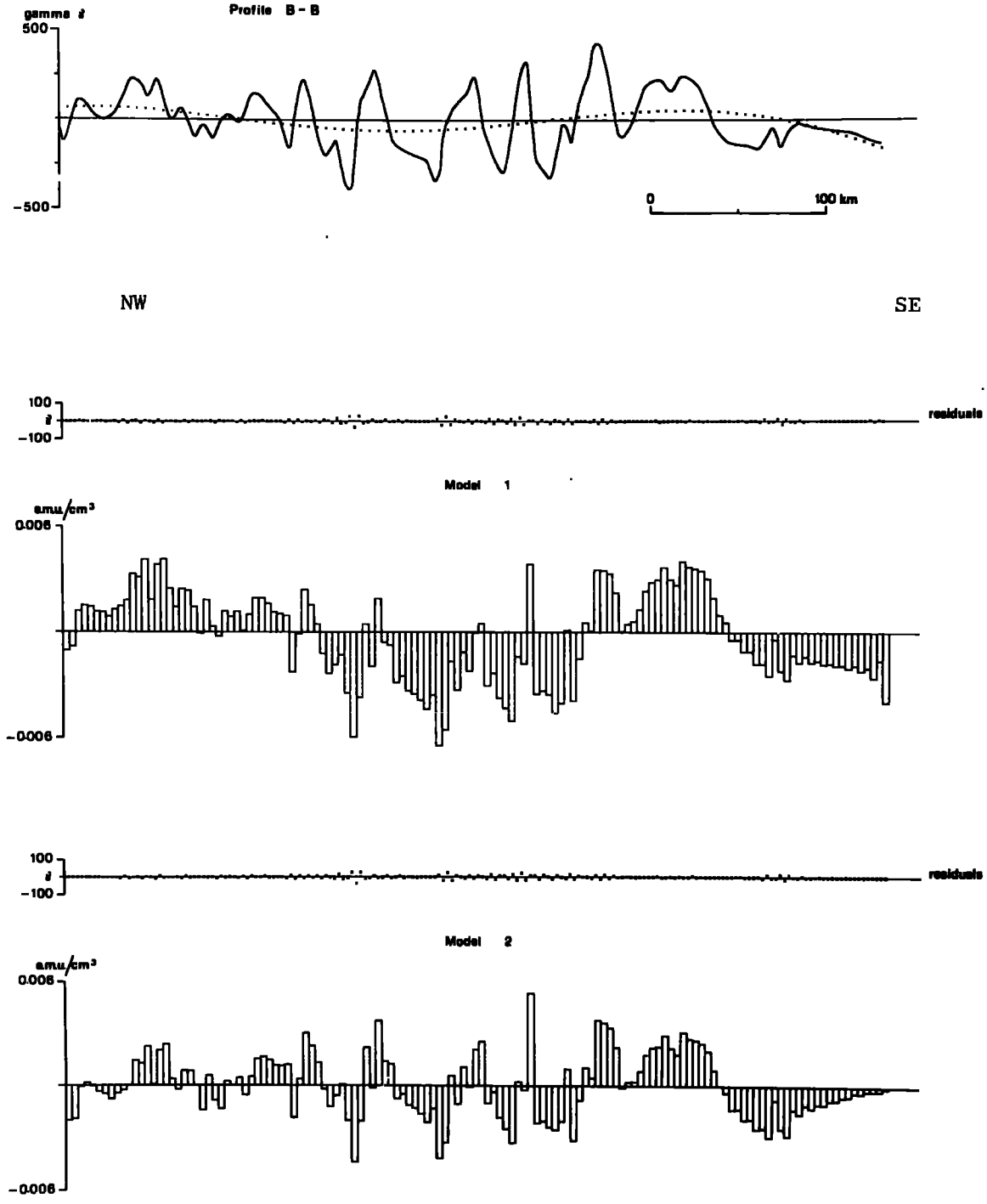

Fig. 3.3 Interpretation of the magnetic profile (B-B), across the Norwegian Sea, in terms of an underlying distribution of magnetization.

changes in the bulk magnetization of the crust is difficult to envisage. More plausibly, long period components of the diurnal variation could introduce long wavelength features into the recorded magnetic profile. Such features would then simply explain apparent long wavelength fluctuations in magnetization. This analysis emphasizes the importance of obtaining accurate magnetic observations for quantitative interpretation. The qualitative mapping of oceanic magnetic anomalies is not subject to this problem and no correction is generally made for diurnal variation.

The removal of a regional trend from marine magnetic surveys has almost always been a rather arbitrary process (Bullard 1967). A general procedure has been to fit a suitable mathematical function, such as a low order polynomial or fourier series, to the observed data. However, with increased survey data becoming available a recent development has been to define a world reference field in terms of a series of spherical harmonics (Cain et al 1965; Anon. 1969). The consistent use of such a standard reference field would allow an immediate comparison of magnetic anomaly maps from adjacent survey areas.

Single oceanic magnetic profiles require a slightly different form of treatment as such traverses are generally widely spaced and are often of a reconnaissance nature. The latest spherical harmonic analysis of the main geomagnetic field (Anon. 1969), though an excellent first estimate, may still not provide a regional background suitable for quantitative interpretation. The effect of a misplaced regional level, on magnetization distributions resulting from the direct interpretation of oceanic magnetic profiles, will be to produce unrealistic large-amplitude values of magnetization and/or introduce spurious long period fluctuations.

When dealing with single magnetic profiles extending over hundreds of kilometres it has been found convenient to adopt the following standard procedure. An initial and generally adequate approximation to the regional magnetic field is obtained by removing, by the method of least squares (Appendix 3), a linear gradient from the total field observations. However, for a given profile of length L, fourier components of maximum wavelength 2L, may still remain within the resulting anomaly profile particularly because of diurnal variation. From earlier considerations such long wavelength components may mask the true polarity of individual magnetization values and obscure true long wavelength variations in magnetization. Low order fourier components, representing these long wavelength features, are therefore removed from the magnetic anomaly profile prior to final interpretation (Appendix 4). This general procedure has been found to be consistently satisfactory in the present work.

3.4 The Resolution of Short Wavelength Magnetic Anomalies

Since magnetic measurements at sea are taken at or above the surface of the sea and several kilometres above the ocean floor, local magnetic anomalies will always be smoothed and attenuated. If we consider a two-dimensional magnetic anomaly of amplitude A and wavelength λ, then this may be expressed as a particular solution of Laplace's equation in the following form:

$$\phi(x) = A \sin\left(\frac{2\pi}{\lambda} x\right)$$

where x is the horizontal co-ordinate.

Providing no magnetic material is encountered, the magnetic anomaly at depth z is given by:

$$\phi_z(x) = A \sin\left(\frac{2\pi}{\lambda} x\right) e^{\frac{2\pi}{\lambda} z}$$

If $z = \lambda/2$ the amplitude for $\phi_z(x)$ is increased by a factor of e^{π} (= 23.2), and if $z = \lambda$ by a factor of $e^{2\pi}$ (= 538), (Bott & Stacey 1967). Hence, when any form of downward continuation is attempted, unless a smoothing function is introduced, the resulting amplification of short wavelength components within the magnetic anomaly rapidly causes problems in stability.

The Linear Inverse technique is essentially the downward continuation of a field subject to Laplace's equation and the formation of an equivalent layer. In practice an incipient 'instability' or oscillation, within the computed values of magnetization, rapidly becomes apparent when block widths less than about 0.6-0.5 times the depth to the top of the model are chosen, assuming an adequate digitization of the magnetic anomaly. The reality of this effect is directly dependent on the accuracy of the short wavelength components within the reduced observations, and the validity of the model used. This form of interpretational procedure therefore imposes a practical limitation, because of errors of observation, on the model block width that may be satisfactorily resolved at a given depth. When applying the Linear Inverse technique it is therefore important to select an adequate block width for the model which properly balances resolution against stability (Bott & Hutton 1970a; Emilia & Bodvarsson 1970).

This limiting situation may be demonstrated by considering the magnetization distribution required to explain a single 'error' anomaly of one gamma for several model configurations. Fig. 3.4 A shows the model used - a horizontal layer formed by equal sized rectangular blocks, with a magnetic anomaly of one gamma at the centre of the model and zero elsewhere. Anomaly points are located

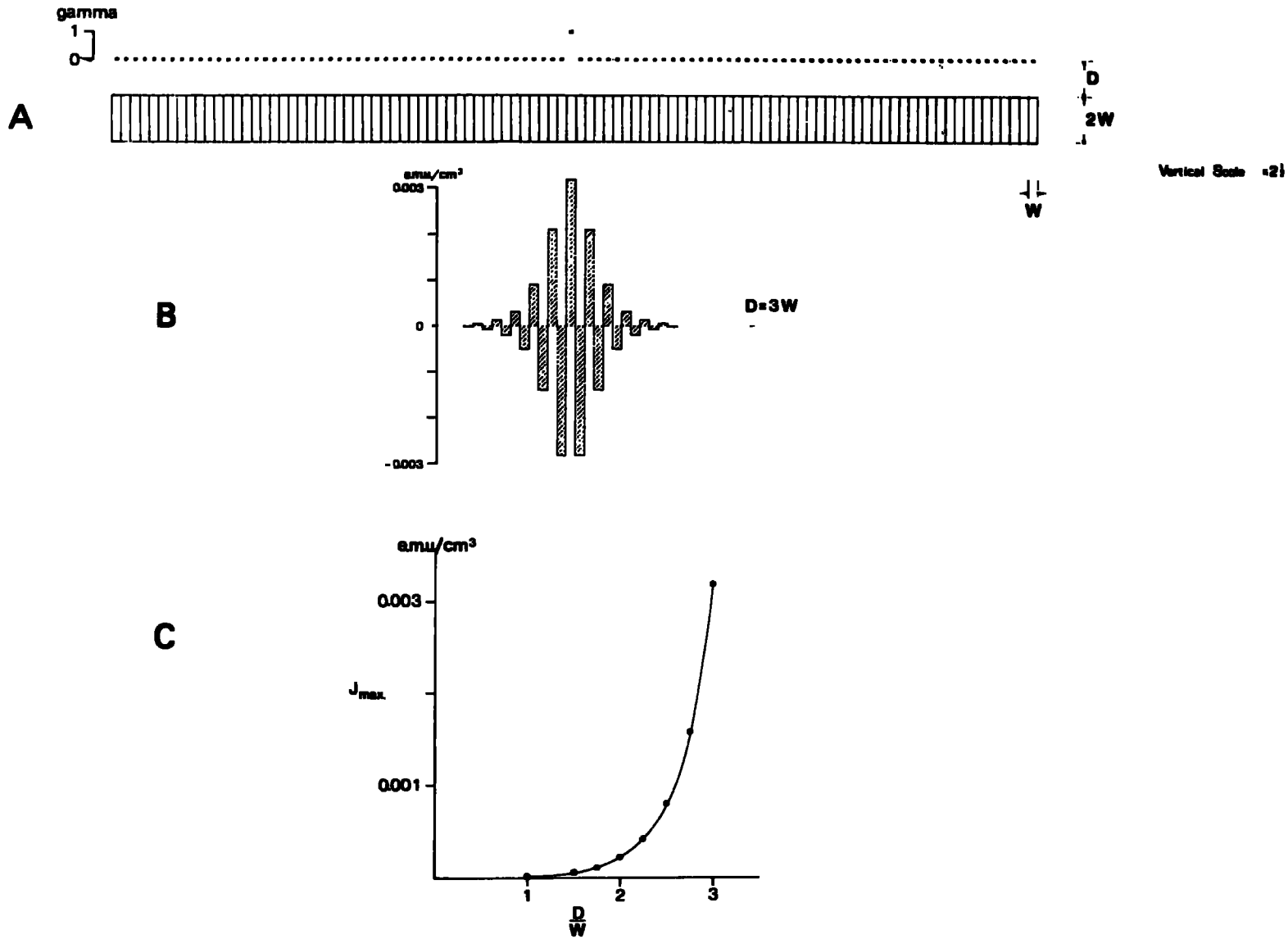
gamma
1
0
A
D
2W
Vertical Scale =2
W
B
emu/cm³
0.003
0
-0.003
D=3W
C
emu/cm³
0.003
$J_{max.}$
0.001
1
2
3
D/W

above the centre of each block. The dip of the earth's field is assumed to be 60^{o} and the profile is east-west. Fig. 3.4 B shows the typical pattern of oscillating magnetization values resulting from these experiments, scaled for the particular condition D/W = 3. The maximum value of magnetization occurs at the block beneath the one gamma anomaly, giving a maximum peak-to-peak fluctuation between adjacent blocks of 0.006 e.m.u./cm^{3}. A plot of this central value of intensity of magnetization as a function of the value D/W is shown in Fig. 3.4 C. The maximum peak-to-peak fluctuation is almost twice the plotted magnetization. This diagram clearly shows that values of D/W greater than about 2 produce unacceptably large fluctuations in the values of magnetization between adjacent blocks. Hence, when dealing with magnetic observations of one gamma accuracy, obtained over a magnetic layer at 3 kilometres depth, a realistic value for the minimum strip-width detectable at the sea surface is about 1.5 kilometres. If errors of observation exceed one gamma then the ratio D/W should be chosen to be less than 2. However, a value of D/W less than one would produce relatively large residuals between the chosen field-points and hence potential information from the magnetic profile would be ignored. Similar results and conclusions (not shown) have been obtained by the use of suitable random error values, distributed along the entire length of the model.

The Vine-Matthews hypothesis predicts that oceanic magnetic anomalies associated with the mid-ocean ridge system represents a record of the history of reversals of the earth's magnetic field. This information supplements and extends the radiometric time scale for geomagnetic reversals as established by Cox et al (1968). The application of the Linear Inverse technique to such oceanic magnetic anomalies directly evaluates this polarity pattern and permits a

precise description of the magnetization variation within the oceanic crust. However, the practical limitation in possible resolution directly controls the minimum geomagnetic polarity event discernible from oceanic magnetic anomalies. Clearly magnetometer measurements made close to the sea floor will reveal shorter wavelengths and higher amplitudes than are observed at the sea surface (Luyendyk et al, 1968). The interpretation of such data in terms of a variable magnetization distribution will then allow the use of much narrower block widths - of the order of 500 metres (Luyendyk 1969).

These resolution estimates also have a direct bearing on the accuracy of rates of crustal spreading determined from oceanic magnetic anomalies. Le Pichon (1968) suggests that the precision of such determinations is probably not better than about $\pm$0.1 cm/yr. Dickson et al (1968) noted that the probable error in the spreading rate for the Vema 20 profile in the South Atlantic is of the order of $\pm$0.2 cm/yr. This estimate is based on the assumption of a linear spreading rate out to anomaly No. 5 (Heirtzler et al 1968). These errors are mainly introduced from the difficulty of defining optimum polarity reversal boundaries from model studies (Johnson 1969). Direct methods allow a more precise definition of possible reversal boundaries ($\pm$ W/2) - although these positions are still subject to navigational uncertainty.

CHAPTER 4

MAGNETIC PROFILES IN THE NORTH ATLANTIC OCEAN

4.1 Introduction

Over the last decade a number of magnetic surveys have been carried out in the North Atlantic, particularly by the U.S. Naval Oceanographic Office. Numerous isolated magnetic profiles across the mid-Atlantic ridge have revealed a systematic magnetic pattern associated with the ridge system and a characteristic, large amplitude anomaly over the ridge crest (Heezen 1953; Ewing et al 1957; Keen 1963; Heirtzler & Le Pichon 1965). On approaching the continental rise a distinctive magnetic boundary is noted parallel to the continental shelf (Heirtzler & Hayes 1967). This boundary separates typically oceanic magnetic anomalies from a smooth undisturbed region, the so called 'quiet-zone', that extends up to the continental shelf. Recent areal magnetic surveys in the North Atlantic (Heirtzler et al 1966; Godby et al 1968; Avery et al 1968; Avery et al 1969) have confirmed the existence of extensive 'Pacific-type' (Mason & Raff 1961; Raff & Mason 1961) oceanic magnetic lineations, associated with the ridge system; and have provided impressive support for the theory of sea-floor spreading.

The interpretation of magnetic profiles across the mid-Atlantic ridge has been carried out almost exclusively in terms of the Vine-Matthews hypothesis of sea-floor spreading. Pitman & Heirtzler (1966), Vine (1966) and Talwani et al (1968) have calculated ocean-floor spreading rates of about 1 cm/yr/limb at the Reykjanes Ridge. Phillips (1967) and Phillips et al (1969) have found similar, though somewhat ambiguous, rates of spreading of about 1.25 cm/yr/limb at 27^{o}N and

near 43°N, respectively. In both areas these authors conclude that the magnetic profile data indicates a slowing down in spreading around 4-5 m.y. B.P., assuming no major error in the reversal time scale used. Loncarevic & Parker (1970) suggest that magnetic data from 45° - 45.5°N correlates well with a magnetic model spreading westwards at 1.25 cm/yr and eastwards at 1.1 cm/yr.

Bullard et al (1965) and Le Pichon (1968) have demonstrated respectively that; the fit of the continents bordering the Atlantic, and ocean-floor spreading rates and fracture zone trend data from the North Atlantic, are consistent with the idea of Eurasia and Greenland-America moving apart, as rigid plates, about a common pole of rotation. There is now a large amount of observational evidence supporting the general theory of continental drift and sea-floor spreading in the North Atlantic Ocean. Relevant geophysical literature for this general area is extensive. Summaries are given by Ewing & Ewing (1959), Nafe & Drake (1969) and Allen (1969).

4.2 The Mid-Atlantic Ridge at 45°N

4.2.1 The Profile Data

During June and July 1968 the author accompanied an oceanographic cruise on C.S.S. HUDSON to the mid-Atlantic ridge near 45°N. This section describes the interpretation of three combined magnetic and bathymetric profiles obtained across the crestal zone of the ridge system (Loncarevic - private communication). The data was collected by the Atlantic Oceanographic Laboratory, Bedford Institute, Canada, as part of their special study programme for this area of the mid-Atlantic ridge (Loncarevic et al 1966). The three profiles considered are situated to the north east of the main survey area (Loncarevic & Parker 1970). These traverses cover an east west distance of about

300 km and a north south distance of 37 km, their location with respect to the axis of the mid-Atlantic ridge is shown in Fig. (4.1). Navigational control for the survey was established by a satellite navigation system (Aumento & Loncarevic 1969). The bathymetric contours of Fig. (4.1) are based on information compiled by the National Institute of Oceanography England, at a scale of 1:1000000. The black dots mark U.S.C.G.S. earthquake epicentres (1963-1968) made available from the U.K.A.E.A. data bank.

The three profiles, Fig. (4.2), were recorded on approximately east west courses and for the purpose of two-dimensional interpretation have been projected at right angles to the local ridge axis. Detailed contour maps for this general area (Loncarevic - private communication) confirm a linear pattern of magnetic and bathymetric features elongated parallel to the median valley, with an approximate trend of 019°. The bathymetric profiles were constructed from corrected soundings (Matthews 1939) made at five minute intervals at an approximate speed of ten knots. The magnetic observations were not corrected for the diurnal variation of the earth's magnetic field, though observatory records from Bedford Institute, Canada (Srivastava 1969) were inspected for magnetic storms. None were evident during the survey period. The magnetic readings used for interpretation were taken at two minute intervals. For each profile, anomaly values were computed by subtracting a linear regional gradient, using the method of least squares, and then removing the principal low order fourier components (section 3.3).

The recorded magnetic anomaly profiles, shown in Fig. (4.2) as a continuous line, reveal anomalies ranging in amplitude from 100 to 300 gamma with widths of 10-30 km. These profiles show correlatable features, although the small scale detail from profile to profile is

Fig. 4.1 General bathymetry of the Mid-Atlantic Ridge near 45°N, showing major morphological features and the location of magnetic profiles used for interpretation.

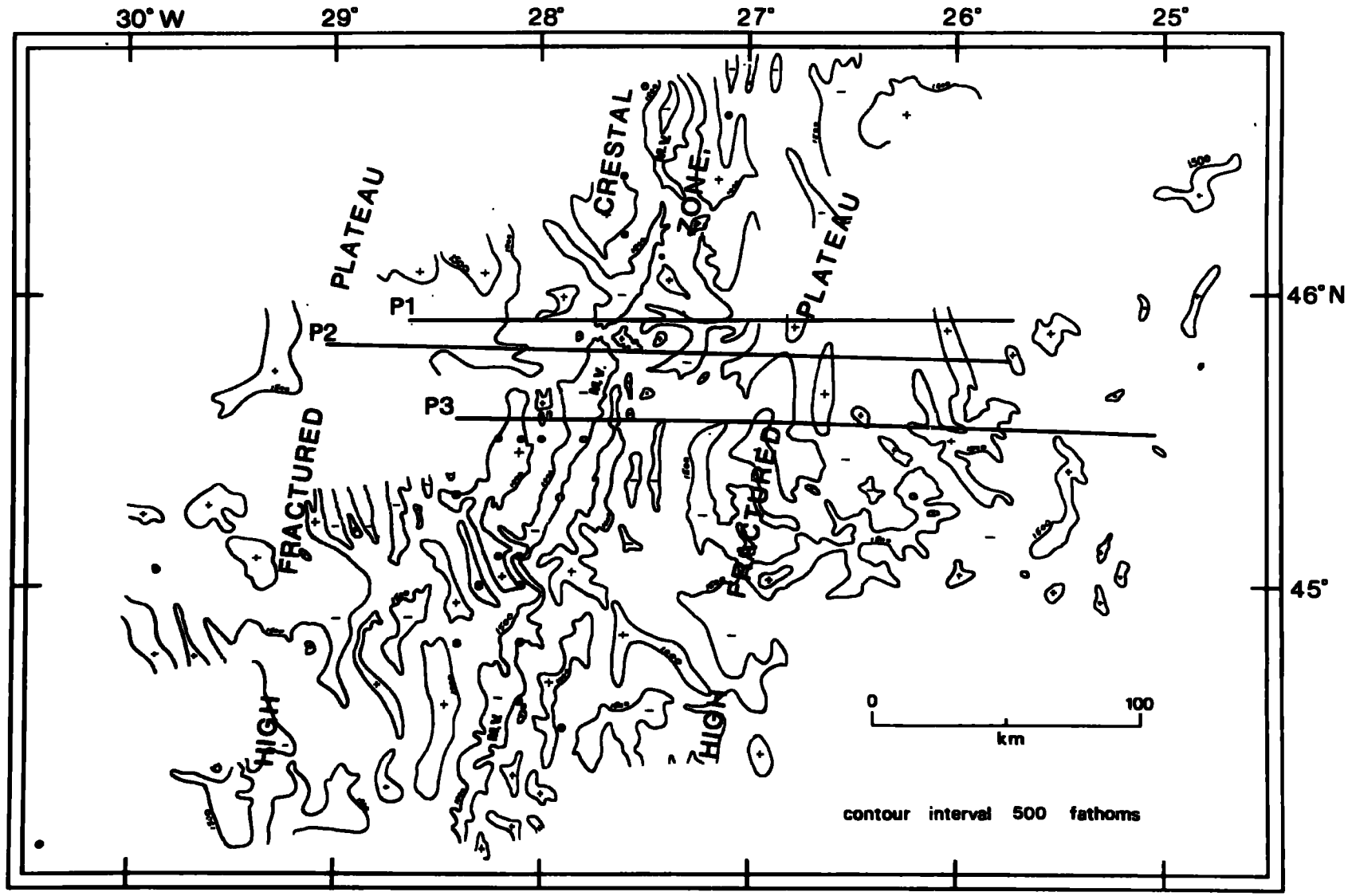

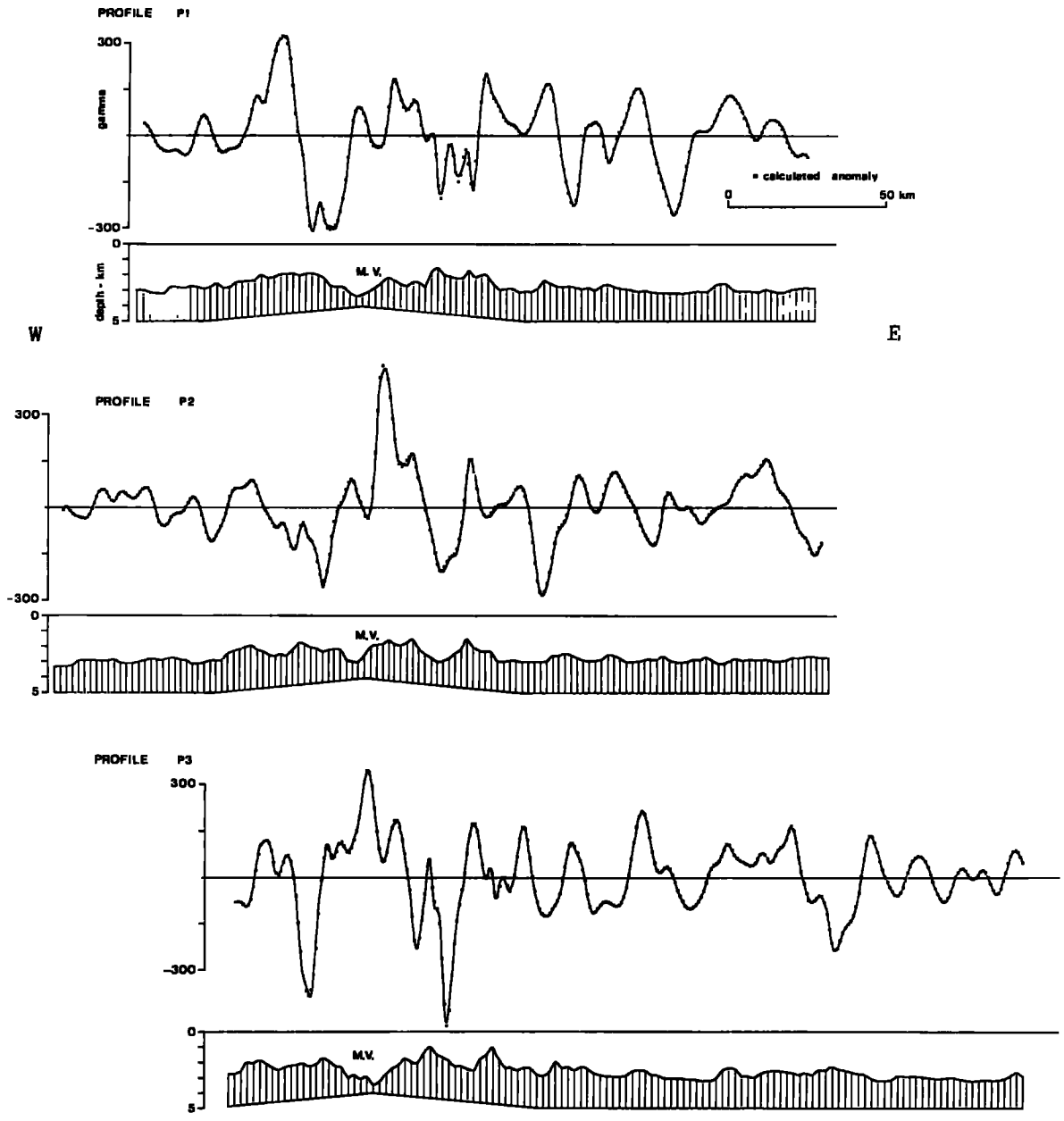
PROFILE P1
300
gamma
-300
= calculated anomaly
0
50 km
0
depth - km
M. V.
5
W
E
PROFILE P2
300
-300
0
M.V.
5
PROFILE P3
300
-300
0
M.V.
5

variable. Certain general features can be recognised at approximately the same distance from the ridge axis on all profiles, although a symmetrical pattern is not readily apparent. A distinctive composite positive magnetic anomaly is associated with the area of the median valley (m.v.) though, in Profile P1, the amplitude of this feature is comparatively reduced. The apparent absence of a large magnetic anomaly associated with the median valley of the mid-Atlantic ridge at this point and further to the north has been noted by Hill (1960) and Loncarevic et al (1966).

The bathymetric record for each traverse reveals an average depth of 2-3 km and shows a rough topography particularly near the median valley area, where changes in relief of the order of 1 km or more occur. Loncarevic et al (1966) report that this crestal topography appears to represent a series of ridge and trough-like features trending sub-parallel to the median valley. Also many of the minor bathymetric features, seen in en echelon pattern, have a general elongation of about 4:1. Away from the Crestal Mountains towards the High Fractured Plateau (Heezen et al 1959) the bathymetric relief appears more subdued, individual features are more isolated, and contour information suggests a weakly orientated relief pattern. Sedimentary deposits are known to gradually increase in thickness away from the ridge crest (Keen & Manchester 1970) and this may be responsible for the more gentle relief.

4.2.2 Interpretation

Because of the general lack of sediment (Ewing et al 1964; Keen & Manchester 1970) and the jagged bathymetric relief observed over the mid-Atlantic ridge in general, it has been assumed that the recorded bathymetry for each profile represents the upper surface of Layer 2 i.e. the adopted magnetic layer. Detailed dredging and bottom photography within the main survey area (Aumento 1968; Aumento & Loncarevic

1969) support this view by revealing basement rock abundantly exposed on the sea-floor with only slight sediment cover. Allowance for this highly uneven sea-floor relief should considerably improve the reliability of the resulting magnetic interpretation (cf. Vogt & Ostensjo 1966). The form of the lower surface of Layer 2 is not known. It is assumed to be located at a depth of about 2 km below the sea-floor, rising slightly at the ridge axis. This is in accord with general refraction results obtained in the North Atlantic (Le Pichon et al 1965).

In each profile the adopted model for Layer 2 was then subdivided into a large number of vertical, adjacent trapezia each assumed to be uniformly magnetized in the direction of the earth's average geocentric dipole field. The Linear Inverse technique was then used to estimate directly the variation in magnetization, within this layer, required to explain the observed magnetic anomaly profiles. Details of the model specifications are set out in Table II, for all three profiles the least squares version of the interpretational method was used.

In each case the observed anomaly profile was almost exactly explained in terms of the assumed magnetic source and a sequence of variable magnetization values. When the theoretical magnetic anomaly profiles (shown as dotted lines in Fig. 4.2), computed from the evaluated distributions of magnetization, are compared with the actual observed profiles no residual value exceeds 28 gamma. The low R.M.S. values emphasize that residual values are appreciably less than this amount, generally being of the order of a few gamma. This accurate simulation of the magnetic profile data is principally due to the optimum block-width value chosen for the magnetic layer. This value of about 2 km permits a good fit of the details of the observed anomaly and avoids excessive amplification of short wavelength components

TABLE II

Specification of Data Points used for the Interpretation of Magnetic Profiles observed at 45°N.

	No. of digitized magnetic anomaly points	*Average sampling interval for magnetic anomaly (km)	No. of model blocks forming the magnetic layer	*Average width of model blocks (km)	Average bathymetric depth (km)	Overall length of projected profile (km)	Maximum residual value between observed and calculated anomaly (gamma)	R.M.S. residual value (gamma)
Profile (P1)	263	0.8	107	2.0	2.67	210	28	± 5
Profile (P2)	315	0.77	128	1.9	2.67	241	26	± 4
Profile (P3)	311	0.8	125	2.0	2.56	249	27	± 5

* The linear distribution of data points along the profiles varies slightly with the speed of the ship.

within the data (section 3.4). Larger residuals would be expected when dealing with steeper magnetic gradients, such as those observed near the crest of the Reykjanes Ridge, and/or with less accurate data points.

The distributions of magnetization computed from the observed magnetic anomalies are shown in Fig. (4.3). These distributions reveal systematic variations in the intensity of magnetization in a direction perpendicular to the strike of the median valley. Each histogram shows groupings of values of approximately equivalent magnitude and sign, separated by comparable sets of values of reversed sign. The boundaries between adjacent groups are marked by fairly abrupt changes in magnetization, generally of the order of 0.002-0.003 e.m.u./cm^3.

For all three profiles there is a distinctive zone of positive magnetization underlying the axial anomaly, within the area of the median valley. On Profiles P1 and P2 these values appear to be associated with bathymetric features observed within the median valley, which probably represent outpourings from two volcanoes which have erupted through the valley sides (Loncarevic et al 1966). For Profile P1 the amplitude of this central group of magnetization values is significantly reduced due to the local decrease in size of the axial anomaly. This reduction may result from some form of local demagnetization associated with the suggested volcanism although the adjacent Profile P2 does not appear to have been affected. Within the axial zones those values of magnetization exceeding about 0.004 e.m.u./cm^3 may be somewhat unrepresentative as the magnetic layer is thinned at these points - due to the topographic valley and the rising base of Layer 2. Whilst these axial zone magnetization values clearly exist as a separate group they do not appear to be significantly larger in amplitude than those associated with the flanking anomalies. This situation is comparable to the

Fig. 4.3 Distributions of magnetization computed from the magnetic anomaly profiles and source models shown in Fig. (4.2).

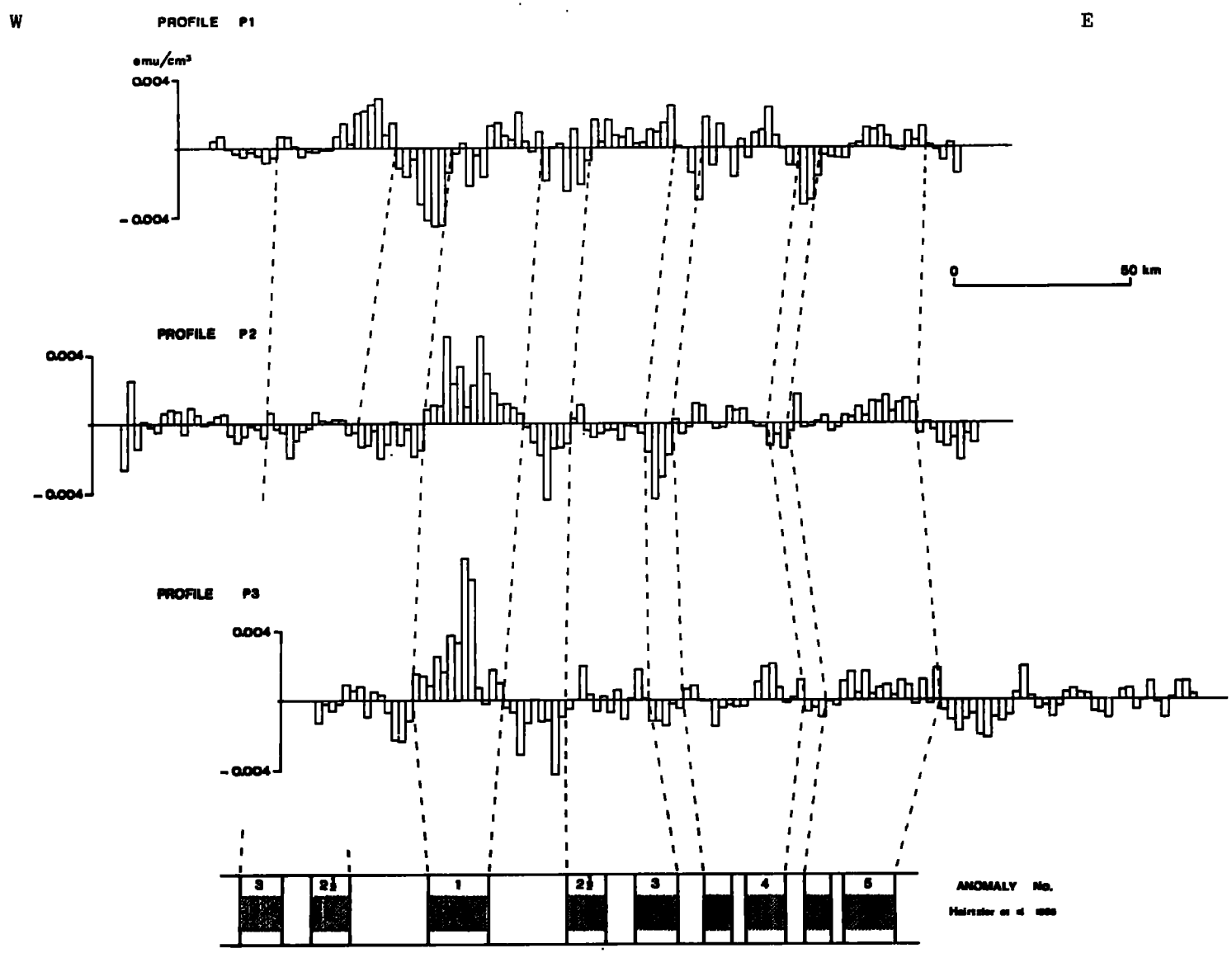

results of other authors (Bott 1967; Emilia & Bodvarsson 1969), although in contrast to results obtained in the Gulf of Aden (Bott & Hutton 1970b).

The positive and negative groups of magnetization shown in Fig. (4.3) have been interpreted in terms of the Vine-Matthews hypothesis of sea-floor spreading and provisionally identified with the sequence of geomagnetic field reversals established by Heirtzler et al (1968). Distinctive reversal boundaries have been traced from profile to profile though certain intermediate polarity transition points are less obvious and have not been identified on all profiles. The correlations indicated suggest an average spreading rate of about 1.2 cm/yr/limb - although this conclusion is biased slightly as the profiles extend mainly to the east of the median valley. The time scale drawn at the bottom of Fig. (4.3) has been scaled for a spreading rate of 1.25 cm/yr/limb.

The identified pattern of sea-floor spreading is not regular or symmetrical in detail. If the rate of spreading was uniform with time along the ridge axis then the correlating lines shown in Fig. (4.3) would be parallel, assuming that the three profiles had been correctly aligned with respect to the axis of spreading. For the three profiles the zone of positive magnetization underlying the axial anomaly is wider than that predicted for a constant spreading rate of 1.25 cm/yr/limb and comparable variations may be noted at a number of other points. Loncarevic & Parker (1970) suggest that between 45^{o}N and 45.5^{o}N, spreading rates deduced from a statistical sumation of magnetic profile data are 1.28 cm/yr to the west and 1.10 cm/yr to the east. These estimates have been obtained using the indirect method of interpretation and are based on rates of spreading that are assumed to be constant in time. It is to be noted that the three profiles considered in the present work are situated to the north of latitude 45.5^{o}N and represent a small fraction of the total information (some 50,000 data points)

considered by Loncarevic and Parker in their analysis.

Aumento (1969) has suggested that a variable rate of sea-floor spreading is indicated for this general area mainly on the basis of radiometric ages determined from dredge samples. His calculated spreading rates fall into two distinct groups: a faster rate on the Crest Mountains (average 3 cm/yr/limb); and a slower rate on the High Fractured Plateau (average 1 cm/yr/limb). Loncarevic & Parker (1970) have commented in detail on age discrepancies between dates predicted from magnetic anomalies and those from the radiometric work (Aumento 1969). Loncarevic & Parker favour a hypothesis explaining the occurrence of 'anomalous' young ages but find difficulty in explaining certain older dates located within a zone predicted to be younger from the magnetic evidence. This conflict has not yet been resolved, the situation is complicated by problems encountered in determining accurate K-Ar dates for young rocks (e.g. Noble & Naughton 1968).

The correlations shown in Fig. (4.3) indicate a locally variable rate of ocean-floor spreading and to some extent support the ideas of Aumento (1969) in that there appears to have been a faster (2 cm/yr/limb) rate of spreading over the last 0.7 million years. A plot of the identified reversal boundaries against distance from the ridge axis suggests that over a period of 10 million years the average spreading rate normal to the ridge axis was 1.25 cm/yr/limb. Away from the ridge crest this value varies between 1.1 to 1.3 cm/yr/limb. This discussion assumes that the geomagnetic time scale established by Heirtzler et al (1968) is essentially correct and that reversal boundaries have been correctly identified.

During the course of the Atlantic Oceanographic Laboratory's study of the mid-Atlantic ridge between 45^{o}N and 46^{o}N a number of dredge hauls,

yielding rock samples, have been carried out in the area, spaced from 150 km west to 70 km east of the median valley. The bulk of the rock material gathered was basalt. Irving et al (1970) report that palaeomagnetic results from 27 dredge hauls (75 samples) indicate that the basalts have a mean remanent magnetization of 92×10^{-4} e.m.u./cm^3, and a mean susceptibility of 0.9×10^{-4} e.m.u./cm^3. The remanence values of basalt vary with distance from the ridge axis. They average about 40×10^{-4} e.m.u./cm^3 on the High Fractured Plateau, about 60×10^{-4} on the Crestal Mountains and then increase sharply towards the median valley where one station gave a value (average of 5 samples) of about 1000×10^{-4}.

The implications of these relatively high remanent magnetization values, assuming no sample bias and no significant vertical variation in magnetization, is that the magnetic layer is considerably thinner than is normally assumed in model work (Irving et al 1970; Carmichael 1970). A number of the sample sites discussed by Irving et al (1970) and Carmichael (1970) are situated about 45°-40'N, mainly over the crestal mountains and extending to the west. This is the approximate position of Profile P3 (Fig. 4.1), although this traverse extends mainly to the east. Accepting that the remanent magnetization values are symmetrically representative (cf. Fig. 2, Irving et al 1970), Profile P3 may be used to examine the hypothesis of a thin, highly-magnetized layer constituting the top of Layer 2.

Accordingly this profile was re-interpreted with the Linear Inverse technique, using the known bathymetry as the upper surface of the magnetic layer and an identical surface set at a lower level for the base. A number of models were tested - the magnetic layer was finally modified to represent a layer of constant thickness (0.5 km) except for the median valley area where a thickness of 0.1 km was adopted. This

model was concluded to be most satisfactory in that the computed distribution of magnetization gave good agreement with the values obtained by Irving et al (1970). This estimate assumes that the intensity of magnetization of the measured samples is representative of the whole magnetic layer, since most of the dredge hauls probably came from the top metre of basaltic flows on the sea-floor. A mantling layer of 0.1 km thickness along the complete length of the profile required magnetization values, at the ridge flanks (about 140 km from the ridge axis), to be about 0.02 - 0.04 e.m.u./cm^3, i.e. almost a factor of ten larger than the average values quoted by Irving et al (1970).

Fig. (4.4) shows the magnetic profile used for the interpretation and the theoretical magnetic anomaly computed from the resulting distribution of magnetization. The 'degree of fit' of the computed and observed anomaly is satisfactory; the maximum residual value obtained was 33 gamma with an overall R.M.S. value of $\pm$6 gamma. The computed distribution of magnetization reveals intensity values similar to those obtained by Irving et al (1970) and the interpretation supports the general idea of a thin magnetic layer (Carmichael 1970). The exceptionally large values of magnetization are located fairly closely within the limits of the median valley. Distinctive groups of positive and negative magnetization away from the ridge axis have been correlated with the reversal time scale (Heirtzler et al 1968) in accord with the hypothesis of sea-floor spreading. No significant difference is noted between these correlations and those shown in Fig. (4.3) obtained with a thicker magnetic layer.

The above interpretation demonstrates that a highly magnetic 'upper-Layer 2' can accurately explain the observed magnetic profile and remain consistent with the Vine-Matthews hypothesis of sea-floor

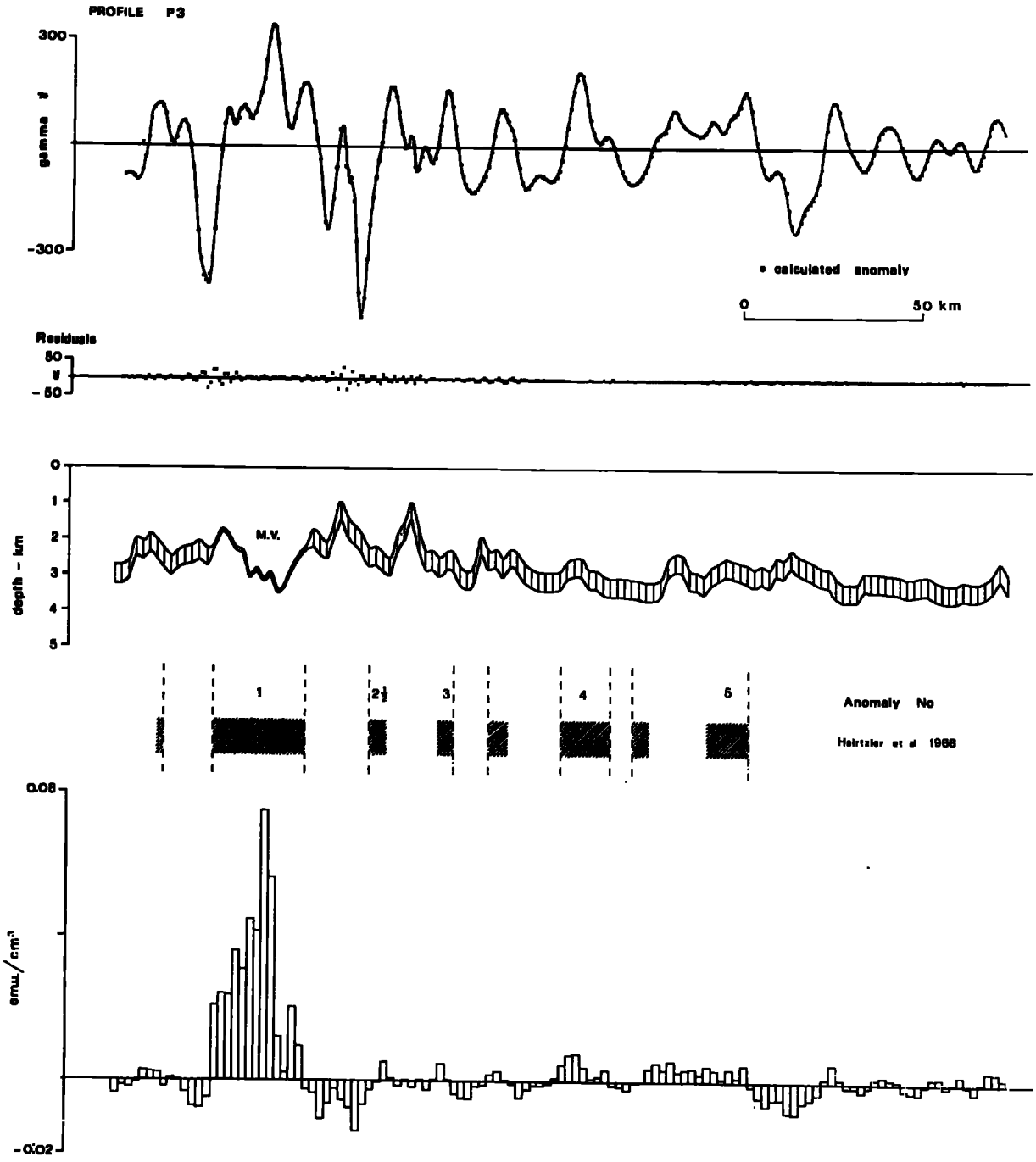

Fig. 4.4 Interpretation of magnetic anomaly profile P3 in terms of a 'thin' magnetic layer.

spreading. Irving et al (1970) suggest that the dramatic local decrease in remanent magnetization intensity, away from the ridge axis, may be due to demagnetization effects resulting from thermal cycling within the narrow, volcanic axial zone. The change in thickness of the magnetic layer away from the median valley, shown in Fig. (4.4), supports this suggestion. The thicker section of the magnetic layer (o.5 km), away from the median valley, would represent lava flows that had been erupted within the median valley and gradually thickened and demagnetized by successive eruptions during the process of sea-floor spreading.

4.3 The Mid-Atlantic Ridge at 60°N

4.3.1 The Profile Data

In September 1967 several shipboard traverses were made across the Reykjanes Ridge at approximately 60°N by the R/V TRIDENT of the University of Rhode Island. The survey operations carried out involved systematic dredging accompanied by bottom photography, seismic profiling and total magnetic field measurements (De Boer et al 1969). A combined magnetic and seismic-profiler traverse obtained in this work has been made available for study (Krause - private communication). This profile extends for about 175 km across the crestal region of the Reykjanes Ridge in a direction approximately perpendicular to the north east strike of the ridge axis. The end points of the profile are located at (60° - 33'N, 30° - 59'W) and (59° - 35.6'N, 28° - 27.8'W).

The Reykjanes Ridge is a continuous north east trending segment of the mid-Atlantic ridge, which extends from latitude 55°N to the Reykjanes Peninsula of south west Iceland. A detailed aeromagnetic survey over the ridge (Heirtzler et al 1966) has revealed a remarkably linear pattern of magnetic anomalies which are approximately symmetric and parallel to the ridge axis. More recent survey work by Godby

et al (1968) and Avery et al (1969) has demonstrated the extension of this magnetic pattern, which is now known to range from the continental slope of Greenland to the western margin of the Rockall Plateau.

At 60°N the observed axial anomaly (Fig. 4.5) has an amplitude of about 1600 gamma and width of about 15 km. The flanking anomalies are smaller in width and have a lower amplitude - generally about 500 gamma. A striking feature of the profile, and of the area in general, are the sharp magnetic gradients recorded. This is particularly noticeable near the axial zone where gradients of the order of 300 gamma/km occur. The average depth of water recorded across the profile is between 1 and 2 km. The crestal zone of the ridge is nearly devoid of sediment and up to about 100 km either side of the axis, sediment thicknesses are a few hundred metres at most (Fig. 1, De Boer et al 1969). The basement surface is therefore somewhat shallower than is observed over other parts of the mid-ocean ridge system and this may partly account for the steep magnetic gradients observed. The general bathymetry of the Reykjanes Ridge has been summarized by Heirtzler et al (1966). The available information indicates a continuous ridge crest, the absence of a median rift and suggests that small local basement features, sub-parallel to the ridge axis, are not greatly continuous beyond a few kilometres.

Unfortunately, magnetograms from the magnetic observatory at Leirvogur, Iceland, revealed a serious magnetic disturbance during the period of the magnetic survey. A computed plot of the total field variation during this disturbance revealed a number of fluctuations of the order of 100 gamma superimposed on a longer period component also having an amplitude of about 100 gamma. A correction for the long period variation has been carried out, although the shorter period

fluctuations have had to be neglected. Magnetic anomaly values shown in Fig. (4.5) were computed by subtracting a linear, least squares regional gradient and the principal low order fourier components, from the total field values (section 3.3).

4.3.2 Interpretation

The acoustic basement, determined from the seismic profiler traverse, has been assumed to represent the upper surface of Layer 2, i.e. the magnetic layer. The form of the lower surface of Layer 2 is not known. Seismic refraction lines in this area (E3, E4; Ewing & Ewing 1959) suggested a crustal structure of 3-4 km of a relatively high velocity basement (5.6-5.8 km/sec) overlying a 7.2 to 7.6 km/sec material, thought to represent altered mantle. However, more recent sonobuoy refraction work on the inner flank of the Reykjanes Ridge (Talwani et al 1968) has demonstrated a 4.5 km/sec velocity material, 1.5-3.5 km thick, overlying a 6.5 km/sec velocity layer. These results suggest that the 5.6-5.8 km/sec layer of Ewing & Ewing (1959) may consist of the two layers of Talwani et al (1968). Layer 2 has therefore been assumed to be approximately 2 km thick, the lower surface rising slightly towards the ridge crest in order to maintain a fairly uniform thickness (Fig. 4.5).

The seismic basement profile was then sampled at an average interval of 0.6 km, yielding 299 points. These points were later combined within the interpretation programme (section 2.3.3) to represent 115 individual model blocks, with an average width of 1.5 km. These model elements were assumed to be uniformly magnetized in the direction of the average geocentric dipole field. The magnetic anomaly profile was digitized at an average interval of 0.8 km yielding 223 values. The least squares version of the Linear Inverse technique was then used to evaluate the distribution of magnetization, within Layer 2,

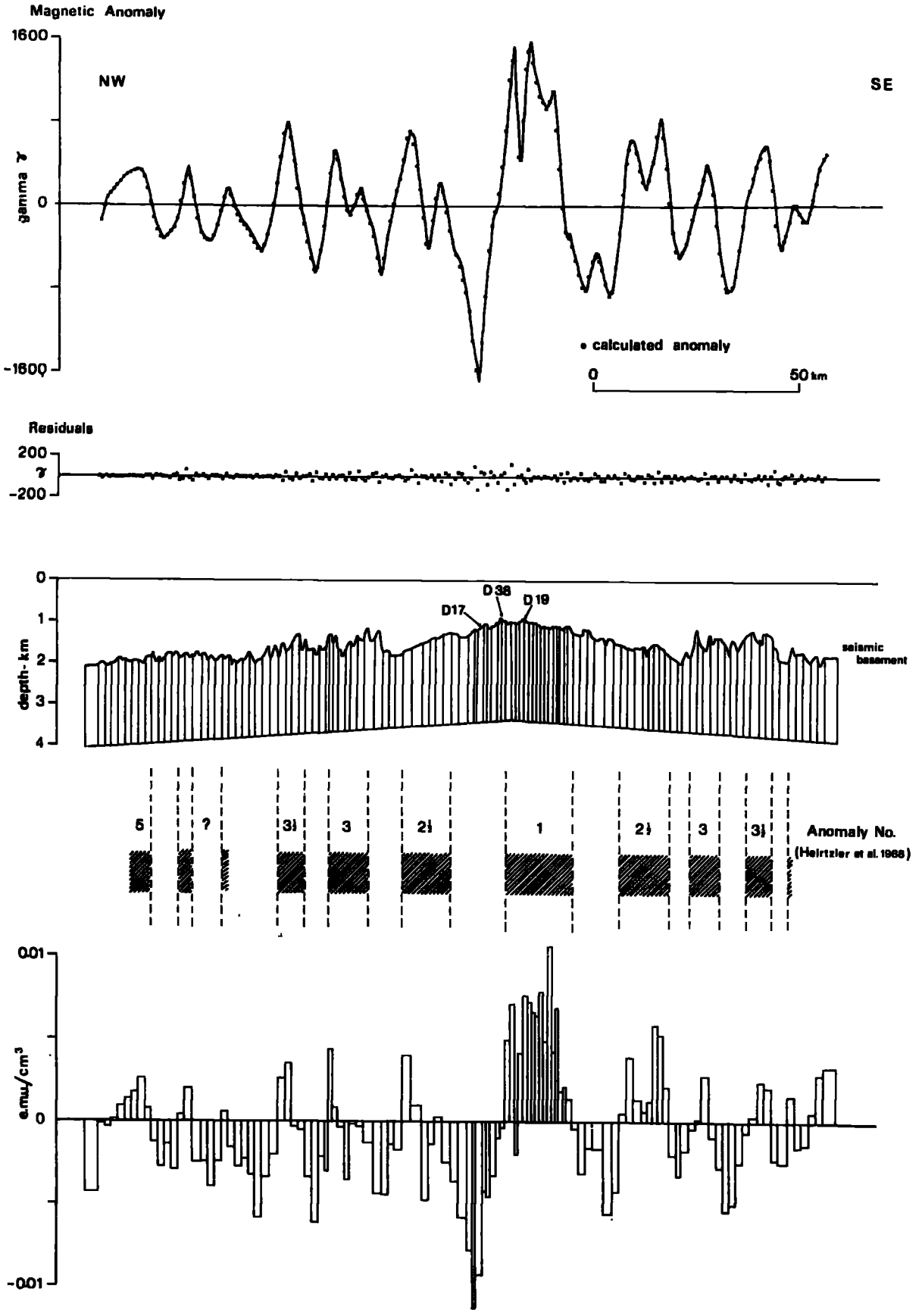

Fig. 4.5 Interpretation of a magnetic anomaly profile across the Reykjanes Ridge.

required to explain the observed magnetic profile.

The resulting interpretation is shown in Fig. (4.5). The theoretical magnetic anomaly computed from the evaluated magnetization distribution is shown by the dotted line. Visually the fit to the observed profile is satisfactory. However, a maximum residual value of 131 gamma is obtained near the ridge crest and the overall R.M.S. value for the profile is $\pm$32 gamma. This degree of fit is not as good as would be expected and reflects a number of problems encountered in the interpretation. From the residual plot it is seen that the largest errors are obtained near the ridge crest and occur particularly over areas of sharp magnetic gradient. The correct form of the anomaly is simulated but small phase errors, due to the arbitrary position of model block boundaries within the magnetic layer, produce relatively large discrepancies between the theoretical and observed magnetic profiles. The upper surface of the magnetic layer is situated within 1 km of the sea surface at the ridge crest. However, optimum model block widths (section 3.4) are difficult to justify because of possible data errors. Variable block widths have been used in the model, particularly near the axial zone where thinner model elements ($\sim$ 1 km) are essential in order to match the extreme magnetic gradients.

The evaluated magnetization distribution reveals a pattern of discrete groups of magnetization associated with the major magnetic anomalies. The zone of positive magnetization underlying the axial anomaly has an average value of about 0.006 e.m.u./cm^3 and is flanked by adjacent negative groups of comparable and greater values of magnetization. This abrupt change in magnetization at the ridge crest is of the order of 0.01 e.m.u./cm^3 and this compares well with a similar value obtained by Godby et al (1968). Similar sharp contrasts in magnetization (0.005 e.m.u./cm^3) occur across the distribution between

adjacent groups of more positive and more negative values. This pattern is in agreement with the Vine-Matthews hypothesis and the major groups have been provisionally correlated with the numbering sequence of reversals of the geomagnetic field established by Heirtzler et al (1968). Distinctive reversal boundaries are not well defined between Anomaly $3\frac{1}{2}$ and 5 on the north west side of the profile. This is partly due to the weak definition of the magnetic anomaly peaks and partly as a consequence of the wide model block widths used. The identified correlations indicate a spreading rate of about 1.0 cm/yr/limb. The reversal pattern is not precisely symmetrical or regular with respect to the ridge axis although the deduced spreading rate does not depart significantly from the range 0.9-1.0 cm/yr/limb.

It is noted that the dredged rock sample (D 17), reported by De Boer et al (1969, Fig. 1) as showing good evidence for reversed polarity, is situated well within the zone of reversed magnetization between Anomaly No. 1 and $2\frac{1}{2}$ to the north west of the ridge axis (Fig. 4.5). Similarly, samples (D 19) and D 38), identified as representing rocks magnetized with a normal polarity, are located within the area of positive magnetization (sample D 38 is probably just within this zone) corresponding to the present polarity epoch.

Recent work by Talwani et al (1968) in this area has demonstrated that a relatively thin ($\sim$ 0.4 km) surface layer of high magnetization (0.01-0.03 e.m.u./cm^3) may be the principal contributor to the magnetization of the oceanic crust. Magnetic profiles parallel to the ridge axis, following the Vine-Matthews hypothesis, entirely within a zone of uniform polarity, were shown to correlate well with small scale variations in basement relief. Talwani et al have suggested that the simplest explanation of this correspondence is that the magnetic anomalies arise largely from the topographic relief of a uniformly

magnetized layer. Approximate two-dimensional calculations, adopting a 'trial and error' process, were used to determine this magnetization contrast. This value was then used to estimate the thickness of the magnetic layer required to satisfy profile data perpendicular to the strike of the ridge.

The profile shown in Fig. (4.5) has been re-interpreted in terms of a magnetic layer 0.5 km thick situated at the top of Layer 2. The resulting interpretation (not shown) gave a satisfactory simulation of the observed profile although the maximum residual value obtained was now 156 gamma with an overall R.M.S. value of $\pm$37 gamma. This slight decrease in 'degree of fit', compared with the initial interpretation (Fig. 4.5), is not considered to be significant. The resulting magnetization distribution revealed a similar pattern to that obtained with the thicker magnetic layer except that significantly larger, both positive and negative, magnetization amplitudes were required (as for Profile P3, Fig. 4.4). The values computed at the ridge crest reached a maximum of 0.035 e.m.u./cm^3 while values associated with the ridge flanks were about 0.01 e.m.u./cm^3. These estimates compare well with those obtained by Talwani et al (1968) and support the hypothesis of a thin highly magnetized upper-Layer 2. Accepting this hypothesis the upper layer is probably not thicker than about 0.5 km since this is the maximum basement relief observed parallel to the ridge axis (Talwani et al 1968).

However, if variations in magnetization exist parallel to the ridge axis, this must be expected to some extent, then the estimated magnetization contrast obtained by Talwani et al may be too large. Similarly, any significant topographic contribution from a lower surface of the magnetic layer would reduce the effective magnetization required. Hence, it is possible that the magnetic layer is thicker than 0.5 km.

This argument is somewhat weakened by recent work (De Boer et al 1970) which describes certain highly magnetic pillow basalts dredged from near the crest of the Reykjanes Ridge (samples D 17, D 38, D 19 and others). The average magnetic intensity, obtained from 15 samples, was 0.05 e.m.u./cm^3, whilst samples recovered from the crestal zone yielded values of 0.05-0.13 e.m.u./cm^3. Further direct computations, for the magnetic profile shown in Fig. (4.5), show that the effective magnetic layer (in the vicinity of the ridge crest) is required to be about 100 metres thick in order to be consistent with magnetization values of the order of 0.13 e.m.u./cm^3.

4.4 Discussion

Magnetic anomalies associated with the mid-Atlantic ridge between the Azores and Iceland appear to fall into two broad types. Those anomalies associated with the Reykjanes Ridge are characterized by a conspicuous axial anomaly and a strikingly linear pattern of large amplitude flanking anomalies (Heirtzler et al 1966). In direct contrast to this situation magnetic profiles obtained between latitudes 42^{o} - 46^{o}N have been described by Phillips et al (1969) and Loncarevic & Parker (1970) as apparently representing a disturbed magnetic pattern and difficult to correlate with normal ocean-floor spreading models predicted from the Vine-Matthews hypothesis. The interpretations shown in Figs.(4.3 & 4.5) take into account the variable magnetic model parameters, in each case, and confirm a significant difference in the magnetic properties of the two areas.

Near 45^{o}N, the statistical treatment carried out by Loncarevic & Parker (1970), on some 50,000 observation points from their survey data, has successfully extracted an 'average' magnetic profile which is more consistent with the pattern predicted from the hypothesis of sea-floor

spreading. This work emphasizes therefore that for this general area there is a relatively high magnetic 'noise-level' superimposed on individual magnetic profiles. The cause of this disturbance is not clear. Matthews & Bath (1967) and Harrison (1968) suggest that dyke-like bodies, responsible for the observed magnetic anomalies, are randomly injected over several kilometres either side of the ridge axis. Loncarevic & Parker (1970) suggest that contamination of 'blocks' of a particular polarity by material of the opposite polarity may then be responsible for the relatively weak definition of the magnetic pattern. However, the rather abrupt magnetization changes noted in Figs. (4.3 & 4.4), and also by other authors (Emilia & Bodvarsson 1969; Bott & Hutton 1970b), indicate narrow transition zones between sections of normal and reversed polarity. This would suggest therefore that contamination by random dyke-injection is not the major source of disturbance of the magnetic pattern.

Alternately, the observed 'noise-level' may be due to the effect of an irregular configuration of the magnetic layer. A significant topographic effect at 45^{o}N from the jagged 'volcanic' relief has already been demonstrated (Fig. 3.1a). Also, if the magnetic layer of this area of the mid-Atlantic ridge is appreciably thinner than that normally expected (Irving et al 1970; Carmichael 1970); then the disturbed magnetic anomaly pattern may be explained by structural disruption of the magnetic layer. Seismic reflection studies indicate the possible existence of block faulting in this area, with faults aligned both parallel to and at right angles to the ridge axis (Aumento 1970). Topographic profiles across this sector of the mid-Atlantic ridge (Heezen et al 1959) support this idea and suggest the existence of a 'basin and range' structural province near the ridge crest. Further north the Reykjanes Ridge is not characterized by a central rift or such mountainous crestal topography.

If this variation in bathymetric relief may be correlated with local tectonic activity away from the ridge crest then this may provide an explanation for the disturbed magnetic pattern observed near $45^{o}N$.

For comparable magnetic models the computed distribution of magnetization, shown in Figs. (4.3) & (4.5), reveal a significant difference in crustal magnetization between $45^{o}N$ and $60^{o}N$. The values obtained over the Reykjanes Ridge are larger and show more abrupt lateral changes. This confirms the findings of Heirtzler & Le Pichon (1965) who noted the apparent departure of observed axial anomaly amplitudes, between 45^{o} - $49^{o}N$, from that predicted from simple model studies applied to the Atlantic as a whole. The reason for this regional difference is not clear. Van Andel (1968) has suggested that low grade metamorphism, associated with recent tectonic activity near the ridge crest, may degrade the effective crustal magnetization at depth. Such a process may be related with the faulting suggested as being responsible for the apparent disturbance of the observed magnetic pattern near $45^{o}N$.

The direct interpretations presented cannot discriminate, in themselves, between a thick ($\sim$ 2.0 km) or thin ($\sim$ 0.5 km) magnetic layer. Good agreement of observed and computed magnetic anomalies was obtained for both models and each represents a plausible solution. The thin magnetic layer suggests that large dyke swarms, extending for several kilometres in depth, may not have a major role in the generation of oceanic crust at mid-ocean ridges. Pillow lava erupted on the sea-floor and subsidiary intrusions could provide the main magnetic source, with a corresponding high intensity of magnetization consistent with the values obtained from recent dredging operations (Opdyke & Hekinian 1967; Irving et al 1970; De Boer et al 1970). Feeder dykes would exist at depth of course.

However, the ambiguity of the situation can only really be resolved by examination of representative rock samples drilled from the ocean floor. Dredged rock samples are almost certainly obtained from the outer margins of lava flows which have chilled extremely rapidly by direct contact with the sea water. During this quenching process the outer margins solidify quickly, producing very fine-grained magnetic particles which are both more intensely and more stably magnetized than the slowly cooled interiors which have larger particles (Nagata 1961). Hence, we may question whether the very large values of remanent magnetization obtained from dredged samples are representative of larger units, within the oceanic crust, which will have cooled more slowly (Cox & Doell 1962). To date, some magnetic properties have been measured in only about 300 submarine samples, this represents approximately one sample per million square kilometres (Watkins et al 1970).

The points made earlier suggest that data from the Reykjanes Ridge may be more representative if computed magnetization distributions are used to study variations in the palaeo-intensity of the earth's magnetic field. In view of unknown demagnetization effects, particularly at the ridge axis (cf. Godby et al 1968; Irving et al 1970), such a study would best be carried out on several long traverses.

CHAPTER 5

MAGNETIC PROFILES IN THE GULF OF ADEN

5.1 Introduction

Recent oceanographic survey data have confirmed the westward continuation of the Carlsberg Ridge, part of the world wide mid-ocean ridge system, from the North West Indian Ocean into the Gulf of Aden and extending into the Gulf of Tadjura (Laughton 1966; Roberts & Whitmarsh 1968; Laughton et al 1969). Available geophysical information for the Gulf of Aden may be summarized as follows:

(a) The bathymetry shows a 'central rough zone' with a median valley, throughout the Gulf of Aden. This is associated with an earthquake epicentre belt, linear magnetic anomalies and high heat flow (Laughton 1965, 1966; Laughton et al 1969).

(b) The crustal structure, from seismic refraction evidence, is typically oceanic. At the western end of the Gulf the axial region of the 'central rough zone' appears to be underlain by an anomalously low mantle velocity (Laughton & Tramontini 1970).

(c) North east - south west cross faults, thought to be transform faults (Sykes 1968), can be traced across the area and intersect the edges of the continental shelf.

(d) Reconstruction of the fit of opposing continental shelf edges (500 fm. line) reveals that pre-Miocene geological features are generally continuous across the reassembly. This suggests that the crustal blocks of Arabia and Somalia have separated within the last 20 million years (Laughton 1966).

(e) Certain linear magnetic anomalies in the Gulf can be identified with the magnetic pattern consequent of sea-floor spreading and indicate spreading rates, normal to the ridge axis, of about 1 cm/yr/limb (Laughton et al 1969).

5.2 The Profile Data

During March 1967, Cruise 16 of R.R.S. DISCOVERY obtained a number of magnetic and bathymetric profiles in the Gulf of Aden (Matthews et al 1967; Laughton et al 1969). This data was collected by the National Institute of Oceanography, England, as part of the continuing marine geophysical research programme associated with the International Indian Ocean Expedition (Hill 1966). The following sections describe the interpretation of three combined magnetic anomaly and bathymetric profiles obtained from this survey work (Jones - private communication).

The location of these traverses is shown in Fig. (5.1). The bathymetric information is based on data compiled by the National Institute of Oceanography at a scale of 1:2000000. Bathymetric contours show a strong lineation of ridges and troughs trending parallel and sub-parallel to the central valley associated with the East Sheba Ridge. Between 56^{o}E and 57^{o}E the ridge axis undergoes a relatively sharp, though apparently continuous, change in strike from a north west to a more east west trend. Earthquake epicentres (Matthews et al 1967) group in this general area and appear to form part of a belt of earthquakes parallel to but displaced from the local ridge axis, (Jones - private communication). This tectonic activity may be related to small transform faults associated with this section of the ridge although available evidence on this point is not conclusive.

Towards Profile Q-R a further series of bathymetric ridges and valleys trend approximately perpendicular to the axis of the East Sheba Ridge and parallel to the Owen Fracture Zone. The Owen Fracture Zone marks the junction of the East Sheba Ridge and the Carlsberg Ridge. The ridge axes are displaced by about 170 nautical miles in a right lateral sense (Matthews 1966). The East Sheba Ridge suffers another major

Fig. 5.1 General bathymetric chart of the Gulf of Aden (after, Laughton et al 1969), showing the major morphological features and the location of magnetic and bathymetric profiles used for interpretation.

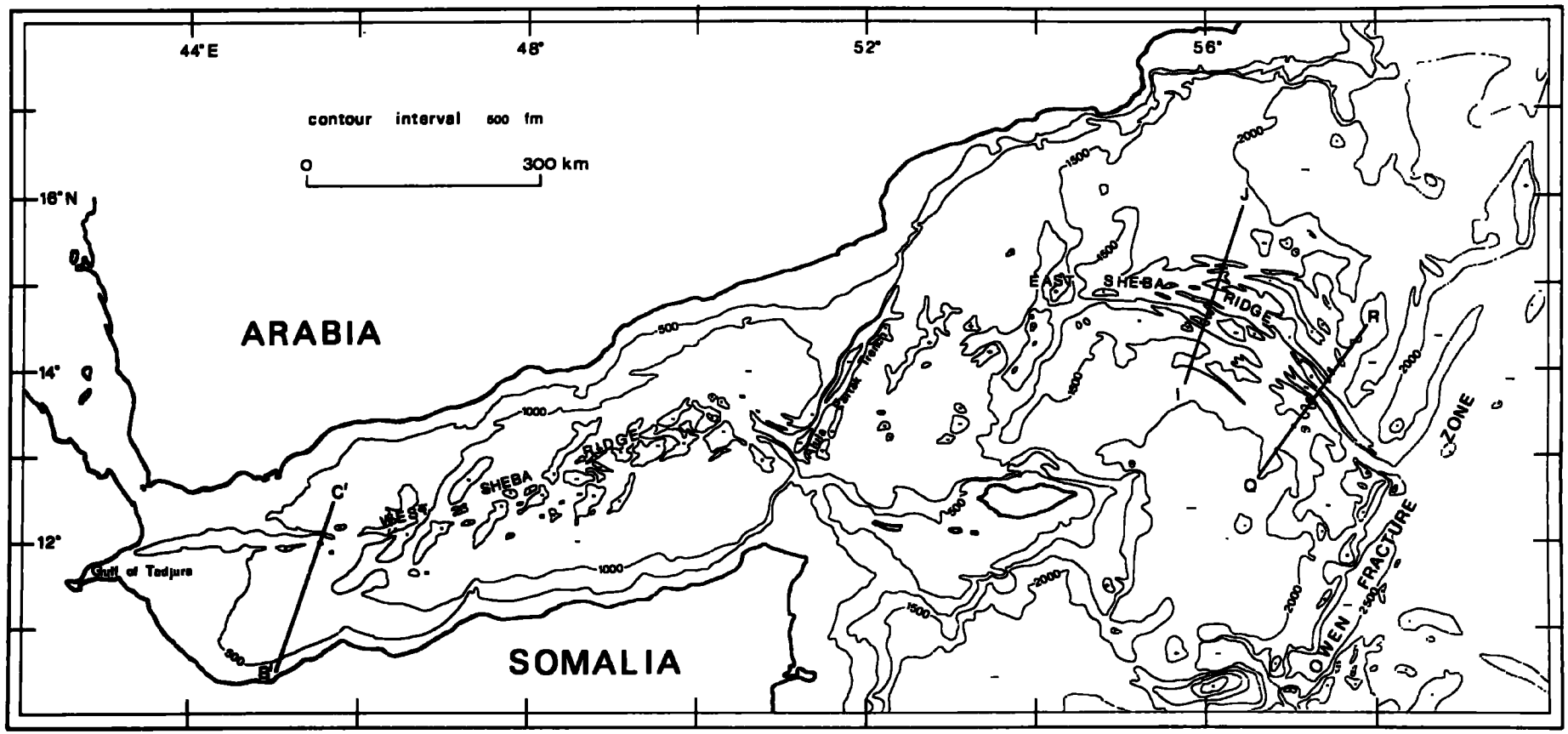

dislocation of some 100 miles in a left lateral sense at the Alua-Fartak trench, identified by Sykes (1968) to be a transform fault.

The westward continuation of the ridge system, the West Sheba Ridge, has a particularly jagged sea-floor relief ($\sim$ 1-1.5 km) and consists mainly of parallel ridges and valleys trending approximately north east - south west. The ridge axis is severely fractured and offset in this region by what are probably a suite of small transform faults (Laughton et al 1969). Further to the west the ridge axis is characterized by a single deep valley striking into the Gulf of Tadjura (Roberts & Whitmarsh 1968). Along the length of the Gulf of Aden the central rough zone is bounded by sediment filled troughs to the north and south. Laughton & Tramontini (1970) report that unconsolidated sediments, within the Gulf, vary in thickness from 0.23 to 1.52 km and generally thicken systematically with distance from the median valley.

Magnetic anomalies recorded in the Gulf of Aden show an approximately linear pattern parallel to the ridge axis and show similar characteristics to those observed over other sections of the mid-ocean ridge system. Over the East Sheba Ridge magnetic profiles may be reasonably interpreted in terms of the Vine-Matthews hypothesis of sea-floor spreading and provide estimates of rates of crustal spreading (Laughton et al 1969). Magnetic profiles obtained near the Owen Fracture Zone and over the West Sheba Ridge are more difficult to relate to this concept and are probably affected by disruptions associated with known faulting. Laughton et al (1969) have demonstrated a generally continuous correlation of magnetic anomalies between adjacent profiles throughout the Gulf. However, a number of 'zones of confusion' exist (generally associated with transform faulting), where anomaly identification is uncertain.

The three magnetic profiles considered in this study, Figs. (5.2, 5.4, 5.5) reveal fairly typical oceanic magnetic anomalies having amplitudes of 100-600 gamma and widths of about 15 km. All profiles show a conspicuous negative anomaly, associated with a well defined local median valley, flanked by comparable positive anomalies. This situation is due to the low magnetic latitude of the area ($+6^{o}$ to $+12^{o}$) which has the effect of producing a dominantly negative magnetic anomaly over a body magnetized in a direction close to the present earth's field. Ridge flank anomalies, generally show a fall off in amplitude away from the ridge crest. This is particularly noticeable in Profiles Q-R and B'-C'.

The original magnetic observations were not corrected for diurnal varation. Anomaly values used for interpretation, in each profile, were computed by subtracting a linear regional gradient (using the method of least squares) from the observations and then removing the principal low order fourier components (section 3.3).

5.3 Interpretation

5.3.1 Profile I-J

This traverse is perpendicular to the local axis of the East Sheba Ridge and to the established trend of the magnetic anomaly pattern, justifying a two-dimensional approach to interpretation. The traverse is situated almost entirely within the central rough zone and the sea-floor relief shows sharp changes in height ($\sim$0.5 to 1.0 km), particularly near the median valley. Because of this rugged relief and general lack of sediment in the area, it has been assumed that the bathymetry recorded along the traverse represents the upper surface of Layer 2, i.e. the magnetic layer. The form of the lower surface of Layer 2 is not known; it has been assumed to be horizontal at a depth of 5 km below sea level

(Fig. 5.2, model (a)). This estimate is consistent with refraction results obtained by Laughton & Tramontini (1970) which indicate that the thickness of Layer 2 varies between 1.8-2.8 km.

Layer 2 was then subdivided into a large number of two-dimensional model blocks, each assumed to be uniformly magnetized in the direction of the earth's average geocentric dipole field. The Linear Inverse technique was then used to directly evaluate the distribution of magnetization within this magnetic layer required to explain the recorded anomaly profile. Model specifications are set out in Table III.

The resulting interpretation is shown in Fig. 5.2b. The theoretical magnetic anomaly, computed from the evaluated distribution of magnetization, is shown as a dotted line and satisfactorily simulates the observed profile. Residual anomaly values do not exceed 62 gamma and are, in general, appreciably less than this. The largest residuals occur near the crest of the ridge where the upper surface of Layer 2 is shallowest and magnetic gradients are particularly steep. These residuals could be reduced by using narrower model blocks. However, justification for such treatment is difficult unless it could be assumed that the magnetic anomaly values were free from short wavelength errors of observations and reduction (section 3.4).

The magnetization histogram reveals a fairly abrupt variation from more positive to more negative groups of values across the profile. There is a distinctive zone of positive magnetization associated with the axial anomaly and located within the sides of the median valley. Changes in magnetization are particularly abrupt near this area and reach 0.01 e.m.u./cm^3. Towards the flanks of the ridge contrasts in magnetization are smaller and of the order of 0.005 e.m.u./cm^3.

TABLE III

Specification of Data Points used for the Interpretation of Magnetic Profiles in the Gulf of Aden

	No. of digitized magnetic anomaly points	Sampling interval for magnetic anomaly (km)	No. of model blocks forming the magnetic layer	Width of model blocks (km)	Average depth to upper surface of magnetic layer (km)	Maximum residual value between observed and calculated anomaly (gamma)	R.M.S. value (gamma)
Profile (I-J)	213	1.15	106	2.3	2.77	62	$\pm$ 12
Profile (Q-R)	207	1.15	103	2.3	3.22	28	$\pm$ 7
Profile (B'-C')	225	1.0	113	2.0	1.93	133	$\pm$ 20

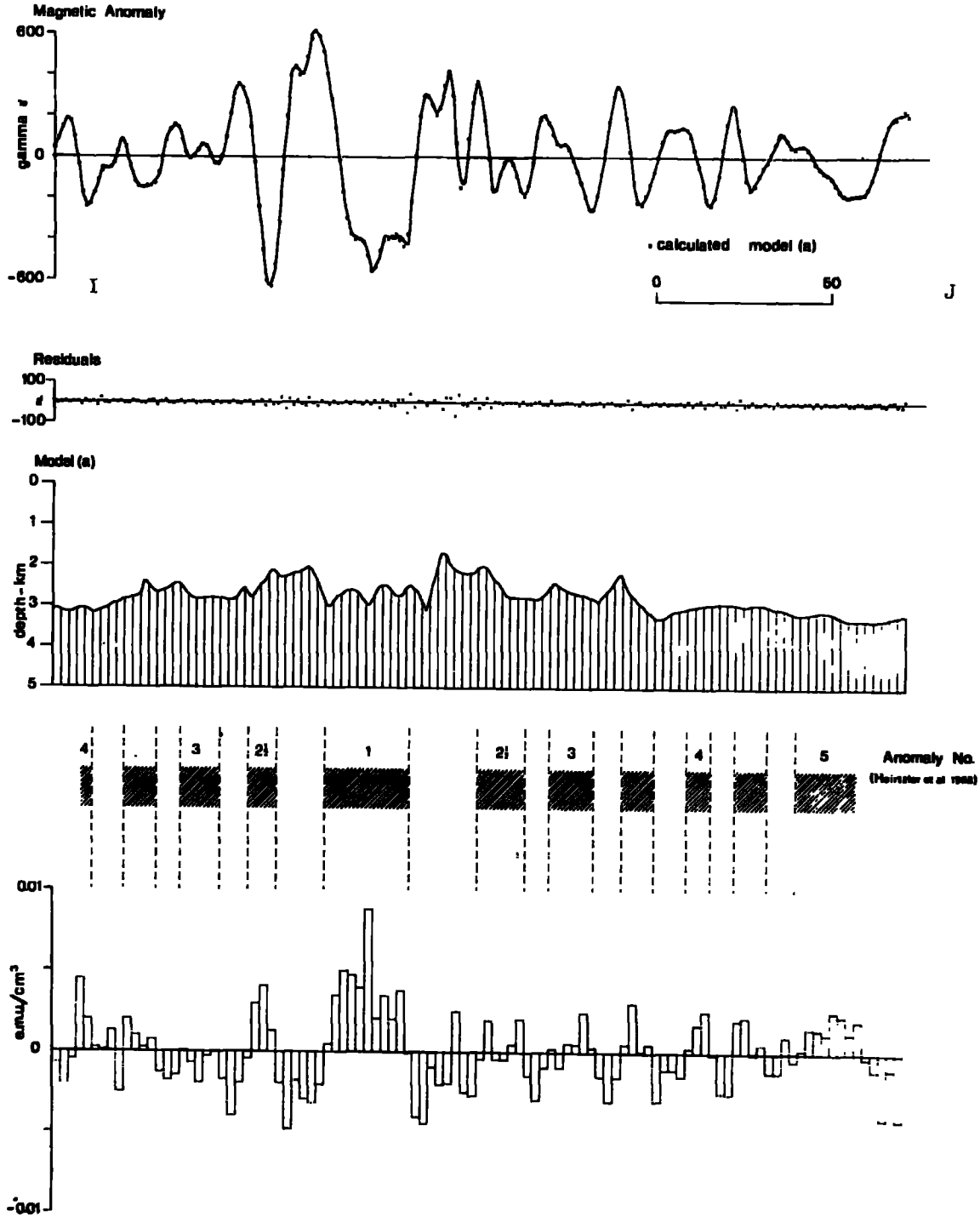

Fig. 5.2 Interpretation of the magnetic profile I-J across the East Sheba Ridge.

The positive and negative groups of magnetization across the profile are in agreement with the Vine-Matthews hypothesis and have been provisionally correlated with the numbering sequence established by Heirtzler et al (1968) for geomagnetic polarity reversals. The correlations indicated suggest an average spreading rate of about 1.1 cm/yr/limb normal to the ridge axis, a value which is consistent with other work in the area (Laughton et al 1969). In detail the reversal boundaries do not appear to reflect a uniform spreading rate. This may be due, in part, to errors of interpretation caused by unknown irregularities associated with the magnetic source, although the computed distribution of magnetization is considered to be essentially representative. The magnetization values correlated with the present polarity epoch (Brunhes) indicate an increased rate of spreading over the last 0.7 million years giving a value of 1.7 cm/yr/limb. The reversal boundaries have been chosen to correspond to areas of abrupt magnetization contrast and slight possible positioning errors would not significantly alter this conclusion. Identified reversal boundaries for the north east limb of the profile also indicate a slightly increased rate of crustal spreading compared with the south west limb. The value obtained is about 1.3 cm/yr. However, this estimate may be somewhat in error if duplication in the anomaly pattern has occurred due to unknown transform faulting.

Results are also presented for two other possible interpretations of the 'unfiltered' version of the Profile I-J, i.e. the long wavelength components have not been removed from the magnetic anomaly profile. Model parameters were as before except that two possible representations of the lower surface of Layer 2 have been assumed: (a) horizontal at a depth of 5 km; and (b) sloping away from the ridge centre (at a depth of 4.5 km) so that Layer 2 retains an approximately uniform thickness.

The resulting interpretations, in terms of these models, are shown in Figs. (5.3a) and (5.3b). Both model (a) and model (b) equally well account for the observed anomaly profile and the R.M.S. residual anomaly value was $\pm$12 gamma in each case. These simulations are very similar to that obtained for the 'filtered' version of Profile I-J and slight differences noted are not considered significant.

The resulting distributions of magnetization computed for models (a) and (b) (Fig. 5.3) are closely alike and show equivalent features to the magnetization pattern described in Fig. (5.2). There is no appreciable change in the identified polarity reversal boundaries. The main difference between the two models shown in Fig. (5.3) is that slightly higher values of magnetization occur beneath the central part of the profile in model (b). This is to be expected due to the thinner Layer 2 at the ridge centre. The interpretations do not otherwise distinguish between the two models although the sloping base of model (b) may be preferred, since it is in more accord with the hypothesis of sea-floor spreading and seismic refraction evidence from various parts of the oceans.

However, both computed distributions of magnetization (Fig. 5.3) show a conspicuous long wavelength component, such that the magnetization values beneath the ridge flanks are predominantly negative. This phenomenon has been discussed previously (section 3.3) and a probable explanation is that lack of correction for the diurnal variation has introduced a spurious long wavelength component in the observed profile. The interpretation discussed earlier for the 'filtered' version of this profile (Fig. 5.2) demonstrates that the removal of the long wavelength components causes the alternating groups of magnetization to be more clearly differentiated on the basis of algebraic sign. This particular study was carried out at an early stage in the present work and the

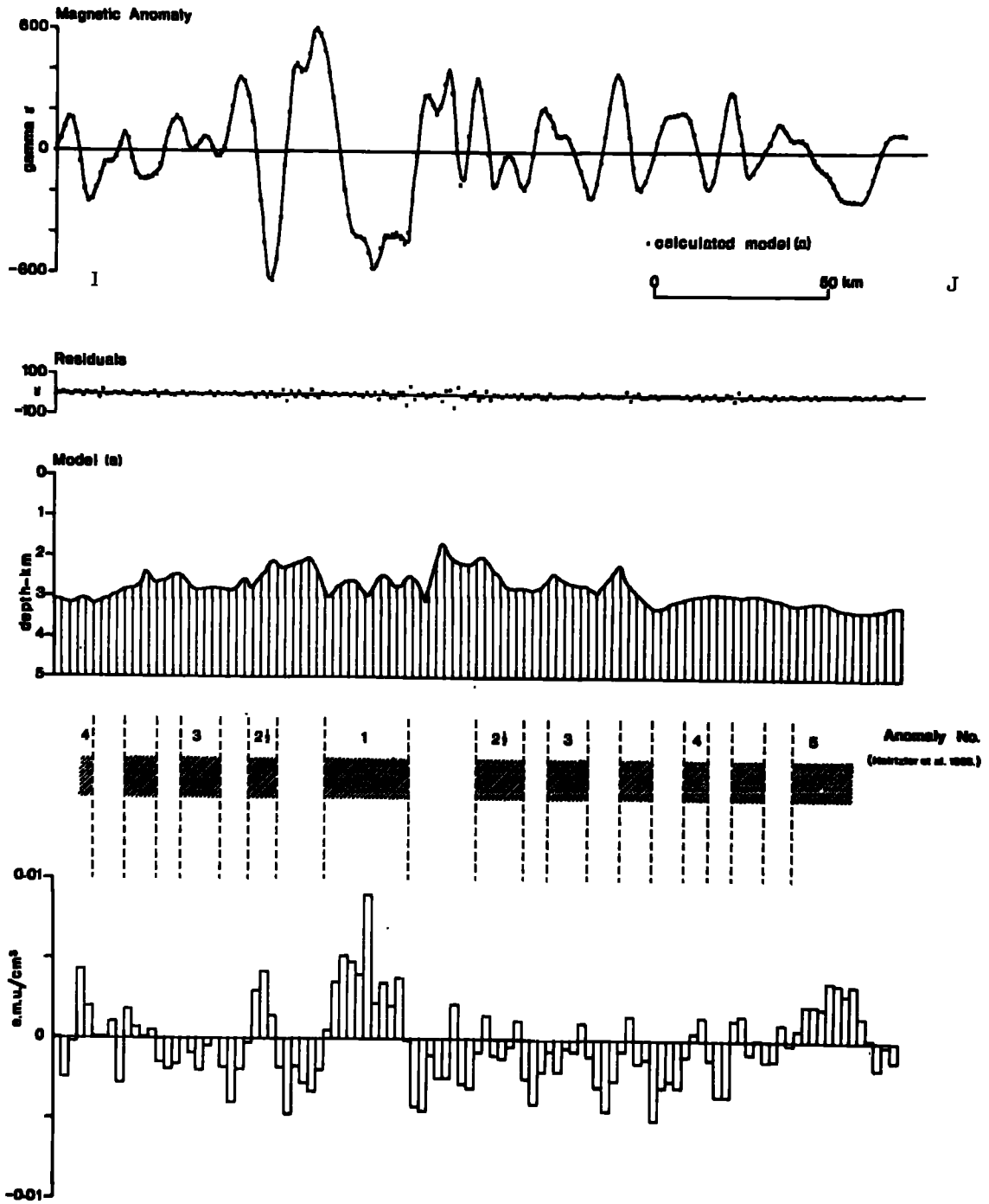

Fig. 5.3a Interpretation of the 'unfiltered' magnetic profile I-J, the base of Layer 2 is assumed to be horizontal.

Fig. 5.3b Interpretation of the 'unfiltered' magnetic profile I-J, the base of Layer 2 is assumed to slope away from the ridge centre.

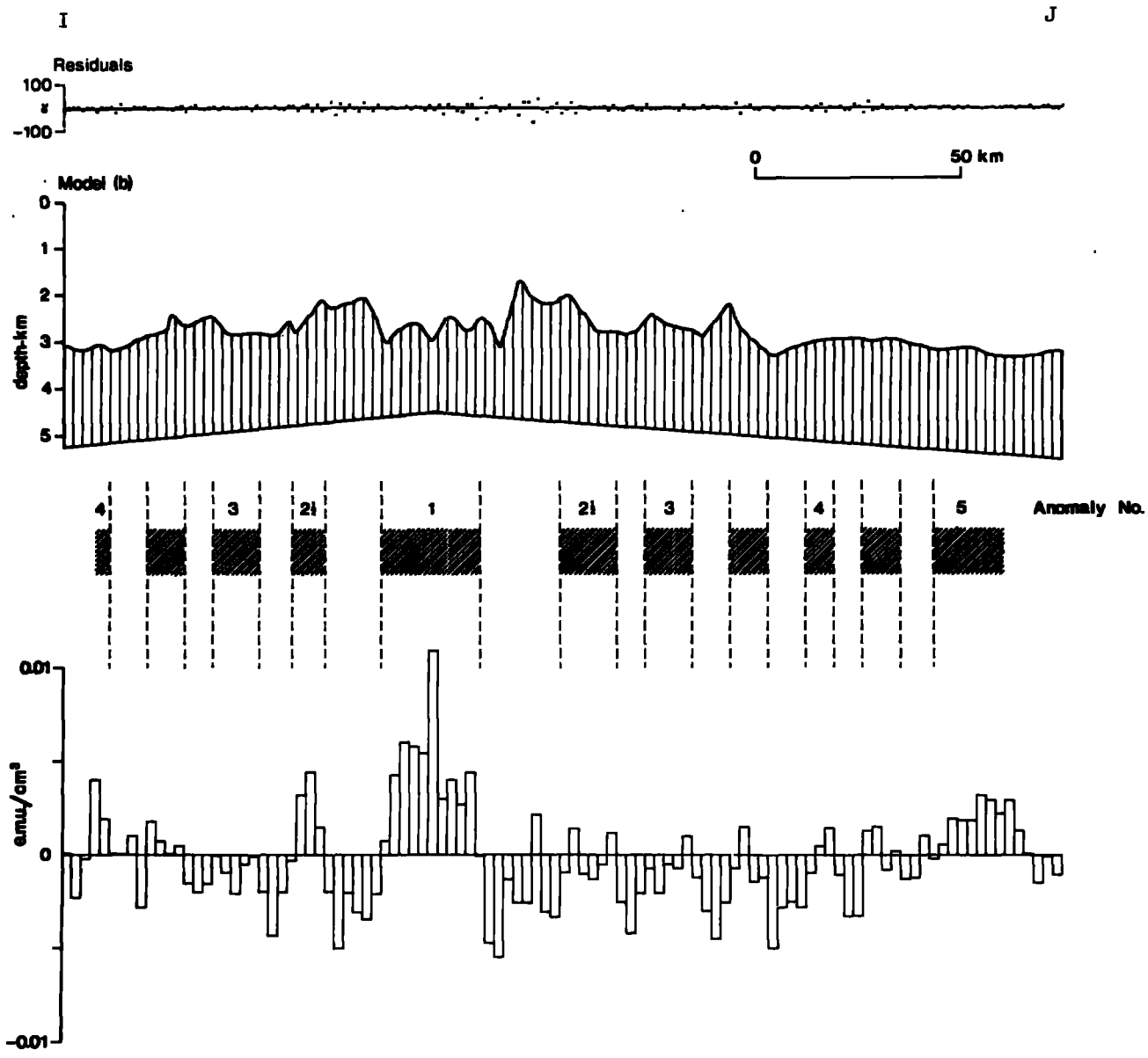

successful extraction of the reversal pattern, by this filtering process, has encouraged standard application of the procedure.

The above results show that small variations in the relief of the lower surface of the magnetic layer, at these depths, are not critical to interpretation. In contrast, errors of observation (within the magnetic data) of quite small amplitude but long wavelength, such as may be caused by the diurnal variation, should be removed as accurately as possible prior to interpretation.

5.3.2 Profile Q-R

This traverse crosses the median valley associated with the East Sheba Ridge, approximately at right angles, and trends parallel to the adjacent Owen Fracture Zone. The bathymetry along the profile reveals a particularly jagged relief, with changes in height of 1-2 km, across the median valley and scarp-like faces of up to a kilometre on either side (Fig. 5.4). This bottom topography strongly suggests that the sea-floor represents a faulted 'volcanic' basement surface with probably very little sediment fill. The bathymetry has therefore been assumed to define the upper surface of Layer 2 (i.e. the magnetic layer), the lower surface has been assumed to be horizontal at a depth of 5 km. As with Profile I-J this source layer was then subdivided into a large number of small two-dimensional model elements and interpretation of the anomaly profile Q-R was carried out using the Linear Inverse technique. Model specifications are given in Table III.

The resulting interpretation is shown in Fig. (5.4). The computed magnetic anomaly closely simulates the observed profile and residual values do not exceed 28 gamma. The larger values occur immediately above the crestal peaks either side of the median valley. The overall improved 'degree of fit' obtained for this profile, compared with that

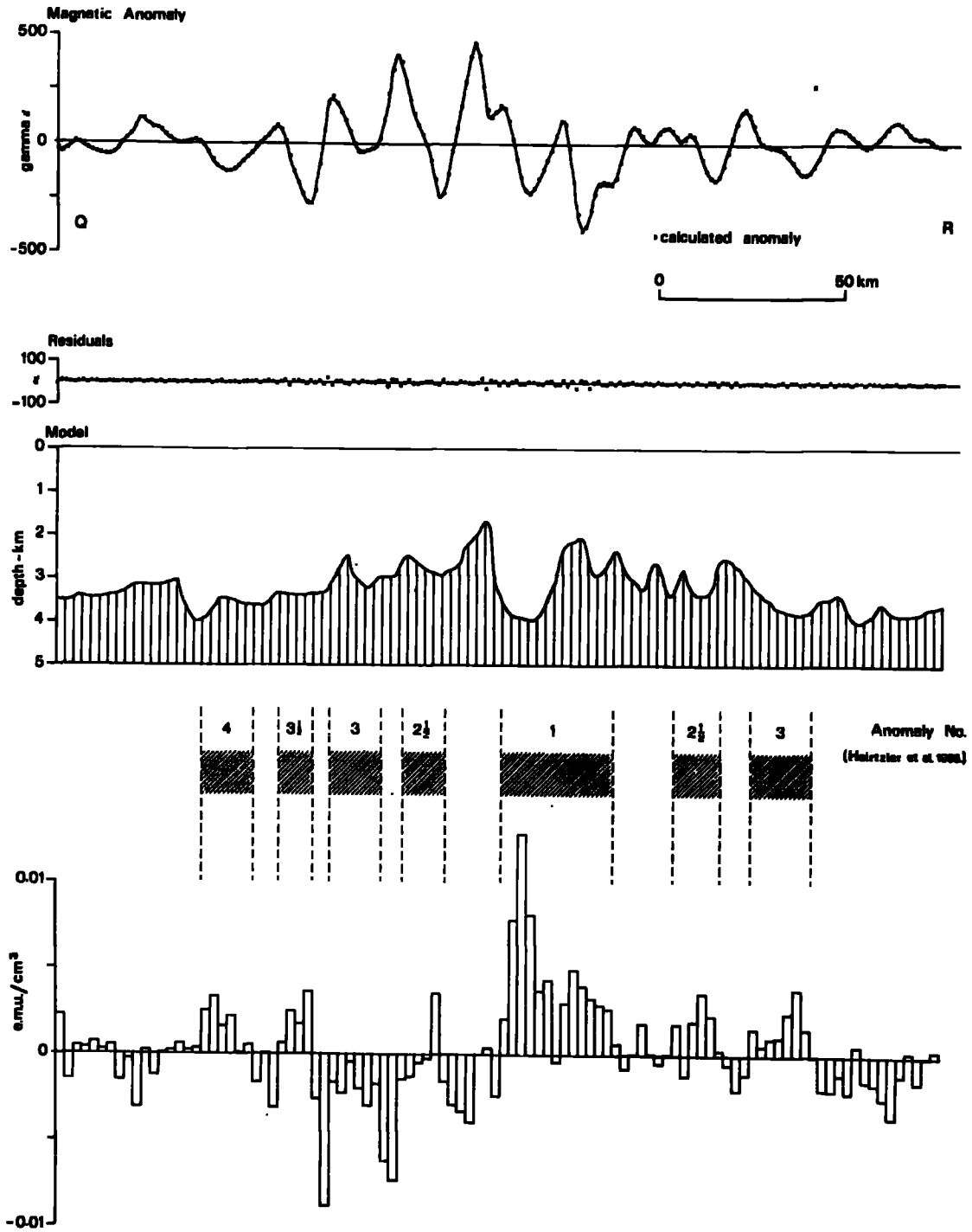

Fig. 5.4 Interpretation of the magnetic profile Q-R across the East Sheba Ridge.

obtained for Profile I-J, is primarily due to the greater depth of water with respect to the model block width used. The dominant feature of the calculated magnetization distribution is a large group of positively magnetized values associated with the ridge crest. Unlike Profile I-J these values appear to extend beyond the limits of the median valley and suggest an unusually wide axial zone. The axial magnetic anomaly observed on this profile is somewhat subdued compared with those recorded on Profiles I-J and B'-C'. This must be due, in part, to the topographic effect of the massive local relief although other unknown irregularities associated with the jagged bathymetry may be responsible.

Discrete groups of magnetization, varying from more positive to more negative values, are observed across the calculated distribution. Changes in magnetization from group to group are abrupt and as for Profile I-J the larger contrasts appear near the axial zone. However, those central values exceeding about 0.006 e.m.u./cm^3 may be unrepresentative because of the locally thin magnetic layer. The distribution of magnetization is in broad agreement with the Vine-Matthews hypothesis although the pattern is not symmetrical in detail. Provisional correlations with polarity reversal boundaries, after Heirtzler et al (1968), are indicated in Fig. (5.4). The correlations identified suggest an average spreading rate of 1.2 cm/yr/limb for the profile except at the axial region where an apparent rate of 2 cm/yr/limb is indicated for the last 0.7 million years.

There is some ambiguity associated with correlations identified towards the north east side of the profile because of the apparent large axial zone. This feature could result from duplication in the magnetic anomaly sequence due to a transform offset. However, the general

bathymetry for the area (Fig. 5.1) indicates an essentially continuous median valley in the vicinity of Profile Q-R. The profile is situated very close to the Owen Fracture Zone which has an associated series of ridges and valleys striking at right angles to the local median valley. Hence, certain errors in interpretation could be caused by serious deviation of the bathymetry, recorded along the profile, from a true two-dimensional structure. Matthews et al (1965) have suggested that extensive brecciation and hydrothermal alteration of permanently magnetized rocks in a fault zone may seriously modify the original magnetic pattern. Magnetic profiles recorded nearer to the main shear area of the Owen Fracture Zone support this idea, showing a subdued magnetic relief (Matthews et al 1967). However, magnetization values computed both to the north east and south west of the axial zone on Profile Q-R do not show a significant reduction in amplitude or gradient compared with values obtained for Profile I-J. This suggests, therefore, that structural dislocation of the magnetic layer may be more responsible for the usually wide axial zone and hence the model adopted for interpretation may be an oversimplification.

5.3.3 Profile B'-C'

This profile extends from near the Somalia coast to some 40 km beyond the median valley to the north east. The profile has been projected along a north south line so as to be approximately at right angles to the east west strike of the ridge axis in this region. The magnetic profile is characterized by a large negative axial anomaly, having an amplitude of about 1200 gamma, with distinctive flanking anomalies near the ridge crest. About 90 km away from the ridge axis, towards the Somalia coast, the magnetic pattern shows a rapid transition to a zone where magnetic anomalies are characterized by low amplitudes and much broader wavelengths. Evidence from seismic refraction work

(Laughton & Tramontini 1970) suggests that southwards along the traverse B'-C' the top of Layer 2 deepens from about 1.5 km at 25 km from the median valley to 2.5 km at a distance of 130 km. Also Layer 2 increases in thickness over this interval from about 1.7 to 2.8 km (Stations 6239-6233, Laughton & Tramontini 1970). This information has been used to construct a dipping magnetic layer, representing Layer 2, about 2 km thick on average. Near the ridge crest the upper surface of this layer is defined by the recorded bathymetry whilst at a greater distance the Layer 1/2 interface is assumed to be a plane surface. The base of Layer 2 is assumed to be parallel to this plane surface.

The resulting interpretation of the magnetic anomaly profile B'-C' in terms of a distribution of magnetization confined to this layer, is shown in Fig. (5.5). Model specifications are given in Table III. The theoretical magnetic anomaly, computed from the evaluated distribution of magnetization shows a satisfactory simulation of the observed profile except near the ridge crest. Here a few residual anomaly values exceed 100 gamma although they are appreciably less elsewhere. The large residuals are associated with a small positive anomaly located within the main axial anomaly. This local anomaly appears to be associated with a bathymetric ridge, situated inside the median valley, reaching within one kilometre of the sea surface. The resolution of this local feature would be considerably improved by use of model blocks less than 2 km wide. However, much narrower blocks could not be used with justification over the deeper portions of the profile unless short wavelength errors of observation and reduction could be accurately eliminated from the magnetic data. Other residual values obtained in this general area similarly reflect the shallow depth of water relative to the model block width used. The essential form of the axial and flanking anomalies have

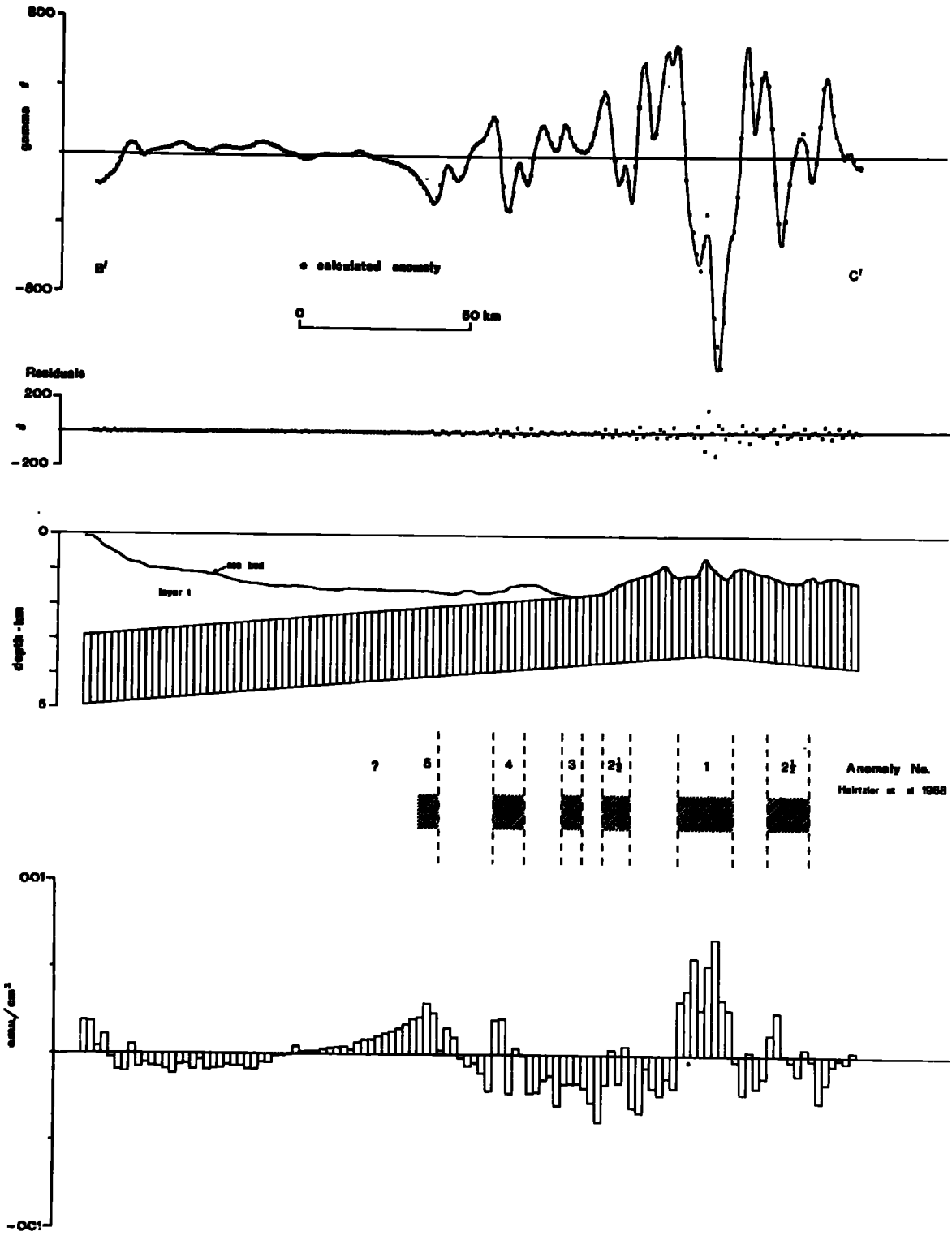

Fig. 5.5 Interpretation of the magnetic profile B'-C' across the West Sheba Ridge, Layer 2 is assumed to dip uniformly away from the ridge crest.

been reproduced and residual values mainly represent small displacements between the observed and computed profiles.

The computed distribution of magnetization shows a conspicuous group of positive values associated with the axial anomaly, and as Profile I-J, located within the walls of the local median valley. The overall magnetization pattern is in broad agreement with the Vine-Matthews hypothesis and provisional correlations with the numbering sequence adopted by Heirtzler et al (1968) for geomagnetic field reversals are indicated (Fig. 5.5). The reversal boundaries identified reveal an average spreading rate of 0.8-0.9 cm/yr for the southern limb. The reversal pattern is fairly regular within these limits although transition points between normal and reversed epochs are not well defined between Anomaly Nos. $2\frac{1}{2}$ and 4. This lack of definition is principally due to the low rate of crustal spreading, which results in a reduction in width of the observed magnetic anomalies, and the model block width used for interpretation.

Beyond Anomaly 5, which is well detailed in terms of its magnetization amplitude, there are no distinctive changes in magnetization observed. The computed values show a gradual 'tailing-off' in magnitude to a fairly uniform level. The fluctuations observed at the end of the profile, near the Somalia coast, are partly due to end-effects in the computations while the magnetic feature observed is probably of very local origin. Accepting that the model representation of Layer 2 is reasonably correct, then these results show that abrupt changes in magnetization at depth (confined to Layer 2), are not required to explain the small magnetic anomalies recorded over this section of the profile. This implies either that the normal mechanism of sea-floor spreading has not occurred or that the remanent magnetization of Layer 2 has been selectively destroyed or degraded in some way.

5.4 Discussion

Magnetic anomalies in the Gulf of Aden do not generally show a simple linear pattern although, in places, the observed pattern is correlatable to that expected from the Vine-Matthews hypothesis of sea-floor spreading. This difficulty may only be apparent since present track spacings are quite wide and persistent correlations between adjacent profiles are clearly subject to some ambiguity. Transform faults are known to offset the ridge axis at a number of points and their effects may explain the wide axial zone encountered with Profile Q-R and possibly the apparent increase in spreading rate to the north west obtained for Profile I-J. Also, throughout the central rough zone in the Gulf of Aden, the sea-floor relief has a mountainous aspect and this must contribute to the complexity of the observed magnetic field.

The interpretations presented, for the three profiles considered, demonstrate that accurate simulations can be obtained for magnetic profiles of a relatively complex nature. The magnetic models used are based on available bathymetric and seismic refraction evidence and are considered to be essentially representative of the true configuration of Layer 2. The computed distributions of magnetization obtained for the three profiles are in agreement with the Vine-Matthews hypothesis and uniquely support the general correlations made by Laughton et al (1969). The results obtained for Profile I-J are most satisfactory in this respect and clearly indicate a sequence of positive and negative groups of magnetization across the profile. Deduced spreading rates, normal to the ridge axis, vary from about 1.1 to 1.2 cm/yr/limb for Profiles I-J and Q-R, whilst Profile B'-C' has a spreading rate of 0.8-0.9 cm/yr to the south. This decrease in spreading rate is to be expected since plate theory predicts that spreading rates derived in

the Gulf of Aden should reflect the angular rotation of Arabia from Somalia. The spreading rates deduced in the present work are in good agreement with the estimates obtained by Laughton et al (1969), using an indirect approach to interpretation, for these profiles. Laughton et al (1969) have demonstrated that these and other spreading rates derived in the Gulf of Aden, resolved parallel to the strike of the transform faults, are proportional to the sine of the angular distance from the pole of rotation established by Le Pichon (1968).

Profiles B'-C' and I-J both reveal a distinctive group of positive magnetization values associated with the axial anomaly and closely sited within the axial region of the ridge crest, identified to be the local median valley. The distinctive transition points, located within one model block width - either side of this zone - to reversely magnetized sections confirm the abrupt nature of this boundary. The most widely accepted mechanism for bringing mantle material to the surface at the ridge crest is that of dyke injection. The above results give strong support to this hypothesis and in view of the narrow transition zones suggest an origin localized within the median valley.

It is of some interest that for the three profiles considered, the positive magnetization values associated with the axial anomaly are somewhat wider in extent than predicted from the average spreading rate determined for the complete profile. The results from Profile Q-R may be in error due to possible structural disruptions associated with the Owen Fracture Zone. However, the identified polarity boundaries for Profiles I-J and B'-C' have been chosen to correspond with abrupt changes in the magnetization distribution and slight errors in position would not change the general conclusion. The polarity epoch boundary at 0.69 million years B.P. is considered to be a highly reliable age date (Cox et al 1968) and provides a firm 'tie-line' between radiometric

dating and palaeomagnetic stratigraphy. The interpretations presented therefore suggest a relatively recent increase in the rate of sea-floor spreading rather than possible errors in the reversal time scale.

A significant feature observed on all magnetic profiles in the Gulf of Aden is the apparent absence of identifiable magnetic anomaly peaks after Anomaly 5. Profile B'-C' (Fig. 5.5) illustrates this point well, the computed distribution of magnetization does not indicate any magnetic record beyond about 10 million years B.P. (i.e. the approximate age of Anomaly 5). The isochron map established by Laughton et al (1969) traces Anomaly 5 roughly along the edge of the central rough zone bordering the sediment filled troughs to the north and south. Laughton et al (1969) suggest that this line may delineate a boundary between simple vertical dyke injection and more horizontal beds of flood basalt. The latter structures would reduce the amplitude of the observed magnetic anomalies and hence decrease the required, apparent magnetization obtained in direct computations. Magnetic bodies of very low inclination ($\sim 10^{o}$), would require much larger contrasts in magnetization to explain the observed low amplitude anomalies and hence may remain consistent with a modified hypothesis of sea-floor spreading. The presence of Layer 2 beyond Anomaly 5 (Station 6233, Laughton & Tramontini 1970) and lack of identifiable magnetic reversals within the magnetization pattern computed for Profile B'-C' suggests that the above hypothesis is more likely than any abrupt cessation in spreading at about 10 million years B.P. (Ewing & Ewing 1967; Le Pichon & Heirtzler 1968). However, this evidence is somewhat weakened by the striking difference, between the sediment free central rough zone and the adjacent thickly sedimented troughs, which suggest that these two provinces of the Gulf were due to separate periods of spreading (Laughton 1966).

CHAPTER 6

AN INVESTIGATION INTO THE INCLINATION OF BODIES CAUSING OCEANIC MAGNETIC ANOMALIES

6.1 Introduction

Magnetic measurements at sea, particularly across mid-oceanic ridges, indicate the presence of important lateral boundaries within the oceanic crust. At present these boundaries are generally not resolvable with other geophysical techniques and have been inferred almost exclusively from the Vine-Matthews hypothesis of sea-floor spreading.

Vine & Matthews (1963) concluded that the steep gradients and large amplitudes of typical magnetic anomalies observed over oceanic ridges required abrupt vertical boundaries between adjacent sections of the oceanic crust. These contacts were postulated to represent normal-reverse polarity changes and hence could produce a considerable magnetic contrast without requiring any lateral change in the petrology of the crustal material. Geologically, the vertical-sided 'blocks' in this model are thought to represent the bulk contribution of a large number of relatively narrow 'basaltic dykes'. The magnetic models of Vine & Matthews, Vine & Wilson (1965) and others are essentially simplifications which express the basic idea of adjoining crustal strips having normal and reversed magnetic polarity.

The characteristic jagged sea-floor relief observed over mid-ocean ridges almost certainly results from submarine fissure eruptions and the effects of subsequent faulting. However, comparatively little is directly known about the emplacement and structure of this intrusive material at depth. Layer 2 is generally agreed to be the

main source of oceanic magnetic anomalies and probably consists of basaltic material, overlying more or less metamorphosed basalt and possibly incorporating a few layers of consolidated sediment. Structural interpretations of this layer are principally based on bathymetric evidence, dredged rock samples and limited seismic profiling (e.g. Van Andel 1968).

However, magnetic anomalies - particularly those associated with the mid-ocean ridge system - provide an alternative approach to interpretation. Linear oceanic magnetic anomalies were first described and interpreted by Mason (1958) and subsequently by Mason & Raff (1961) and Raff & Mason (1961). These authors suggested several possible source models that could equally account for individual magnetic anomalies (section 1.2). It is significant that those models located within the volcanic layer (5.3 km/sec) showed sloping lateral boundaries. Mason (1958) and Mason & Raff (1961) suggested that these models could be explained as basic lava flows within Layer 2 - although there was an apparent lack of topographic and seismic expression.

The Vine-Matthews hypothesis successfully avoided the problems implied by such isolated structures by postulating an essentially uniform composition to Layer 2. Subsequent interpretations, in the light of this hypothesis, have always emphasized the vertical aspect of lateral boundaries within the magnetic layer (Vine 1966; Pitman & Heirtzler 1966; Heirtzler et al 1968) and ignored the possibility of inclined structures.

Nevertheless, Loncarevic et al (1966) note that vertical sided blocks are not a necessary requisite to explain magnetic anomalies observed over the crest of the mid-Atlantic ridge at latitude 45^{o}N. These authors present two types of model simulation: those in which

the contacts between differently magnetized blocks are sloping, and those in which the contacts are vertical. However, preference is indicated for the vertical-model combined with a gradational magnetization pattern, on the grounds of a plausible geological origin.

Heirtzler et al (1966) have suggested that magnetic anomalies observed over the Reykjanes Ridge may be produced by subhorizontal lava flows and not vertical dykes. However, detailed model simulations for profiles observed over the survey area are not presented. Their arguments are based on the possible extension of a simplified geological section from the main graben on Iceland, across to the Reykjanes Ridge. This section incorporates very low angle (4^{o}-8^{o}) lava flows of alternately positive and negative polarity. Pitman & Heirtzler (1966) have subsequently presented a re-interpretation of the Reykjanes Ridge magnetic anomalies in terms of a magnetic model formed from a sequence of vertical-sided blocks of alternating polarity. This is more in accord with an origin due to dyke injection and sea-floor spreading.

The available literature suggests that possible structural alternatives to vertical 'dyke-like' bodies may exist within the upper part of the oceanic crust. However, it is not clear as to whether such models could satisfactorily explain observed magnetic anomalies and remain consistent with current ideas concerning the creation of oceanic crust, by the process of sea-floor spreading. The following sections describe a quantitative attempt to test and compare the validity of various source models as applied to typical oceanic magnetic anomalies.

6.2 The Direct Approach

The attitude of lateral boundaries within the oceanic crust would be most satisfactorily examined with a highly penetrating, deep sea, seismic profiling technique. However, it has been possible to obtain certain estimates of the reasonableness of various magnetic models by application of the Linear Inverse technique. The procedure used permits model elements of irregular cross-section to be incorporated within the magnetic layer (section 2.3.2). Several possible structural models were tested against two magnetic profiles considered to be representative of oceanic magnetic anomalies. The profiles were chosen from the Juan de Fuca Ridge (Vine & Wilson 1965, Fig. 4a) and the Pacific-Antarctic Ridge (Pitman & Heirtzler 1966, Eltanin-19).

6.2.1 The Juan de Fuca Profile

This profile was recorded across the crestal area of the Juan de Fuca Ridge, effectively at right angles to the well established magnetic lineation pattern (Raff & Mason 1961). The profile is about 330 km long on a true bearing of 110°; the ridge crest is located at 47°N, 129.2°W (Wilson 1965b, Fig. 3 profile-a). This profile was originally described by Vine & Wilson (1965) together with two other profiles, spaced at intervals of 45 km along the ridge axis. These authors presented a general interpretation (adopting an indirect approach) for the central magnetic profile and concluded that the essential features of their source models supported the Vine-Matthews hypothesis of sea-floor spreading.

The magnetic anomaly profile, denoted (a) in Fig. 4 of Vine & Wilson (1965), has been sampled at intervals of 2 km yielding a total of 167 field points along the profile. The crustal model adopted for the magnetic source was a horizontal Layer 2, extending between 3.3 and 5.0 km, i.e. as Vine & Wilson (1965). This layer was then sub-

divided into 112 vertical model units, each having a width of 3 km and assumed to be uniformly magnetized in the direction of the average geocentric dipole field. The Linear Inverse technique was then used to directly evaluate the distribution of magnetization within Layer 2 required to explain the observed profile.

Initial interpretation indicated that low amplitude, long wavelength components within the magnetic data were depressing the computed magnetization values. Low order fourier components were therefore removed from the data (section 3.3) and a re-interpretation carried out. This filtering process in no way affects the resulting conclusions.

Fig. (6.1) shows the resulting interpretation obtained for this profile. The theoretical magnetic anomaly values, computed from the evaluated magnetization distribution, show a satisfactory fit to the observed profile. Residual anomaly values do not exceed 51 gamma and are in general appreciably less than this, the R.M.S. value for the complete profile is $\pm$13 gamma. The larger residual values are associated with steep gradients near the central part of the profile. Improved topographic control for the upper surface of the magnetic layer would improve the fit (cf. Vine & Wilson 1965), as would the use of narrower model blocks. However, in view of possible errors within the basic magnetic data used, the use of narrower model blocks is not desirable (Bott & Hutton 1970a).

The computed distribution of magnetization is in agreement with the Vine-Matthews hypothesis of sea-floor spreading and major geomagnetic polarity reversal boundaries, following the time scale of Heirtzler et al (1968), have been denoted. These correlations indicate an average crustal spreading rate of 2.7 cm/yr/limb (cf. Vine 1966, 2.9 cm/yr/limb) although the resulting polarity pattern shows small local variations

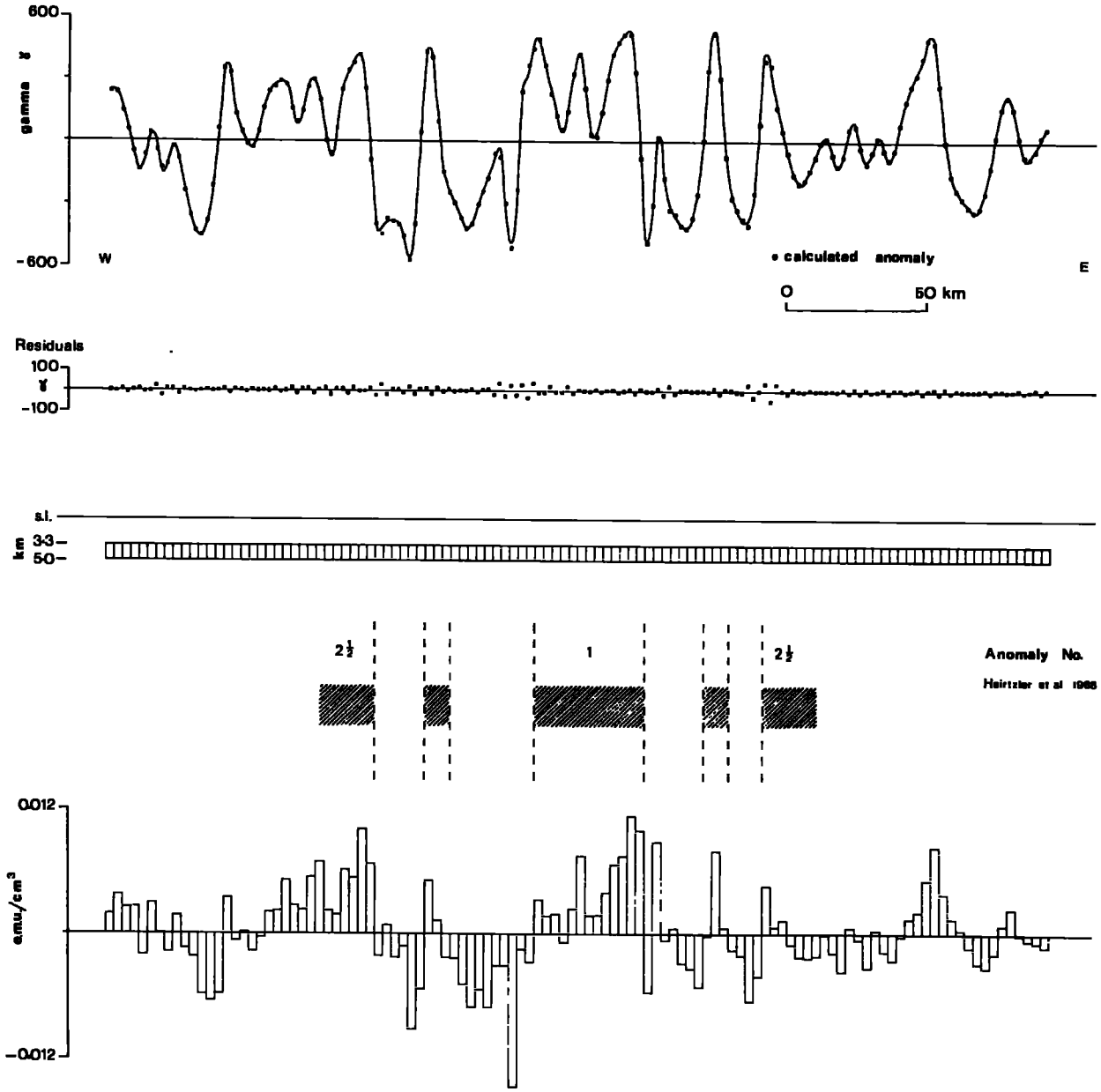

Fig. 6.1 Interpretation of a magnetic anomaly profile across the Juan de Fuca Ridge.

($\pm$0.2 cm/yr) away from this value. This pattern is only roughly symmetrical and suggests a slightly higher rate of spreading towards the north west. However, recent work by Peter & Lattimore (1969, Fig.1) suggests that a major transcurrent fracture pattern may be responsible for the complex structural configuration of this general area of the ridge system. The associated faulting indicates that duplication and offsets in the magnetic anomaly lineations occur, particularly to the north and west of the axial zone on the profile considered. The identification of possible reversal boundaries beyond Anomaly 2½ is not clear and further correlations would be best attempted in conjunction with other profile data. The interpretation presented supports the conclusion of Bott (1967), obtained from the analysis of a shorter section of the same profile, in that there is no indication of excessively strong magnetization required to explain the axial anomaly.

The rectangular model units within the magnetic layer were then modified to represent adjacent trapezia sloping inwards towards the centre of the profile. The angle of dip of these bodies ($\sim 40^{\circ}$) is kept constant throughout the model, except for a few blocks near the centre which have a more vertical attitude. The magnetic profile shown in Fig. (6.1) was then re-interpreted in terms of this second model. The resulting interpretation is shown in Fig. (6.2a). Again a satisfactory fit to the observed anomaly was produced, the maximum residual value obtained being 61 gamma with an overall R.M.S. value of $\pm$16 gamma. The slight increase in the 'degree of misfit', compared with the previous model, is not considered to be significant.

The results of this second interpretation are essentially similar, both in 'degree of fit' to the observed profile and in the computed magnetization pattern, to those produced from the original model. Small arrows shown on Fig. (6.2a) denote those areas of more obvious change

within the computed magnetization values, although the distribution is equally as acceptable as the former, (Fig. 6.1). The differences noted show an increased rate of change in the intensity of magnetization, particularly towards the centre of the profile near areas of steep magnetic gradient. This suggests that the computed values will show an increasing degree of sensitivity towards further major changes in slope of the model blocks within the magnetic layer.

The model blocks were then re-modified to represent low angle ($\sim 10^{o}$), 'sheet-like' bodies, again sloping inwards towards the centre of the profile. The resulting interpretation in terms of this third model is shown in Fig. (6.2b). The fit to the observed magnetic anomaly profile was adequate, although the maximum residual value obtained was 87 gamma with an overall R.M.S. value of $\pm$18 gamma. Although this degree of fit is somewhat poorer than that obtained for the two previous models this effect may not be a direct consequence of the magnetic model used. An improved degree of fit could be obtained, by the use of narrower model elements, if short wavelength errors within the magnetic data were eliminated.

However, the distribution of magnetization obtained for this model is significantly different from the previous cases. The original simple pattern has been completely changed - the distribution now consists of rapidly oscillating values of magnetization with no coherent form across the profile. Computed values are significantly increased in amplitude reaching 0.045 e.m.u./cm^3, compared with a maximum value of 0.014 e.m.u./cm^3 obtained with earlier models. The pattern shows very rapid variations in magnetization, of the order of 0.08 e.m.u./cm^3. The larger values are principally associated with areas of steep magnetic gradient. If narrower model block widths had been used, within the magnetic layer, this oscillation would have been much more pronounced.

Fig. 6.2a

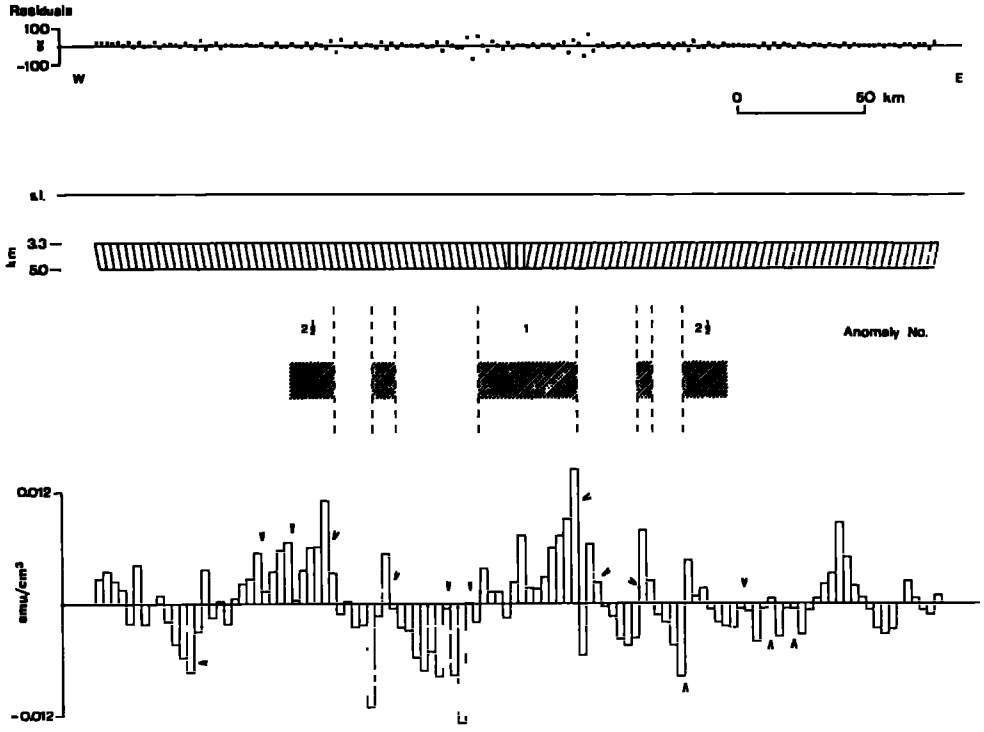

Fig. 6.2b

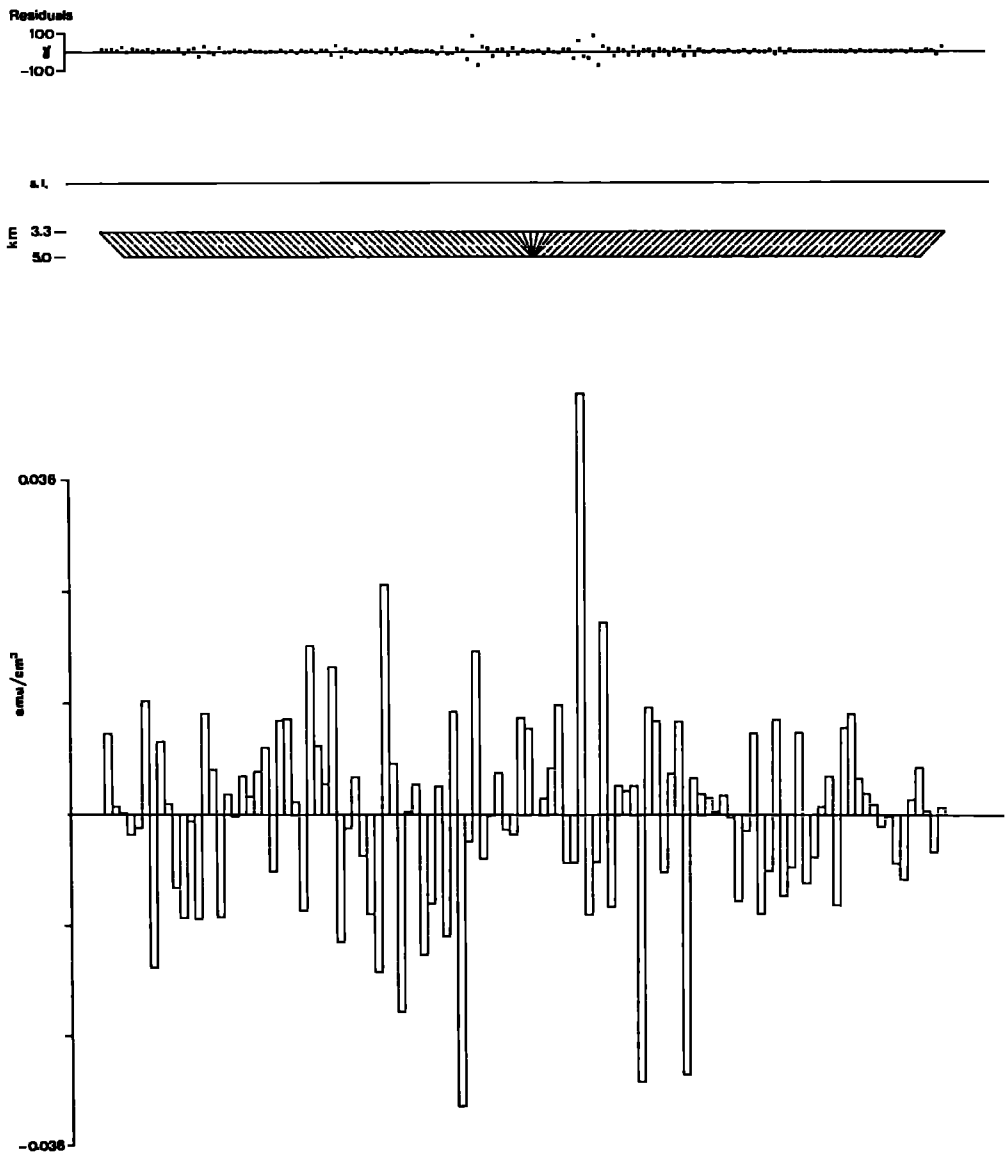

Intermediate stages of these computations (not presented) have confirmed the general trend shown by these three models. As the vertical dip of the model elements are successively reduced to a near horizontal form, increasing fluctuations in magnetization values combine to confuse and remove any simple pattern.

6.2.2 The Eltanin-19 Profile

This profile is one of four long traverses carried out across the Pacific-Antarctic ridge, between 40^{o}S and 55^{o}S, by the U.S.S. ELTANIN during 1965. These profiles were first described by Pitman & Heirtzler (1966) and subsequently by Pitman et al (1968). The excellent broad scale symmetry of the Eltanin-19 magnetic profile, about the crest of the ridge, has well established this traverse within the literature of sea-floor spreading.

The central section of this traverse has been projected along an azimuth normal to the local strike of the Pacific-Antarctic ridge (040^{o}) and is about 350 km long. The ridge crest is located at 51.6^{o}S, 117.8^{o}W. The magnetic profile was sampled at an interval of 2 km yielding 174 field points along the profile. These values were taken from the original total field readings which were made available at intervals of 15 minutes and better (Herron - private communication). Clearly for quantitative interpretation it is desirable to use magnetic observations made at a closer interval than 10-15 minutes, if available. However, those interpolated values used are considered to be essentially representative of the observed profile. Magnetic anomaly values, shown in Fig. (6.3), were computed by subtracting a linear least squares regional gradient and the principal low order fourier components, from the total field values.

The general bathymetry of the Pacific-Antarctic ridge reveals a generally subdued relief which has the form of a very broad and gently sloping arch (Menard & Chase 1965). Seismic profiler evidence from the South Pacific (Ewing et al 1969) indicates that, for an assumed mean sediment velocity of 2 km/sec, the sediment cover along the profile considered is less than 100 metres. It is therefore assumed that the bathymetry recorded along the profile represents the upper surface of Layer 2 (the adopted magnetic layer). Bathymetric readings for the profile were available at intervals of 5 minutes or better.

The lower surface of Layer 2 was assumed horizontal at a depth of 5 km. This estimate is generally consistent with the crustal model presented by Talwani et al (1965) for the East Pacific Rise near 16^{o}S. Use of a sloping surface for the Layer 2/3 interface would not significantly change the interpretation.

Layer 2 was then subdivided into 118 vertical sided model blocks 3 km wide, assumed to be uniformly magnetized in the direction of the earth's average geocentric dipole field. The Linear Inverse technique was then used to evaluate the distribution of magnetization, within this magnetic layer, from the observed magnetic anomalies. The resulting interpretation is shown in Fig. (6.3). The computed magnetic anomaly profile shows a reasonable simulation of the observed profile. The maximum residual value obtained was 84 gamma with an overall R.M.S. value of $\pm$19 gamma for the complete profile. The larger residual values are principally associated with areas of abrupt change in magnetic gradient. An improved simulation could have been obtained by the use of narrower model blocks - particularly near the ridge crest where the depth of water is less than 3 km. However, in view of possible

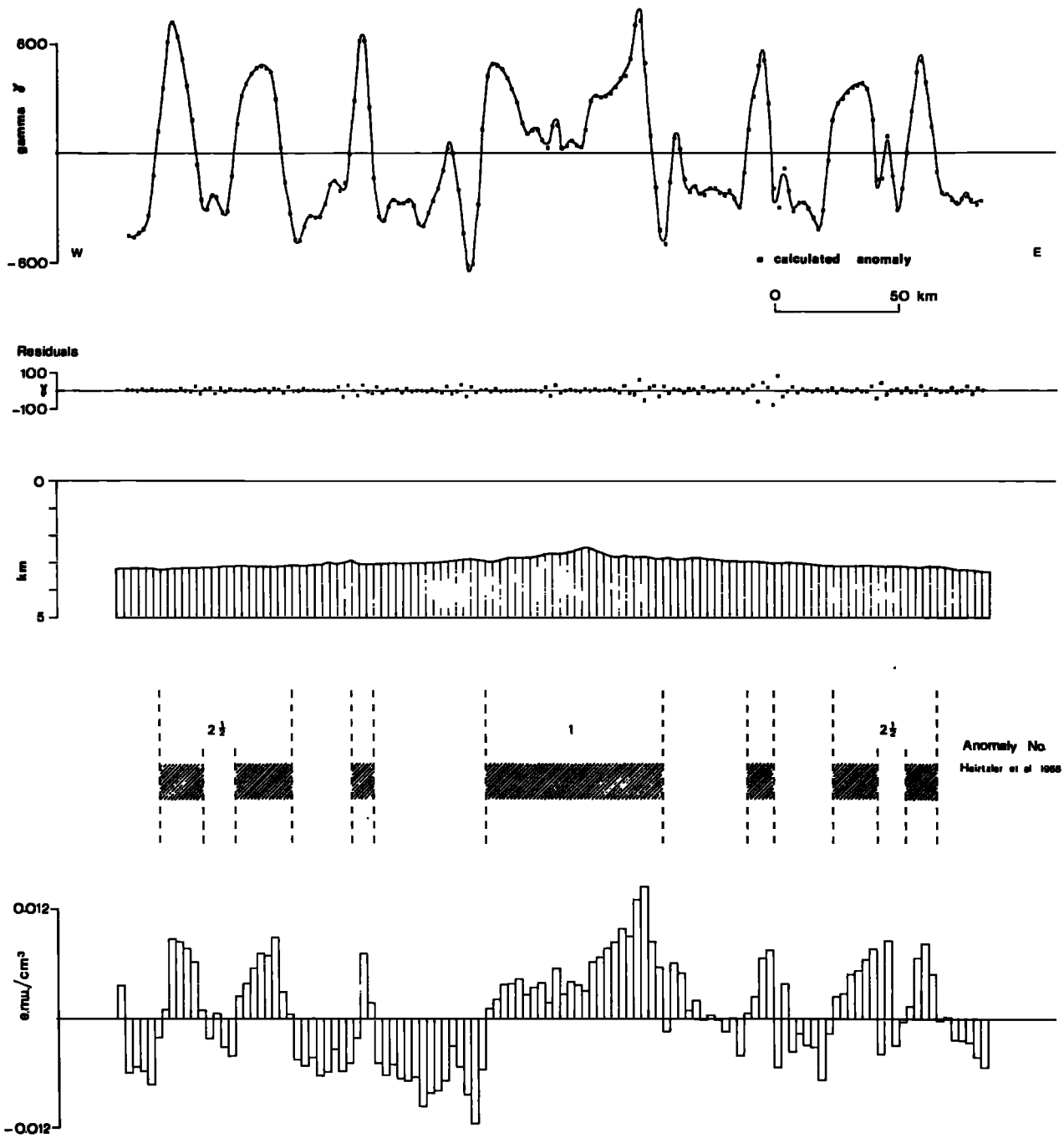

Fig. 6.3 Interpretation of the magnetic anomaly profile Eltanin-19, across the Pacific-Antarctic Ridge.

interpolation errors within the magnetic observations this procedure was not considered justifiable.

The resulting distribution of magnetization is in agreement with the Vine-Matthews hypothesis of sea-floor spreading and provisional correlations with the geomagnetic time scale established by Heirtzler et al (1968) are indicated. The identified reversal boundaries give an average spreading rate of 4.7 cm/yr/limb for the profile although there is some indication of a slightly reduced spreading rate for the south east limb. Emilia & Bodvarsson (1969) have presented a similar interpretation for this particular profile, in terms of an underlying distribution of magnetization confined to Layer 2.

The model elements of Fig. (6.3) were then modified to represent sloping bodies, by advancing their lower x - co-ordinates by 3 km towards the centre of the profile (Fig. 6.4a). Block boundaries then showed a gradual increase in dip (30^{o}-39^{o}) towards the centre of the profile, except for those few central elements that were constrained to have a near vertical dip. The observed magnetic profile was then re-interpreted in terms of this second model. The resulting distribution of magnetization and residual plot is shown in Fig. (6.4a).

As for the Juan de Fuca profile the computed magnetization pattern has remained essentially similar to that obtained with the magnetic model incorporating vertical sided blocks. Small arrows denote those areas of more obvious change. These areas show mainly small increases in amplitude and slightly more abrupt changes in magnetization. Again a satisfactory fit to the observed anomaly profile was obtained, with a maximum residual value of 48 gamma and an overall R.M.S. value of $\pm$12 gamma. This 'degree of fit' is an improvement when compared with that obtained for the previous model (Fig. 6.3). This is in contrast

to the situation observed across the Juan de Fuca ridge where residual values showed a slight increase under similar circumstances. Comparison of the residual plots shown in Fig. (6.3) and Fig. (6.4a) reveals that this result is principally due to the reduction in size of a few large residual values. The positions of these points corresponds to those areas of the magnetization distribution, noted earlier as displaying more abrupt local variations (Fig. 6.4a). Hence, larger residual differences would be expected at points intermediate to those considered.

The model elements were then re-adjusted to represent very low angle bodies (10^{o}-12^{o}) dipping towards the centre of the profile. The resulting interpretation of the observed magnetic profile in terms of this third model is shown in Fig. (6.4b). The computed magnetic profile again satisfactorily simulates the observed profile, the maximum residual value obtained being 64 gamma with an overall R.M.S. value of $\pm$14 gamma for the complete profile. This is only a small increase in misfit when compared with that obtained for the previous model. However, the computed distribution of magnetization now shows a significantly changed form, from that shown in Fig. (6.3). The histogram reveals an irregular oscillating pattern with fluctuations in the computed values reaching 0.036 e.m.u./cm^3. This distribution has very similar features to those obtained for the Juan de Fuca profile, under comparable conditions of low angle model elements (Fig. 6.2b). Rapid variations in intensity values are not so significant over the central section.of the ELTANIN-19 profile. This is partly due to compensation introduced from the assumed increase in thickness of the magnetic layer at the ridge crest.

Fig. 6.4a

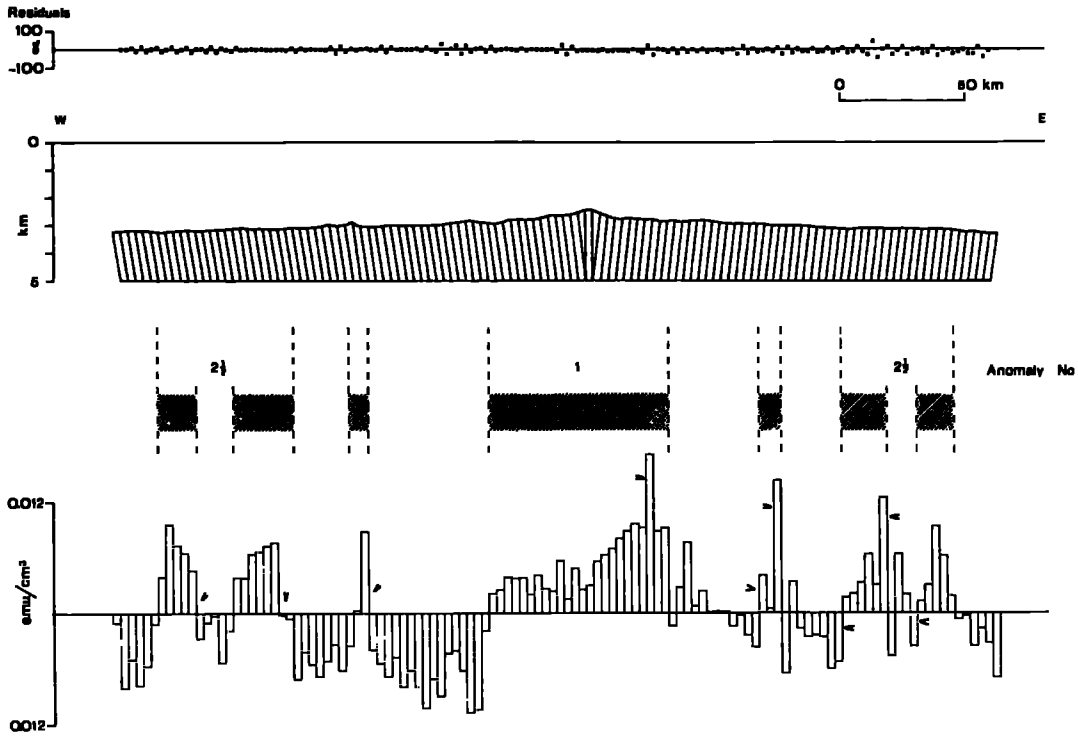

Fig. 6.4b

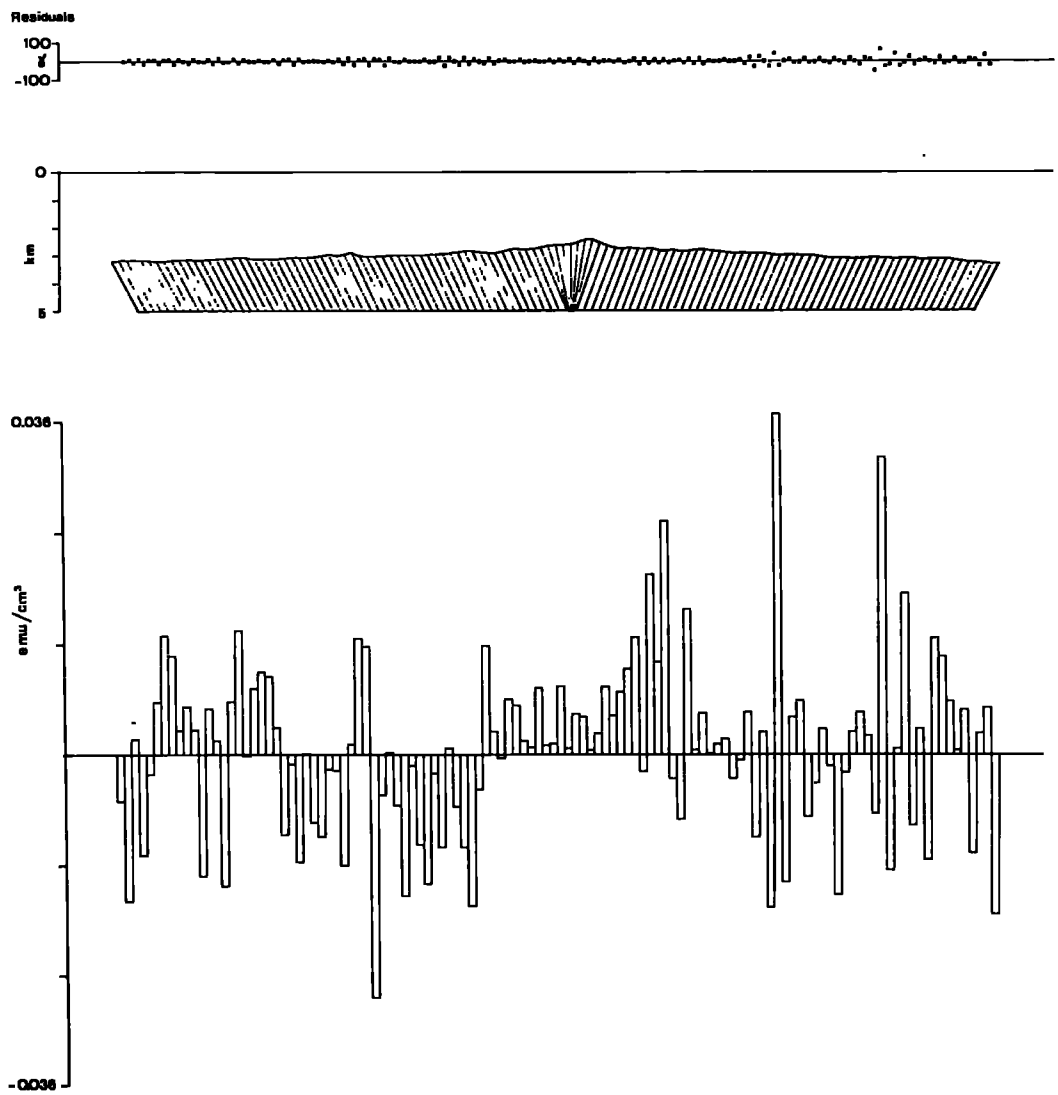

6.3 Discussion

The interpretations presented demonstrate that magnetic structures within Layer 2, inclined up to about 50° from the vertical, can explain typical oceanic magnetic anomalies. Those magnetic models incorporating bodies of very low inclination (10° and less, from the horizontal) appear unsuitable in view of the highly irregular values of magnetization required. Dredged rock samples having comparable magnetization values to those computed for these models (0.03-0.04 e.m.u./cm^3) have been reported from the mid-Atlantic ridge (e.g. Irving et al 1970). However, these rocks were obtained from the median valley zone where samples were found to be ten times more magnetic than those at a greater distance from the ridge axis. Furthermore, these values are most probably not representative of the true magnetization at depth, since this would cause very much larger magnetic anomalies than are observed. Also, the geological origin of extensive low angle structures near the ridge crest is difficult to understand. This is particularly so in view of the jumbled 'volcanic' sea-floor relief characteristic of crestal areas.

Because of the difficulty in accurately defining the magnetic gradients of oceanic anomalies, it is not possible to place more than a broad distinction between those magnetic models which are plausible and those which are not. It is considered that possible models may include bodies inclined up to 50° from the vertical whilst sheet-like bodies dipping at 15° and less are improbable. The general applicability of this conclusion depends largely on the severity of local magnetic gradients. Gradients observed at the crests of the Reykjanes Ridge and the Sheba Ridge, for example, would be difficult to explain in terms of anything other than a near vertical structure. However, within the indicated limits, the feasibility of magnetic models incorporating sloping bodies is acceptable. The distributions of

magnetization computed for these models, from the observed anomalies, remain compatible with the Vine-Matthews hypothesis of sea-floor spreading and radical complications are not envisaged. The rate of horizontal movement of the sea-floor is not affected as inferred polarity boundaries remain almost constant in position with respect to the sea-bed. Although the models considered in this study only include bodies sloping towards the ridge axis, comparable results would be expected for bodies inclined away from the ridge.

The implications of inclined intrusive structures, within the upper part of the oceanic crust, in terms of an emplacement mechanism are more significant. Current theories concerning the formation of crustal material at the axis of a mid-ocean ridge, almost exclusively require some form of vertical dyke injection in response to deep seated convection within the mantle (Dietz 1961; Hess 1962; Vine & Matthews 1963). Matthews & Bath (1967) and Harrison (1968) have both suggested models of dyke-injection which incorporate the bulk of such intrusive material over zones 10 and 6 km wide, respectively. Cann (1968) suggests that basalt may be discharged from uprising mantle currents at a depth of about 30 km in a zone about 20 km wide. However, a surface area of comparable width to this estimate, formed from intrusive structures inclined towards the ridge centre, would imply a narrower zone of injection at depth.

Structural controls that appear suitable for inclined intrusive bodies have been demonstrated by a number of authors. Sykes (1967) has shown that, from the interpretation of earthquake mechanisms, typical ridge crest faults are normal ones, with a fault plane striking nearly parallel to the ridge axis and dipping at about 60^{o}. Atwater & Mudie (1968) interpret step-like structures, observed across the rift valley

walls of the Gorda Rise, as the upper surfaces of tilted blocks. The boundaries of these features are considered to be inclined faults dipping at about 30^{o} towards the centre of the rift. Comparable fault systems have also been postulated by Van Andel (1968) and Van Andel & Bowin (1968) in an attempt to explain the structural development of the mid-Atlantic ridge. The fracture pattern indicated by Van Andel (1968, Fig. 9) suggests that basaltic material emplaced at the ridge crest may be subsequently faulted by fairly low angle faults, in response to renewed uplift of the ridge. Hence, this could give rise to a complex of inclined fault blocks, forming the basaltic layer and possibly extending for some 500 km away from the ridge crest.

It is interesting to note the somewhat anomalous situation reported by Cox & Doell (1962), Raff (1963) and Vine & Matthews (1963) concerning the experimental drilling phase of the Mohole project - Guadalupe site. Basalt samples retrieved from drill hole EM7 were found to be reversely magnetized, although the implied crustal polarity, deduced from the magnetic anomaly recorded above the drill site, was in the opposite sense. Raff (1963, Fig. 2) suggests that a thin isolated layer of reversely magnetized lava overlies a normally magnetized block. This situation could perhaps be readily explained in terms of a thin offshoot from an adjacent inclined (as opposed to vertical) structure of reversed polarity.

It is concluded therefore that vertical 'dyke-like' bodies commonly assumed to form the bulk of Layer 2 may be an oversimplification of the true structure. Magnetic models incorporating inclined structures provide good simulations of observed profiles and remain compatible with the theory of sea-floor spreading and the principal structural controls known to exist at mid-ocean ridge crests. However, the magnetic interpretations presented can not distinguish between near vertical and

semi-inclined structures, although near horizontal bodies are considered to be unreasonable in view of the unlikely distribution of magnetization required to explain the observed anomalies. It is to be emphasized that those models examined are only simplified representations of the structural form of Layer 2. Clearly a more irregular distribution of structural elements would be expected within the oceanic crust due to the combined effect of both vertical and inclined intrusive bodies and any subsequent faulting.

CHAPTER 7

SUMMARY AND DISCUSSION

7.1 The Method of Interpretation

The task of interpreting oceanic magnetic anomalies generally reduces to the problem of either defining a magnetic basement, as the upper surface of a uniformly magnetized source body, or evaluating the variation in magnetization within a defined basement layer. The latter problem is encountered in interpreting oceanic magnetic anomalies associated with mid-ocean ridges. These anomalies can generally be treated as two-dimensional and may be reasonably interpreted in terms of a magnetic source within Layer 2. The distribution of magnetization within this basement layer can be directly determined, from the observed magnetic anomalies, by a linear inverse technique. This technique is based on the numerical solution of a linear integral equation (Bott 1967) which is approximated by a finite set of linear algebraic equations. These equations relate (n) observed magnetic anomaly field points (A_i) to (m) unknown magnetization values (J_j):

$$A_i = \sum_{j=1}^{m} K_{ij} J_j \qquad (i = 1,2.....n)$$

The solution of this system of equations specifies the distribution of magnetization required to explain the observed magnetic anomaly profile. The values of magnetization relate to a series of two-dimensional model blocks incorporated within the magnetic layer. Model blocks may be of irregular cross-section and the procedure provides a solution to both the completely determined and over-determined problem (i.e. $n \geq m$).

A completely determined system of equations, i.e. as many field points as model blocks within the magnetic layer (n=m), permits an exact solution of the problem. This is because every field point considered can be completely explained by the resulting magnetization distribution. However, solution of an overdetermined system (n> m), adopting a minimization procedure, is a more desirable form of interpretation. This procedure permits the consideration of an increased number of data points, from the observed magnetic anomaly, in terms of a magnetic model that may be subsequently modified for purposes of comparison.

Limitations in the method of interpretation principally arise from the instability inherent in any form of downward continuation of fields derived from potentials which satisfy Laplace's equation. The excessive amplification of short wavelength components within the magnetic data results in unwanted fluctuations of similar wavelength within the computed magnetization distribution. This incipient instability imposes a practical limitation on the model block width that may be satisfactorily resolved at a given depth. It is recommended that model block widths should be chosen to be comparable to, and not less than x(0.6), the depth to the upper surface of the magnetic layer, depending on the accuracy of the reduced observations.

Unwanted large amplitude fluctuations in magnetization result from the effect of quite small amplitude but long wavelength components within the magnetic observations. These components may result from the lack of correction for diurnal variation, or an unsuitable regional gradient. Their effect may mask the true polarity of magnetization values over sections of the profile considered and may also obscure true long wavelength variations in magnetization. Such fluctuations can be partially eliminated by suitable filtering or applying accurate corrections for the diurnal variation.

7.2 The Magnetic Layer

The magnetic layer causing oceanic magnetic anomalies is generally chosen to correspond with the seismic Layer 2. This layer is considered to be formed from a volcanic assemblage, principally of basaltic material. Initially Mason (1958), Mason & Raff (1961) and Vine & Matthews (1963) considered that the magnetic source, responsible for oceanic anomalies, could extend throughout the oceanic crust. At a later stage Vine & Wilson (1965) concluded that it was more reasonable to assume that the greatest contribution came from Layer 2. This was more in accord with the ideas of Hess (1962) who considered that the oceanic crust was formed from a thin veneer of basalt (1-2 km), on top of the main crustal layer of serpentinized peridotite which was considered to be weakly magnetic (Cox et al 1964).

However, recent work indicates that serpentinite possesses a strong magnetization (Opdyke & Hekinian 1967; Irving et al 1970). Since the remanent magnetization of Layer 3 is probably not as significant as that of Layer 2, from other considerations (Bott 1967; Carmichael 1970), the above results argue against a serpentinite composition for Layer 3. Support for a basaltic or gabbroic composition for Layer 3 is based primarily on the rejection of serpentinite as a major constituent of the oceanic crust. Cann (1968) suggests that while Layer 2 is metamorphosed at depth to a greenschist facies meta-basalt (Melson & Van Andel 1966), Layer 3 corresponds to a higher grade of metamorphism: the amphibolite facies.

Measurements of the magnetic properties of rocks dredged from the mid-Atlantic ridge (Luyendyk & Melson 1967; Opdyke & Hekinian 1967) have revealed that, in general, basalts show a range of magnetic intensity that extends over four orders of magnitude while metamorphics are another order lower than the lowest basalts. Melson & Van Andel (1966) suggest

that the alteration of basalts to a greenschist facies, at about 2 km beneath the sea-floor, effectively demagnetizes the basaltic material. Hence if there was a regional level below which all basalts were metamorphosed to greenschist facies, then this level would represent the base of the magnetic layer (Van Andel 1968).

Recent determinations of high remanent magnetization values from the mid-Atlantic ridge (Irving et al 1970; De Boer et al 1970) suggest that the effective magnetic layer may even be confined to within 0.5 km of the upper surface of Layer 2. However, this interpretation is subject to some ambiguity in view of a possible sampling bias.

7.3 Interpretational Results

Interpretations of magnetic profiles in the North Atlantic, Gulf of Aden and the Pacific, are presented in terms of computed distributions of magnetization confined to Layer 2. The resulting magnetization patterns, reveal a characteristic sequence of values alternating between more positive and more negative values and give strong support to the Vine-Matthews hypothesis of sea-floor spreading. The identification of geomagnetic reversal boundaries (Heirtzler et al 1968), chosen by consideration of changes in magnetization, provide estimates of rates of crustal spreading. Computed rates are generally consistent with values obtained by other authors, using indirect simulation techniques, although small variations are noticed for most profiles considered. These variations may be due, in part, to errors of observations and technique although they suggest that the rate of injection of material at the ridge axis is locally irregular.

General results, assuming a uniform thickness for Layer 2, suggest certain regional differences in the bulk magnetization of the oceanic crust. Interpretations from the Pacific and central North Atlantic

(near 45°N) show that crestal sections of the magnetic layer are not significantly more magnetic than adjacent sections. However, results from the Reykjanes Ridge and the Gulf of Aden indicate that the median zone of the ridge system is slightly more magnetic than flanking areas. Reasons for these apparent differences are not clear. Local demagnetization effects at the ridge crest may be responsible in part (cf. Irving et al 1970).

Within the computed distributions of magnetization transition zones, between areas identified to be of normal and reversed polarity, are generally quite abrupt. Profiles in the North Atlantic and Gulf of Aden show a close correspondence of those values of magnetization, associated with the axial anomaly, within the local median valley. This suggests that volcanic material is emplaced within a narrow band width and contamination of adjacent crustal sections is not significant.

Studies of representative magnetic profiles have shown that both vertical and inclined source bodies, within Layer 2, are plausible structures and can explain the observed anomalies. The interpretations presented do not distinguish between these models, although it is concluded that extensive, sub-horizontal bodies (dipping at 10° and less) are unlikely in view of the unreasonable distributions of magnetization required.

Model studies confirm the feasibility of a thin magnetic layer (0.5 km), situated just below the sea-floor. Subsequent disruption of this thin layer could account for the somewhat irregular magnetic pattern observed over certain parts of the ridge system (e.g. near 45°N on the mid-Atlantic ridge). This model suggests that extensive dyke-injection of material may be unnecessary and volcanic activity at the crests of mid-ocean ridges may be more comparable to that in Iceland,

where there is little evidence for dense swarms of dykes (Walker 1960). However, verification of this model rests with precise seismic reflection and refraction work, combined with palaeomagnetic studies of representative rock samples drilled from the sea-floor.

REFERENCES

AL-CHALABI, M. 1970. Unpublished Ph.D. thesis. University of Durham. (in preparation).

ALLEN, T.D. 1969. A review of marine geomagnetism. Earth-Sci. Rev. 5, 217-254.

ANDERSSEN, R.S. 1969. On the solution of certain overdetermined systems of linear equations that arise in geophysics. J. Geophys. Res. 74, 1045-1051.

ANONYMOUS. 1969. International geomagnetic reference field. 1965. J. Geophys. Res. 74, 4407-4408.

ATWATER, T.M. and MUDIE, J.D. 1968. Block faulting on the Gorda Rise. Science. 159, 729-731.

AUMENTO, F. 1968. The Mid-Atlantic Ridge near 45°N. II.Basalts from the area of Confederation Peak. Can. J. Earth Sci. 5, 1-21.

———— 1969. The Mid-Atlantic Ridge near 45°N. V. Fission track and ferro-manganese chronology. Can. J. Earth Sci. 6, 1431-1440.

———— 1970. Geology of the Mid-Atlantic Ridge at 45°N. Symposium of petrology of rocks from the ocean floor. London: Roy. Soc. Spec. Paper. (in press).

AUMENTO, F. and LONCAREVIC, B.D. 1969. The Mid-Atlantic Ridge near 45°N. III. Bald Mountain. Can. J. Earth Sci. 6, 11-23.

AVERY, O.E., BURTON, G.D. and HEIRTZLER, J.R. 1968. An aeromagnetic survey of the Norwegian Sea. J. Geophys. Res. 73, 4583-4600.

AVERY, O.E., VOGT, P.R. and HIGGS, R.H. 1969. Morphology, magnetic anomalies and evolution of the Northeast Atlantic and Labrador Sea - Part 2. Magnetic anomalies. Trans. Am. Geophys. Un. 50, 184.

BARRET, D.L. 1967. Frequency modulation of a shipborne proton magnetometer signal due to the hydrodynamic instability of the towed vehicle. J. Geophys. Res. 73, 5327-5334.

BARTELS, J. 1957. Geomagnetic measures for the time-variations of solar corpuscular radiation. I.G.Y. Annals. 4, London: Pergamon Press. 227-236.

BOTT, M.H.P. 1963. Two methods applicable to computers for evaluating magnetic anomalies due to finite three dimensional bodies. Geophys. Prosp. 11, 292-299.

BOTT, M.H.P. 1967. Solution of the linear inverse problem in magnetic interpretation with application to oceanic magnetic anomalies. Geophys. J.R. astr. Soc. 13, 313-323.

———— 1969a. Durham University geophysical computer programme specification No. 2. MAGN.

———— 1969b. Computation of the magnetic anomalies caused by two-dimensional bodies. Geophys. J.R. astr. Soc. 18, 251-256.

BOTT, M.H.P. and HUTTON, M.A. 1970a. Limitations on the resolution possible in the direct interpretation of marine magnetic anomalies. Earth Planet. Sci. Lett. 8, 317-319.

———————————— 1970b. A matrix method for interpreting oceanic magnetic anomalies. Geophys. J.R. astr. Soc. 20, 149-157.

BOTT, M.H.P. and STACEY, A.P. 1967. Geophysical evidence on the origin of the Faeroe Bank Channel - II. A gravity and magnetic profile. Deep-Sea Res. 14, 7-11.

BRUCKSHAW, J.M. and KUNARATNAM, K. 1963. The interpretation of magnetic anomalies due to dykes. Geophys. Prosp. 11, 511-522.

BULLARD, E.C. 1967a. Electromagnetic induction in the earth. Quart. J. Roy. astr. Soc. 8, 143-160.

———— 1967b. The removal of trend from magnetic surveys. Earth Planet. Sci. Lett. 2, 293-300.

BULLARD, E.C. and MASON, R.G. 1961. The magnetic field astern of a ship. Deep-Sea Res. 8, 20-27.

BULLARD, E.C., EVERETT, J.E. and SMITH, A.G. 1965. The fit of the continents around the Atlantic. Phil. Trans. Roy. Soc. Lond. A, 258, 41-51.

BUTLER, P.F. 1968. The interpretation of magnetic field anomalies over dykes by optimization procedures. Unpublished M.Sc. thesis. University of Durham. 55pp.

CAIN, J.C. 1965. Models of the earth's magnetic field. Goddard Space Flight Centre, Res. Rept. X-612-65-400.

CANN, J.R. 1968. Geological processes at mid-ocean ridge crests. Geophys. J.R. astr. Soc. 15, 331-341.

CANN, J.R. and VINE, F.J. 1966. An area on the crest of the Carlsberg Ridge: petrology and magnetic survey. Phil. Trans. Roy. Soc. Lond. A, 259, 198-217.

CARMICHAEL, C.M. 1970. The Mid-Atlantic ridge near 45°N. VII. Magnetic properties and opaque mineralogy of dredged samples. Can. J. Earth Sci. 7, 239-256.

CHAPMAN, S. 1961. The earth's magnetism. London: Methuen & Co. Ltd.

COX, A. 1969. Geomagnetic reversals. Science. 163, 237-245.

COX, A. and DOELL, R.R. 1962. Magnetic properties of the basalt in hole EM7, Mohole Project. J. Geophys. Res. 67, 3997-4004.

COX, A., DOELL, R.R. and DALRYMPLE, G.B. 1963. Geomagnetic polarity epochs and Pleistocene geochronometry. Nature, Lond. 198, 1049-51.

———————————— 1964. Reversals of the earth's magnetic field. Science. 144, 1537-1543.

———————————— 1968. Time scale for geomagnetic reversals. In: The history of the earth's crust, NASA Symposium. New Jersey: Princeton University Press. 101-108.

COX, A., DOELL, R.R. and THOMPSON, G. 1964. Magnetic properties of serpentinite from Mayaguez, Puerto Rico. In: A study of serpentinite NAS-NRC Publ. no. 1188, 49-60.

DALRYMPLE, G.B., COX, A., DOELL, R.R. and GROMME, C.S. 1967. Pliocene geomagnetic polarity epochs. Earth Plant. Sci. Lett. 2, 163-173.

DE BOER, J., SCHILLING, J.-G. and KRAUSE, D.C. 1969. Magnetic polarity of pillow basalts from Reykjanes Ridge. Science. 166, 996-998.

———————————— 1970. Reykjanes Ridge: Implications of magnetic properties of dredged rock. Earth Planet. Sci. Lett. 9, 55-60.

DICKSON, G.O., PITMAN, W.C. and HEIRTZLER, J.R. 1968. Magnetic anomalies in the South Atlantic and ocean floor spreading. J. Geophys. Res. 73, 2087-2100.

DIETZ, R.S. 1961. Continent and ocean basin evolution by spreading of the sea floor. Nature, Lond. 190, 854-857.

DOELL, R.R. and DALRYMPLE, G.B. 1966. Geomagnetic polarity epochs - a new polarity event and the age of the Brunhes-Matuyama boundary. Science. 152, 1060-1061.

ELSASSER, W.M. 1967. Convection and stress propagation in the upper mantle. Princeton University Technical Rept. 5.

EMILIA, D.A. and BODVARSSON, G. 1969. Numerical methods in the direct interpretation of marine magnetic anomalies. Earth Planet. Sci. Lett. 7, 194-200.

———————————— 1970. More on the direct interpretation of magnetic anomalies. Earth Planet. Sci. Lett. 8, 320-321.

EWING, J. and EWING, M. 1959. Seismic refraction measurements in the Atlantic Ocean basins, in the Mediterranean Sea, on the Mid-Atlantic Ridge, and in the Norwegian Sea. Bull. Geol. Soc. Am. 70, 291-318.

———————————— 1967. Sediment distribution on the mid-ocean ridges with respect to spreading of the sea floor. Science. 156, 1590-1592.

EWING, M., EWING, J.I. and TALWANI, M. 1964. Sediment distribution in the oceans: The Mid-Atlantic Ridge. Bull. Geol. Soc. Am. 75, 17-36.

EWING, M., HEEZEN, B.C. and HIRSHAM, J. 1957. Mid-Atlantic Ridge seismic belts and magnetic anomalies. Seismol. Assoc. Intern. Union Geodesy Geophys. Gen. Assembly: Toronto. (abstract).

EWING, M., HOUTZ, R. and EWING, J. 1969. South Pacific sediment distribution. J. Geophys. Res. 74, 2477-2493.

GAY, S.P. 1963. Standard curves for interpretation of magnetic anomalies over long tabular bodies. Geophysics 28, 161-200.

GODBY, E.A., HOOD, P.J. and BOWER, M.E. 1968. Aeromagnetic profiles across the Reykjanes Ridge southwest of Iceland. J. Geophys. Res. 73, 7637-7649.

GOLUB, G. 1965. Numerical methods for solving linear least squares problems. Numerische Mathematik. 7, 206-216.

HARRISON, C.G.A. 1968. Formation of magnetic anomaly patterns by dyke injection. J. Geophys. Res. 73, 2137-2142.

HAYS, J.D. and OPDYKE, N.D. 1967. Antarctic Radiolaria, magnetic reversals and climatic change. Science. 158, 1001-1011.

HEEZEN, B.C., EWING, M. and MILLER, E.T. 1953. Trans-Atlantic profile of total magnetic intensity and topography, Dakar to Barbados. Deep-Sea Res. 1, 25-33.

HEEZEN, B.C., THARP, M. and EWING, M. 1959. The floors of the oceans, 1. the North Atlantic. Geol. Soc. Am. Spec. Paper. 65, 126pp.

HEIRTZLER, J.R., DICKSON, G.O., HERRON, E.M., PITMAN, W.C. and LE PICHON, X. 1968. Marine magnetic anomalies, geomagnetic field reversals and motions of the ocean floor and continents. J. Geophys. Res. 73, 2119-2136.

HEIRTZLER, J.R. and HAYS, D.E. 1967. Magnetic boundaries in the North Atlantic Ocean. Science. 1957, 185-187.

HEIRTZLER, J.R. and LE PICHON, X. 1965. Crustal structure of the mid-ocean ridges, 3. Magnetic anomalies over the Mid-Atlantic Ridge. J. Geophys. Res. 70, 4013-4033.

HEIRTZLER, J.R., LE PICHON, X. and BARON, J.G. 1966. Magnetic anomalies over the Reykjanes Ridge. Deep-Sea Res. 13, 427-443.

HESS, H.H. 1962. History of ocean basins. In: Petrological Studies. A volume to honour A.F. Buddington. Geol. Soc. Am., New York. 599-620.

HILL, M.N. 1959. A ship-borne nuclear-spin magnetometer. Deep-Sea Res. 5, 309-311.

———— 1960. A median valley of the Mid-Atlantic Ridge. Deep-Sea Res. 6, 193-205.

———— 1966. A discussion concerning the floor of the northwest Indian Ocean. Phil. Trans. Roy. Soc. Lond. A, 259, 133-298.

HOLMES, A. 1965. The principles of physical geology. London: Nelson.

HYDROGRAPHER-NETHERLANDS. 1967. Navado III. Bathymetric, magnetic and gravity investigations H. Neth. M.S. SNELLIUS, 1964-1965. Hydrographic Newsletter, Special Publ. no. 3, 8-9.

I.B.M. 1968. System/360, scientific subroutine package (360A-CM-03X). Version III. Programmer's manual. New York: I.B.M.

——— 1969. System/360, scientific subroutine package (PL/1) (360A-CM-07X). Programme Description and operations manual. New York: I.B.M.

IRVING, E., ROBERTSON, W.A. and AUMENTO, F. 1970. The Mid-Atlantic Ridge near 45°N. VI. Remanent intensity, susceptibility and iron content of dredged samples. Can. J. Earth Sci. 7, 226-238.

ISACKS, B. and MOLNAR, P. 1969. Mantle earthquake mechanisms and the sinking of the lithosphere. Nature, Lond. 223, 1121-1124.

ISACKS, B., OLIVER, J. and SYKES, L.R. 1968. Seismology and the new global tectonics. J. Geophys. Res. 73, 5855-5899.

JACOBS, J.A. and WESTPHAL, K.O. 1964. Geomagnetic micropulsations. In: Physics and chemistry of the earth. 5, London: Pergamon Press. 157-224.

JOHNSON, W.W. 1969. A least squares method of interpreting magnetic anomalies caused by two-dimensional structures. Geophysics. 34, 65-74.

KEEN, M.J. 1963. Magnetic anomalies over the Mid-Atlantic Ridge. Nature, Lond. 197,888-890.

KEEN, M.J. and MANCHESTER, K.S. 1970. The Mid-Atlantic Ridge near 45°N. X. Sediment distribution and thickness from seismic reflection profiling. Can. J. Earth Sci. 7, 735-747.

LAUGHTON, A.S. 1965. The Gulf of Aden, in relation to the Red Sea and the Afar depression of Ethiopia. In: The world rift system, Report of U.M.C. symposium. Ottawa: Geol. Surv. Paper 66-14, 78.

———————— 1966. The Gulf of Aden. Phil. Trans. Roy. Soc. Lond. A, 259, 150-171.

LAUGHTON, A.S. and TRAMONTINI, C. 1970. Recent studies of the crustal structure in the Gulf of Aden. Geophys. J. R. astr. Soc. (in press).

LAUGHTON, A.S., WHITMARSH, R.B. and JONES, M.T. 1969. The evolution of the Gulf of Aden. Proc. Roy. Soc. Lond. (in press).

LE PICHON, X. 1968. Sea-floor spreading and continental drift. J. Geophys. Res. 73, 3661-3697.

LE PICHON, X. and HEIRTZLER, J.R. 1968. Magnetic anomalies in the Indian Ocean and sea-floor spreading. J. Geophys. Res. 73, 2101-2117.

LE PICHON, X., HOUTZ, R.E., DRAKE, C.L. and NAFE, J.E. 1965. Crustal structure of the mid-ocean ridges. 1. Seismic refraction measurements. J. Geophys. Res. 70, 319-339.

LONCAREVIC, B.D., MASON, C.S. and MATTHEWS, D.H. 1966. Mid-Atlantic Ridge near 45°N. I. The median valley. Can. J. Earth Sci. 3, 327-349.

LONCAREVIC, B.D. and PARKER, R.L. 1970. Mid-Atlantic Ridge near 45°N. XI. Magnetic anomalies and ocean floor spreading. Can. J. Earth Sci. (in press).

LUYENDYK, B.P. 1969. Origin of short-wavelength magnetic lineations observed near the ocean bottom. J. Geophys. Res. 74, 4869-4881.

LUYENDYK, B.P. and MELSON, W.G. 1967. Magnetic properties and petrology of rocks near the crest of the Mid-Atlantic Ridge. Nature, Lond. 215, 147-149.

LUYENDYK, B.P., MUDIE, J.D. and HARRISON, C.G.A. 1968. Lineations of magnetic anomalies in the northeast Pacific observed near the ocean floor. J. Geophys. Res. 73, 5951-5957.

MASON, R.G. 1958. A magnetic survey off the west coast of the United States between latitudes 32° and 36°N, longitudes 121° and 128°W. Geophys. J. R. astr. Soc. 1, 320-329.

MASON, R.G. and RAFF, A.D. 1961. Magnetic survey off the west coast of North America, 32°N. latitude to 42°N. latitude. Bull. Geol. Soc. Am. 72, 1259-1266.

MATTHEWS, D.H. 1966. The Owen fracture zone and the northern end of the Carlsberg Ridge. Phil. Trans. Roy. Soc. Lond. A, 259, 172-186.

MATTHEWS, D.H. and BATH, J. 1967. Formation of magnetic anomaly pattern of Mid-Atlantic Ridge. Geophys. J. R. astr. Soc. 13, 349-357.

MATTHEWS, D.H., VINE, F.J. and CANN, J.R. 1965. Geology of an area of the Carlsberg Ridge, Indian Ocean. Bull. Geol. Soc. Am. 76, 675-682.

MATTHEWS, D.H., WILLIAMS, C. and LAUGHTON, A.S. 1967. Mid-ocean ridge in the mouth of the Gulf of Aden. Nature, Lond. 215, 1052-1053.

MATTHEWS, D.J. 1939. Tables of the velocity of sound in pure water and sea water for use in echo-sounding and echo-ranging. 2nd ed. Brit. Admiralty Hydrograph. Dept. Publ. H.D. 282.

MAXWELL, A.E., VON HERZEN, R.P., JINGHWA HSÜ, K., ANDREWS, J.E., SAITO, T., PERCIVAL, S.F., MILOW, E.D. and BOYCE, R.E. 1970. Deep sea drilling in the South Atlantic. Science. 168, 1047-1059.

McKENZIE, D.P. 1969. Speculations on the consequences and causes of plate motions. Geophys. J. R. astr. Soc. 18, 1-32.

McKENZIE, D.P. and PARKER, R.L. 1967. The North Pacific: an example of tectonics on a sphere. Nature, Lond. 216, 1276-1280.

MELSON, W.G. and VAN ANDEL, T.H. 1966. Metamorphism in the Mid-Atlantic Ridge, 22°N latitude. Marine Geol. 4, 165-186.

MENARD, H.W. and CHASE, T.E. 1965. Tectonic effects of upper mantle motion. In: Upper mantle symposium, New Delhi. New York: McGraw-Hill. 29-36.

MORGAN, W.J. 1968. Rises, trenches, great faults and crustal blocks. J. Geophys. Res. 73, 1959-1982.

NAFE, J.E. and DRAKE, C.L. 1969. Floor of the North Atlantic - summary of geophysical data. In: North Atlantic - geology and continental drift, Memoir 12, The Am. Ass. Petroleum Geologists.

NAGATA, T. 1961. Rock magnetism. Tokyo: Maruzen Company Ltd.

NOBLE, C.S. and NAUGHTON, J.J. 1968. Deep-ocean basalts: inert gas content and uncertainties in age dating. Science. 162, 265-266.

OPDYKE, N.D. and GLASS, B.P. 1969. The palaeomagnetism of sediment cores from the Indian Ocean. Deep-Sea Res. 16, 249-261.

OPDYKE, N.D., GLASS, B., HAYS, J.D. and FOSTER, J. 1966. Palaeomagnetic study of Antarctic deep-sea cores. Science. 154, 349-357.

OPDYKE, N.D. and HEKINIAN, R. 1967. Magnetic properties of some igneous rocks from the Mid-Atlantic Ridge. J. Geophys. Res. 72, 2257-2260.

OZIMA, M., OZIMA, M. and KANEOKA, I. 1968. Potassium-argon ages and magnetic properties of some dredged submarine basalts and their geophysical implications. J. Geophys. Res. 73, 711-723.

PETER, G. and LATTIMORE, R. 1969. Magnetic structure of the Juan de Fuca-Gorda Ridge area. J. Geophys. Res. 74, 586-593.

PHILLIPS, J.D. 1967. Magnetic anomalies over the Mid-Atlantic Ridge near 27°N. Science. 157, 920-923.

PHILLIPS, J.D., THOMPSON, G., VON HERZEN, R.P. and BOWEN, V.T. 1969. Mid-Atlantic Ridge near 43°N latitude. J. Geophys. Res. 74, 3069-3081.

PITMAN, W.C. and HEIRTZLER, J.R. 1966. Magnetic anomalies over the Pacific-Antarctic Ridge. Science. 154, 1164-1171.

PITMAN, W.C., HERRON, E.M. and HEIRTZLER, J.R. 1968. Magnetic anomalies in the Pacific and sea floor spreading. J. Geophys. Res. 73, 2069-2085.

RAFF, A.D. 1963. Magnetic anomaly over Mohole Drill Hole EM7. J. Geophys. Res. 68, 955-956.

———— 1966. Boundaries of an area of very long magnetic anomalies in the northeast Pacific. J. Geophys. Res. 71, 2631-2636.

RAFF, A.D. and MASON, R.G. 1961. Magnetic survey off the west coast of North America, 40°N. latitude to 52°N. latitude. Bull. Geol. Soc. Am. 72, 1267-1270.

RIKITAKE, T. 1966. Electromagnetism and the earth's interior. Amsterdam: Elsevier.

ROBERTS, D.G. and WHITMARSH, R.B. 1969. A bathymetric and magnetic survey of the Gulf of Tadjura, western Gulf of Aden. Earth Planet. Sci. Lett. 5, 253-258.

ROY, A. 1962. Ambiguity in geophysical interpretation. Geophysics. 27, 90-99.

SCHNEIDER, E.D. and VOGT, P.R. 1968. Discontinuities in the history of sea-floor spreading. Nature, Lond. 217, 1212-1222.

SMITH, R.A. 1960. Some formulae for interpreting local gravity anomalies. Geophys. Prosp. 8, 609-613.

———— 1961. Some theorems concerning local magnetic anomalies. Geophys. Prosp. 9, 399-410.

SRIVASTAVA, S.P. 1969. Magnetic variations for ground station, B.I., for June 1968. B.I. Data series 1968-8-D. Unpublished manuscript.

STACEY, A.P. 1968. Interpretation of gravity and magnetic anomalies in the N.E. Atlantic. Unpublished Ph.D. thesis. University of Durham. 144pp.

STACEY, R.A. 1965. Computer methods for the interpretation of two-dimensional gravity and magnetic anomalies. Unpublished Ph.D. thesis. University of Durham. 169pp.

SYKES, L.R. 1966. The seismicity and deep structure of island arcs. J. Geophys. Res. 71, 2981-3006.

———— 1967. Mechanism of earthquakes and nature of faulting on the mid-ocean ridges. J. Geophys. Res. 72, 2131-2153.

———— 1968. Seismological evidence for transform faults, sea floor spreading and continental drift. In: The history of the earth's crust, NASA Symposium. New Jersey: Princeton University Press. 120-150.

TALWANI, M. and HEIRTZLER, J.R. 1964. Computation of magnetic anomalies caused by two-dimensional structures of arbitrary shape. In: Computers in the mineral industries. Stanford: Stanford University Press. 464-480.

TALWANI, M., LE PICHON, X. and EWING, M. 1965. Crustal structure of the mid-ocean ridges, 2. Computed model from gravity and seismic refraction data. J. Geophys. Res. 70, 341-352.

TALWANI, M., LE PICHON, X. and HEIRTZLER, J.R. 1965. East Pacific Rise: The magnetic pattern and the fracture zones. Science. 150, 1109-1115.

TALWANI, M., WINDISCH, C., LANGSETH, M. and HEIRTZLER, J.R. 1968. Recent geophysical studies on the Reykjanes Ridge. AGU 49th meeting Washington. Trans. Am. Geophys. Un. 49, 201.

TANNER, J.G. 1967. An automated method of gravity interpretation. Geophys. J. R. astr. Soc. 13, 339-347.

ULRICH, J. 1960. Zur topographie des Reykjanes-Rückens. Kieler Meersef. 16, 155-163.

———— 1962. Echolotprofile der Forschungsfahrten von F.F.S. Anton Dohrn and V.F.S. Gauss in I.G.Y. 1957/68. Dt. hydrogr. Z, Erganzungsheft. 4, 15pp.

VACQUIER, V., RAFF, A.D. and WARREN, R.E. 1961. Horizontal displacements in the floor of the northeastern Pacific Ocean. Bull. Geol. Soc. Am. 72, 1251-1258.

VAN ANDEL, T.H. 1968. The structure and development of rifted midoceanic rises. J. Marine Res. 26, 144-161.

VAN ANDEL, T.H. and BOWIN, C.O. 1968. Mid-Atlantic Ridge between 22° and 23° north latitude and the tectonics of mid-ocean rises. J. Geophys. Res. 73, 1279-1298.

VINE, F.J. 1966. Spreading of the ocean floor: New Evidence. Science. 154, 1405-1415.

VINE, F.G. and MATTHEWS, D.H. 1963. Magnetic anomalies over oceanic ridges. Nature, Lond. 199, 947-949.

VINE, F.J. and WILSON, J.T. 1965. Magnetic anomalies over a young oceanic ridge off Vancouver Island. Science. 150, 485-489.

VOGT, P.R. and OSTENSO, N.A. 1966. Magnetic survey over the Mid-Atlantic Ridge between 42°N and 46°N. J. Geophys. Res. 71, 4389-4411.

WATKINS, N.D., PASTER, T. and ADE-HALL, J. 1970. Variation of magnetic properties in a single deep-sea pillow basalt. Earth Planet. Sci. Lett. 8, 322-328.

WALKER, G.P.L. 1960. Zeolite zones and dyke distribution in relation to the structure of the basalts of eastern Iceland. J. Geol. 68, 515-528.

WILSON, J.T. 1965a. A new class of faults and their bearing on continental drift. Nature, Lond. 207, 343-347.

———— 1965b. Transform faults, oceanic ridges and magnetic anomalies south west of Vancouver Island. Science. 150, 482-485.

APPENDIX 1

THE COMPUTER PROGRAMME MXOCEAN III A

This programme uses a least squares matrix technique to directly evaluate a distribution of magnetization, within a specified two-dimensional magnetic layer, which causes a given magnetic anomaly. The magnetic layer is formed from a series of adjacent model blocks, represented by vertical trapezia, having a defined direction of magnetization. The programme prints out details of the magnetic layer used, the observed, calculated and residual (observed minus calculated) magnetic anomalies and the calculated magnetization values. The programme has been written in PL/1 for use on the N.U.M.A.C. I.B.M. 360/67.

Notes on data format

Data items should be written as integer and fixed point decimal numbers in a form appropriate to PL/1. Items follow each other sequentially and must be separated by at least one space or by a comma. Data input points are labelled LO, L2, ... L8 in the programme 'print out'.

LO:

HE, ALFE, HM, ALFM are the values of the dip and azimuth of the earth's field and dip and azimuth of the direction of magnetization, respectively. These are in degrees. The azimuths are measured from the strike towards the positive x-axis and the dips are measured from the azimuth directions downwards towards the positive z-axis.

V = total number of magnetic anomaly points.

W = total number of co-ordinate points defining the upper surface of the magnetic layer used. Number of model blocks within this layer = (W-1) unless block combination required (then see Z:LO and BC, PR:L8).

NO = total number of sections for the profile, normally set = 1 unless variable XSTEP (see L3, L5) required for different sections.

EPS = tolerance parameter (try = 0.0001), I.B.M. S.S.P. (LLSQ)

Z = W unless block combination required, then Z = final number of blocks after regular combination in groups of (BC+1) (see L8).

L2:

DATA = data control trigger,

If DATA = 0 then go to L3.

If DATA = 1 read x - co-ordinates (SX) and z - co-ordinates (SZ) of the magnetic anomaly field points, i.e. for irregular spaced data points.

L3:

Generation of magnetic anomaly field point co-ordinates for regular spaced data.

XO = initial x - co-ordinate of field point values.

ZO = z - co-ordinate for all field point values.

STA = array of numbers (dimension NO, see L1) specifying the final field point at the end of each profile section.

XSTEP = array of numbers (dimension NO) specifying x - increments for each section of the profile.

L4:

BATA = data control trigger,

If BATA = 0 then go to L5.

If BATA = 1 read x - co-ordinates (BX) and z - co-ordinates of upper (BU) and lower (BL) surfaces of magnetic layer; each array has (W) elements. These points define model block junctions.

L5:

Generation of x and z - co-ordinates for a magnetic layer, formed from model blocks having a regular width.

BXO = initial x - co-ordinate for outer edge of first model block.

BZB = z - co-ordinate for a horizontal surface forming the base of the magnetic layer.

SCALE = scaling parameter for z - co-ordinates of upper surface of magnetic layer, use as required.

BSTA = array of numbers (dimension NO) specifying the final body point at the end of each profile section.

BSTEP = array of numbers (dimension NO) specifying the block width for each section of the profile.

L6:

BATH = data control trigger,

If BATH = 0 read single value (POT) as the z - co-ordinate for a horizontal surface forming the top of the magnetic layer.

If BATH = 1 read series (W) of z - co-ordinates defining the upper surface of the magnetic layer.

L7:

AD = array of magnetic anomaly values (dimension V).

L8:

N.B. Automatic option if Z is not set equal to W, else input point is ignored by programme.

BC = number of successive model blocks to be combined with first model block. This procedure then steps along the magnetic layer, combining model blocks in groups of (BC+1).

PR = set = 1 if print out of information on above operation required (advised), else set = 0.

General Notes

(a) Magnetic anomaly values are in units of gamma, x-z units are arbitrary and intensity of magnetization values are in units of e.m.u./cm^3.

(b) Model block widths should be comparable to the depth to the upper surface of the magnetic layer and not less than about x 0.6 this value.

Appendix 1. Programme Print Out

```
//DGP1OFN  JOB  (0107,60,,2),DGP1ORT.M.HUTTON,MSGLEVEL=1,CLASS=G
//        EXEC PL1FCLG,TIME.G=(4,0)
//C.SYSIN   DD   *
          (SUBSCRIPTRANGE)
     MXOIIIA  PROCEDURE OPTIONS (MAIN)
  /*  ********************************************************************  */
  /*                                                                        */
  /*  ********************************************************************  */
  /*                                                                        */
  /*  THIS  PROGRAMME  USES  A  LEAST.SQUARES  MATRIX  TECHNIQUE            */
  /*  TO  DIRECTLY  EVALUATE  A  DISTRIBUTION  OF  MAGNETIZATION            */
  /*  WITHIN  A  SPECIFIED  TWO.DIMENSIONAL  MAGNETIC  LAYER  WHICH         */
  /*  CAUSES  A  GIVEN  MAGNETIC ANOMALY.  ***     A  THEORETICAL           */
  /*  MAGNETIC  PROFILE  IS  THEN  COMPUTED  FROM  THIS MAGNETISATION       */
  /*  DISTRIBUTION  AND  RESIDUAL  VALUES  EVALUATED                        */
  /*  THE  SOURCE  BODY  IS  REPRESENTED  BY  A  MODEL  FORMED  FROM        */
  /*  A  CONTINUOUS  SET  OF  ADJACENT  VERTICAL  TRAPEZIA                  */
  /*  A  DIRECTION  OF  MAGNETIZATION  FOR  THE  MODEL  IS  ASSUMED.        */
  /*  ********************************************************************  */
  /*                                                                        */
  /*  ********************************************************************  */
  /*        ***  PARAMETER  DEFINITIONS  ***                                */
  /*  HM=INCLINATION (D) OF  THE  MAGNETISATION  VECTOR.                    */
  /*  HE=INCLINATION (D) OF  THE  EARTH'S  MAGNETIC  FIELD.                 */
  /*  ALFM= AZIMUTH (D) OF  THE  DIRECTION  OF  MAGNETISATION               */
  /*  MEASURED  FROM  THE  STRIKE  OF  THE  BODY  TOWARDS  THE              */
  /*  POSITIVE  X AXIS.                                                     */
  /*  ALFE= AZIMUTH (D) OF  THE  EARTH'S  FIELD, MEASURED  AS  ALFM.        */
  /*  V=TOTAL  NUMBER  OF  MAGNETIC  ANOMALY  POINTS.                       */
  /*  W=TOTAL  NUMBER  OF  COORDINATES  DELINEATING  THE  UPPER             */
  /*  SURFACE  OF  THE  MODEL. *****  W MUST  NOT  EXCEED  (V+1).           */
  /*  NO=TOTAL  NO.  OF  SECTIONS  FOR  THE  PROFIE.  **  NORMALLY          */
  /*  SET=1  UNLESS  VARIABLE  XSTEP  REQUIRED  FOR  DIFFERENT  SECTIONS.   */
  /*  EPS  PARAMETER  REF.  I.B.M.  SSP  (LLSQ).                            */
  /*  Z= W  UNLESS  BLOCK  COMBINATION  REQUIRED  THEN  Z=FINAL             */
  /*  NUMBER  OF  BLOCKS  AFTER  COMBINATION  IN  GROUPS  OF  (BC+1)        */
  /*  AD= ARRAY STORING  MAGNETIC  ANOMALY  VALUES                          */
  /*  SX= ARRAY STORING  X  CO-ORDINATES OF ANOMALY POINTS                  */
  /*  SZ= ARRAY STORING  Z  CO-ORDINATES OF ANOMALY POINTS                  */
  /*  BX= ARRAY STORING  X  CO-ORDINATES OF MODEL SURFACE                   */
  /*  BU= ARRAY STORING  Z  CO-ORDINATES OF UPPER SURFACE OF MODEL          */
  /*  BL= ARRAY STORING  Z  CO-ORDINATES OF LOWER SURFACE OF MODEL          */
  /*  ********************************************************************  */
  /*                                                                        */
  /*  ********************************************************************  */
```

```
    DECLARE SAVE FILE RECORD SEQUENTIAL
    DECLARE (HM,HE,HHM,HHE,BETA,ALFM,ALFE,A,SBETA,CBETA,EPS,CA,CB,XSA
    ZSA,XSB,ZSB,DD,RA,RL,TA,TB,TT,TBA,THETA,EE,XS,ZS,SCALE,XO,ZO,BZO,
    BXO,DATA,BATA,BATH,POT,R,TEMP,TO1,TO2,PR)
    DECLARE (V,W,NO,Z,BC,IER,IC,IM,NOM)FIXED BINARY
 L0 GET LIST (HM,HE,ALFM,ALFE,V,W,NO,EPS,Z)
    A=SQRT(((COSD(HE))**2)*((SIND(ALFE))**2)+(SIND(HE))**2)*(((COSD(
    HM))**2)*((SIND(ALFM))**2)+(SIND(HM))**2))
    HHM=ATAND(SIND(HM),COSD(HM)*SIND(ALFM))
    HHE=ATAND(SIND(HE),COSD(HE)*SIND(ALFE))
    BETA=(HHE+HHM)
    CBETA=200000.0*COSD(BETA)
    SBETA=200000.0*SIND(BETA)
    IF Z=W THEN Z=(W-1)
/*  ************************************************************  */
    PUT PAGE EDIT ('HM=',HM) (SKIP,A,X(1),F(6,1))
    PUT EDIT ('ALFM=',ALFM) (SKIP,A,X(1),F(6,1))
    PUT EDIT ('HE=',HE) (SKIP,A,X(1),F(6,1))
    PUT EDIT ('ALFE=',ALFE) (SKIP,A,X(1),F(6,1))
    PUT EDIT ('HHM=',HHM) (SKIP,A,X(1),F(6,1))
    PUT EDIT ('HHE=',HHE) (SKIP,A,X(1),F(6,1))
    PUT EDIT ('BETA=',BETA) (SKIP(2),A,X(1),F(6,1))
    PUT EDIT ('STATION POINTS=',V) (SKIP(2),A,X(2),F(6,1))
    PUT EDIT ('BLOCK   EDGES =',W) (SKIP(2),A,X(2),F(6,1))
    PUT EDIT ('NO. OF BLOCKS =',Z) (SKIP(2),A,X(2),F(6,1))
/*  ************************************************************  */
 L1 BEGIN
    DECLARE LINK LABEL
    DECLARE ((BX,BU,BL) (W),(ATB,BTB,ABB,BBB) (W-1),(AD,CAL,SX,SZ,HH)
    (V),(AUX(2*(Z))),H(Z,V),ELEM(W-1),BLOCK(Z*2),(S,IPIV) (Z))
 L2 GET LIST (DATA)
    IF DATA=0 THEN GO TO L3
    GET LIST (SX,SZ)
    GO TO L4
 L3 GET LIST (XO,ZO)
    SX(1)=XO   SZ=ZO
    DECLARE (STA,XSTEP) (NO)
    GET LIST (STA,XSTEP)
    DO I=1 TO NO
    IF I>1 THEN DO J=(STA(I-1)+1) TO STA(I)
    SX(J)=SX(J-1)+XSTEP(I)
    END
    ELSE DO J=2 TO STA(I)
    SX(J)=SX(J-1)+XSTEP(I)
    END   END
 L4 GET LIST (BATA)
    IF BATA=0 THEN GO TO L5
    GET LIST (BX,BU,BL)
    GO TO L7
 L5 GET LIST (BXO,BZB,SCALE)
    BX(1)=BXO
    BL=BZB
    DECLARE (BSTA,BSTEP) (NO)
    GET LIST (BSTA,BSTEP)
    DO I=1 TO NO
    IF I>1 THEN DO J=(BSTA(I-1)+1) TO BSTA(I)
    BX(J)=BX(J-1)+BSTEP(I)
    END
    ELSE DO J=2 TO BSTA(I)
    BX(J)=BX(J-1)+BSTEP(I)
    END   END
```

```
L6 GET LIST (DATA)
   IF DATA=0 THEN DO
   GET LIST (POT)
   BU=POT*SCALE
   END
   ELSE DO
   GET LIST (BU)
   BU=BU*(SCALE)
   END
L7 GET LIST (AD)
   IF Z=(W-1) THEN DO
   N=1
   DO I=2 TO (Z*2) BY 2
   BLOCK(I-1)=N
   BLOCK(I)=N
   N=N+1
   END   END
   ELSE DO
L8 GET LIST (BC,PR)
   BLOCK(1)=1
   DO J=2 TO ((Z*2)-2) BY 2
   BLOCK(J)=BLOCK(J-1)+BC
   BLOCK(J+1)=BLOCK(J)+1
   END
   BLOCK(Z*2)=(W-1)
   IF PR=1 THEN DO
   PUT LIST (BLOCK)SKIP
   PUT SKIP
   DO I=2 TO (Z*2) BY 2
   NOM=BLOCK(I)+1
   PUT LIST (BX(NOM))
   END   END   END
/*  ************************************************************  */
/*            COMPUTATION  OF  COEFFICIENT  MATRIX                */
/*                                                                */
   DO J=1 TO V
   XS=SX(J)  ZS=SZ(J)
   DO I=1 TO (W-1)
   IF J>1 THEN GO TO L9
   CALL TOP(BX(I),BU(I),BX(I+1),BU(I+1),ATB(I),BTB(I))
   CALL TOP(BX(I),BL(I),BX(I+1),BL(I+1),ABB(I),BBB(I))
L9 CA=ATB(I)          CB=BTB(I)
   XSA=BX(I)-XS       ZSA=BU(I)-ZS
   XSB=BX(I+1)-XS     ZSB=BU(I+1)-ZS
   LINK=L10   GO TO L11
L10 DD=EE          CA=ABB(I)          CB=BBB(I)
   ZSA=BL(I)-ZS    ZSB=BL(I+1)-ZS     LINK=L12
L11 RA=XSA*XSA+ZSA*ZSA          RB=XSB*XSB+ZSB*ZSB
   TA=XSA/ZSA    TB=XSB/ZSB    TT=1+TA*TB    TBA=TB-TA
   THETA=ATAN(TBA,TT)
   EE=THETA*CB+LOG(RB/RA)*CA
   GO TO LINK
L12 ELEM(I)=(DD-EE)*A
   END
   N=1
   DO K=1 TO Z
   TEMP=0
   DO I=BLOCK(N) TO BLOCK(N+1)
   TEMP=TEMP+ELEM(I)
   END
   H(K,J)=TEMP
   N=N+2
   END   END
```

```
    PUT LIST('  COEFFICIENT  MATRIX  SUCCESSFULLY  FORMED')SKIP(3)
/*                                                                    */
/*  ***************************************************************  */
/*   STORING  COEFFICIENT  MATRIX (H)  AND  ANOMALY  VALUES (AD)     */
/*    ON  TEMPORARY  DISC-SPACE                                       */
/*                                                                    */
    OPEN FILE(SAVE) OUTPUT
    WRITE FILE(SAVE) FROM(AD)
    DO I=1 TO Z
    HH=H(I,*)
    WRITE FILE(SAVE) FROM(HH)
    END
    CLOSE FILE(SAVE)
/*  ***************************************************************  */
/*   SOLUTION  OF  MATRIX  EQUATION  AD=(H)*(S)  USING  I.B.M.       */
/*    S.S.P.  LLSQ  ROUTINE DESTROYS  ARRAYS (H) AND (AD)            */
/*                                                                    */
    IW=Z    IQ=1
    CALL LLSQ(H(1,1),AD(1),V,IW,IQ,S(1),IPIV(1),EPS,IER,AUX(1))
    PUT LIST (IER)SKIP(2)
    IF IER=0 THEN BEGIN
    PUT LIST('  MATRIX PROCEDURE SUCCESSFUL')
    END
    IF IER¬=0 THEN BEGIN
    S=0
    PUT LIST ('  SSP FAILED,  SOLUTION MATRIX SET TO ZERO')
    END
/*  ***************************************************************  */
/*   RE-WRITING  MATRIX (H)  AND  (AD)  FROM  DISC STORE              */
/*                                                                    */
    OPEN FILE(SAVE)
    READ FILE(SAVE) INTO(AD)
    DO I=1 TO Z
    READ FILE(SAVE) INTO(HH)
    H(I,*)=HH
    END
    CLOSE FILE(SAVE)
/*  ***************************************************************  */
/*   COMPUTATION  OF  THEORETICAL  MAGNETIC  ANOMALY                  */
/*                                                                    */
    T01=0    T02=0
    DO I=1 TO V
    CAL(I)=SUM(H(*,I)*S)
    R=(AD(I)-CAL(I))
    IF R<0 THEN R=-R
    T01=T01+R
    T02=T02+(R*R)
    END
/*  ***************************************************************  */
```

```
/*  OUTPUT OF DATA DESCRIBING MODEL AND ANOMALY PROFILE          */
/*  FOLLOWED BY COMPUTED MAGNETIZATION DISTRIBUTION              */
/*                                                               */
    PUT EDIT ('BLOCK EDGE','X','ZT','ZB') (SKIP(2),A,X(4),A,X(9),A,X(6
    ),A)
    DO K=1 TO W
    PUT EDIT ((K),BX(K),BU(K),BL(K)) (SKIP,F(4),X(6),F(8,3),X(4),F(6,3
    ),X(3),F(6,3))
    END
    PUT EDIT ('ZS=',SZ(1)) (SKIP(2),A,X(2),F(6,2))
    PUT EDIT ('STATION','XS','ANOMALY','CALCULATED ANOMALY','RESIDUALS
    ') (SKIP(2),A,X(5),A,X(6),A,X(5),A,X(6),A)
    DO J=1 TO V
    PUT EDIT ((J),SX(J),AD(J),CAL(J),(AD(J)-CAL(J))) (SKIP,F(4),X(5),F
    (8,3),X(2),F(8,1),X(8),F(8,1),X(14),F(6,1))
    END
    PUT EDIT ('POSITIVE SUM OF RESIDUALS=',TO1) (SKIP(2),A,F(15,2))
    PUT EDIT ('SUM OF SQUARES OF RESIDUALS=',TO2) (SKIP(2),A,F(20,2))
    PUT PAGE EDIT ('BLOCK','MAGNETIZATION') (SKIP,A,X(5),A)
    DO L=1 TO IW
    PUT EDIT ((L),S(L)) (F(4),X(6),F(12,5))SKIP
    END
/*  ************************************************************ */
/*  SUBROUTINE USED IN COMPUTATION OF COEFFICIENT MATRIX         */
/*                                                               */
TOP PROCEDURE (XA,ZA,XB,ZB,CA,CB)
    DECLARE (XA,ZA,XB,ZB,BAR,S,C,DX,DZ,CA,CB)
    DX=(XA-XB)    DZ=(ZA-ZB)
    BAR=SQRT((DX*DX)+(DZ*DZ))
    S=DZ/BAR      C=-DX/BAR
    CA=(0.5)*C*(S*CBETA+C*SBETA)
    CB=C*(S*SBETA-C*CBETA)
    END TOP
/*  ************************************************************ */
    END L1
  END MXOIIIA
*
/L.SYSLIB  DD  DSNAME=SYS1.PL1LIB,DISP=SHR
/  DD  DSNAME=SYS2.LOAD.SSP,DISP=SHR
/  DD  DSNAME=SYS1.FORTLIB,DISP=SHR
/G.SAVE  DD DSNAME=&RED,UNIT=2314,VOLUME=SER=UNE999,                C
/             DISP=(NEW,DELETE),SPACE=(CYL,10),                     C
/             DCB=(RECFM=VT,LRECL=1600,DSORG=PS)
/G.SYSIN   DD  *
*
```

APPENDIX 2

THE COMPUTER PROGRAMME MXOCEAN III B

This programme uses a least squares matrix technique to directly evaluate a distribution of magnetization, within a specified two-dimensional magnetic layer, which causes a given magnetic anomaly. The magnetic layer is formed from a series of adjacent model blocks, represented by either irregular or regular quadrilaterals. The programming procedure represents a combination of two separate computer programmes: MXOCEAN III A (Appendix 1) and MAGN (Bott 1969a). The programme prints out details of the magnetic layer used, the observed, calculated and residual (observed minus calculated) magnetic anomalies and the calculated magnetization values. The programme has been written in PL/1 for use on the N.U.M.A.C. I.B.M. 360/67.

Notes on data format

The data input for this programme is essentially equivalent to that given in Appendix 1 for the computer programme MXOCEAN III A. Data input points labelled L2, L3, ... L7 are identical for both programmes.

LO:

FI, FA, BI, BA are the values of the dip and azimuth of the earth's field and dip and azimuth of the direction of magnetization, respectively. These are in degrees. The azimuths are measured from the strike towards the positive x-axis and the dips are measured from the azimuth directions downwards towards the positive z-axis.

V = total number of magnetic anomaly points.

W = total number of co-ordinates defining the upper surface of the magnetic layer used. Number of model blocks within this layer = (W-1).

NO = total number of sections for the profile, normally set = 1 unless variable XSTEP (see L3, L5) required for different sections.

EPS = tolerance parameter (try = 0.0001), I.B.M. SSP.(LLSQ).

(for details of succeeding data input see Appendix 1).

Appendix 2. Programme Print Out

```
//OPTIONF   JOB  (0107,67,,2),OPTIONF.M.HUTTON,MSGLEVEL=1,CLASS=G
//*HOLD           ***  TIME.G=6 MINS     CLASS=G  ***************
//         EXEC NPLIFCLG,TIME.G=(6,0)
//C.SYSIN   DD   *
         (SUBSCRIPTRANGE)
   MXOIIIB  PROCEDURE OPTIONS (MAIN)
/*  ************************************************************  */
/*                                                                */
/*  ************************************************************  */
/*                                                                */
/*  THIS  PROGRAMME  USES  A  LEAST.SQUARES  MATRIX  TECHNIQUE    */
/*  TO  DIRECTLY  EVALUATE  A  DISTRIBUTION  OF  MAGNETIZATION    */
/*  WITHIN  A  SPECIFIED  TWO.DIMENSIONAL  MAGNETIC  LAYER  WHICH */
/*  CAUSES  A  GIVEN  MAGNETIC  ANOMALY.  **  A  THEORETICAL      */
/*  MAGNETIC  ANOMALY  IS  THEN  COMPUTED  FROM  THIS MAGNETIZATION */
/*  DISTRIBUTION  AND  RESIDUAL  VALUES  EVALUATED.               */
/*  THE  SOURCE  BODY  IS  REPRESENTED  BY  A  MODEL  FORMED  FROM */
/*  A  CONTINUOUS  SET  OF  ADJACENT  QUADRILATERALS.             */
/*  A  DIRECTION  OF  MAGNETIZATION  FOR  THE  MODEL  IS  ASSUMED. */
/*  ************************************************************  */
/*                                                                */
/*  ************************************************************  */
/*            ***  PARAMETER  DEFINITIONS  ***                    */
/*  FI=INCLINATION (D) OF THE  EARTH'S  MAGNETIC  FIELD.          */
/*  BI=INCLINATION (D) OF THE  MAGNETIZATION  VECTOR.             */
/*  FA=AZIMUTH (D) OF  THE  EARTH'S  MAGNETIC  FIELD  MEASURED    */
/*  FROM  THE  STRIKE  OF  THE  BODY  TOWARDS  THE  POSITIVE X.AXIS */
/*  BA=AZIMUTH (D) OF  DIRECTION  OF  MAGNETIZATION,  MEASURED    */
/*  AS  FOR  FA.                                                  */
/*  V=TOTAL  NUMBER  OF  MAGNETIC  ANOMALY  POINTS.               */
/*  W=TOTAL  NUMBER  OF  X CO.ORDINATES  DELINEATING  THE  UPPER  */
/*  SURFACE  OF  THE  MODEL. **** W MUST  NOT  EXCEED  (V+1).     */
/*  NO=TOTAL  NO. OF  SECTIONS  FOR  THE  PROFILE. **  NORMALLY   */
/*  SET=1  UNLESS VARIABLE  XSTEP REQUIRED FOR  DIFFERENT  SECTIONS */
/*  EPS  PARAMETER  REF. I.B.M. SSP (LLSQ). ** (TRY 0.0001).      */
/*  AD= ARRAY  STORING  MAGNETIC  ANOMALY  VALUES.                */
/*  SX= ARRAY  STORING  X  CO-ORDINATES  OF ANOMALY  POINTS.      */
/*  SZ= ARRAY  STORING  Z  CO-ORDINATES  OF ANOMALY  POINTS.      */
/*  BU= ARRAY  STORING  Z  CO-ORDINATES  OF UPPER  MODEL  SURFACE. */
/*  BUX=ARRAY  STORING  X  CO-ORDINATES  OF UPPER  MODEL  SURFACE. */
/*  BL= ARRAY  STORING  Z  CO-ORDINATES  OF LOWER  MODEL  SURFACE. */
/*  BLX=ARRAY  STORING  X  CO-ORDINATES  OF LOWER  MODEL  SURFACE. */
/*  ************************************************************  */
/*                                                                */
/*  ************************************************************  */
    DECLARE SAVE FILE RECORD SEQUENTIAL
    DECLARE (FI,FA,BI,BA,EPS,AL,PX,PXE,PZ,PZE,R,TD1,TD2,X1,X2,XD,Z1,
    Z2,ZD,DATA,BATA,BXD,BZB,SCALE,BATH,PDT)
    DECLARE (V,W,NO,IER,IO,IW)FIXED BINARY
 LO GET LIST (FI,FA,BI,BA,V,W,NO,EPS)
    PX=COSD(BI)*SIND(BA)     PZ=SIND(BI)
    PXE=COSD(FI)    PZE=SIND(FI)    AL=SIND(FA)
/*  ************************************************************  */
    PUT PAGE EDIT ('FI=',FI) (SKIP,A,X(1),F(6,1))
    PUT EDIT ('FA=',FA) (SKIP,A,X(1),F(6,1))
    PUT EDIT ('BI=',BI) (SKIP,A,X(1),F(6,1))
    PUT EDIT ('BA=',BA) (SKIP,A,X(1),F(6,1))
    PUT EDIT ('STATION POINTS=',V) (SKIP(2),A,X(2),F(6,1))
    PUT EDIT ('BLOCK   EDGES =',W) (SKIP(2),A,X(2),F(6,1))
    PUT EDIT ('NO. OF  BLOCKS=',(W-1)) (SKIP(2),A,X(2),F(6,1))
    NSIDE=4    IDE=5
```

```
/*  ************************************************************  *
 L1 BEGIN
    DECLARE ((SX,SZ,AD,HH,CAL) (V),(BUX,BLX,BU,BL) (W),(X,Z) (IDF),
    (SS,IPIV) (W-1),(AUX(2*(W-1))),(H(W-1,V)))
 L2 GET LIST (DATA)
    IF DATA=0 THEN GO TO L3
    GET LIST (SX,SZ)
    GO TO L4
 L3 GET LIST (XO,ZO)
    SX(1)=XO    SZ=ZO
    DECLARE (STA,XSTEP) (NO)
    GET LIST (STA,XSTEP)
    DO I=1 TO NO
    IF I>1 THEN DO J=(STA(I-1)+1) TO STA(I)
    SX(J)=SX(J-1)+XSTEP(I)
    END
    ELSE DO J=2 TO STA(I)
    SX(J)=SX(J-1)+XSTEP(I)
    END    END
 L4 GET LIST (DATA)
    IF DATA=0 THEN GO TO L5
    GET LIST (BU,BL,BUX,BLX)
    GO TO L7
 L5 GET LIST (BXO,BZB,SCALE)
    BUX(1)=BXO
    BL=BZB
    DECLARE (BSTA,BSTEP) (NO)
    GET LIST (BSTA,BSTEP)
    DO I=1 TO NO
    IF I>1 THEN DO J=(BSTA(I-1)+1) TO BSTA(I)
    BUX(J)=BUX(J-1)+BSTEP(I)
    END
    ELSE DO J=2 TO BSTA(I)
    BUX(J)=BUX(J-1)+BSTEP(I)
    END    END
    BLX=BUX
 L6 GET LIST (BATH)
    IF BATH=0 THEN DO
    GET LIST (POT)
    BU=POT*SCALE
    END
    ELSE DO
    GET LIST (BU)
    BU=BU*(SCALE)
    END
    [redacted]
 L7 GET LIST (AD)
```

```
/*  ************************************************************  */
/*            COMPUTATION  OF  COEFFICIENT  MATRIX                */
/*                                                                */
PUT LIST(TIME)SKIP
    DO K=1 TO (W-1)
    X(1)=BUX(K)        Z(1)=BU(K)
    X(2)=BLX(K)        Z(2)=BL(K)
    X(3)=BLX(K+1)      Z(3)=BL(K+1)
    X(4)=BUX(K+1)      Z(4)=BU(K+1)
    X(5)=BUX(K)        Z(5)=BU(K).
    CALL NGAM(X,Z,H(K,*))
    END
PUT LIST(TIME)SKIP.
    PUT LIST ('   COEFFICIENT  MATRIX  SUCCESSFULLY  FORMED')SKIP(3)
/*                                                                */
/*  ************************************************************  */
/*   STORING  COEFFICIENT  MATRIX (H)  AND  ANOMALY  VALUES  (AD)  */
/*     ON  TEMPORARY  DISC-SPACE                                  */
    OPEN FILE(SAVE) OUTPUT
    WRITE FILE(SAVE) FROM(AD)
    DO I=1 TO (W-1)
    HH=H(I,*)
    WRITE FILE(SAVE) FROM(HH)
    END
    CLOSE FILE(SAVE)
/*  ************************************************************  */
/*   SOLUTION  OF  MATRIX  EQUATION  AD=(H)*(SS)  USING  I.B.M.   */
/*    S.S.P.  LLSQ.  *NB* ROUTINE  DESTROYS  ARRAYS (H) AND (AD)  */
/*                                                                */
    IW=(W-1)    IQ=1
    CALL LLSQ(H(1,1),AD(1),V,IW,IQ,SS(1),IPIV(1),EPS,IER,AUX(1))
    PUT LIST (IER)SKIP(2)
    IF IER=0 THEN BEGIN
    PUT LIST('  MATRIX  PROCEDURE  SUCCESSFUL')
    END
    IF IER¬=0 THEN BEGIN
    SS=0
    PUT LIST (' SSP  FAILED,  SOLUTION  MATRIX  SET TO ZERO')
    END
/*  ************************************************************  */
/*  RE-WRITING  MATRIX (H) AND  (AD)  FROM  DISC  STORE           */
/*                                                                */
    OPEN FILE(SAVE) INPUT
    READ FILE(SAVE) INTO(AD)
    DO I=1 TO (W-1)
    READ FILE(SAVE) INTO(HH)
    H(I,*)=HH
    END
    CLOSE FILE(SAVE)
/*  ************************************************************  */
/*   COMPUTATION  OF  THEORETICAL  MAGNETIC  ANOMALY              */
/*                                                                */
    TO1=0    TO2=0
    DO I=1 TO V
    CAL(I)=SUM(H(*,I)*SS)
    R=(AD(I)-CAL(I))
    IF R<0 THEN R=-R
    TO1=TO1+R
    TO2=TO2+(R*R)
    END
/*  ************************************************************  */
```

```
/*   OUTPUT OF DATA DESCRIBING MODEL AND ANOMALY PROFILE          *
/*   FOLLOWED BY COMPUTED MAGNETIZATION DISTRIBUTION              *
/*                                                                *
     PUT EDIT ('BLOCK EDGE','XT','ZT','XB','ZB') (SKIP(2),A,X(4),A,X(8
     ,A,X(12),A,X(11),A)
     DO I=1 TO W
     PUT EDIT ((I),BUX(I),BU(I),BLX(I),BL(I)) (SKIP,F(4),X(5),F(8,3),
     X(5),F(8,3),X(5),F(8,3),X(5),F(8,3))
     END
     PUT EDIT ('ZS=',SZ(1)) (SKIP(2),A,X(2),F(6,2))
     PUT EDIT ('STATION','XS','ANOMALY','CALCULATED ANOMALY','RESIDUAL
     ') (SKIP(2),A,X(5),A,X(6),A,X(5),A,X(6),A)
     DO J=1 TO V
     PUT EDIT ((J),SX(J),AD(J),CAL(J),(AD(J)-CAL(J))) (SKIP,F(4),X(5),
     F(8,3),X(2),F(8,1),X(8),F(8,1),X(14),F(6,1))
     END
     PUT EDIT ('POSITIVE SUM OF RESIDUALS=',TO1) (SKIP(2),A,F(15,2))
     PUT EDIT ('SUM OF SQUARES OF RESIDUALS=',TO2) (SKIP(2),A,F(20,2))
     PUT PAGE EDIT('BLOCK','MAGNETIZATION') (SKIP,A,X(5),A)
     DO L=1 TO IW
     PUT EDIT ((L),SS(L)) (SKIP,F(4),X(6),F(12,5))
     END
/*   ************************************************************   *
/*   SUBROUTINE USED IN COMPUTATION OF COEFFICIENT MATRIX         *
/*                                                                *
NGAM PROCEDURE (X,Z,AN)
     DECLARE ((X,Z) (IDE),(AN,EA,EB) (V),(S,C,P) (NSIDE))
     DECLARE (H,B,D,A,DH,DZ)
     DO I=1 TO NSIDE
     H=SQRT((X(I)-X(I+1))**2+(Z(I+1)-Z(I))**2)
     S(I)=(Z(I+1)-Z(I))/H    C(I)=(X(I)-X(I+1))/H
     P(I)=200000*S(I)
     END
     EA=0    EB=0
     DO I=1 TO NSIDE
     IF S(I)¬=0 THEN DO J=1 TO V
       X1=X(I)-SX(J)        X2=X(I+1)-SX(J)
       Z1=Z(I)-SZ(J)        Z2=Z(I+1)-SZ(J)
     B=X1/Z1    D=X2/Z2    H=B=D    B=1+B*D
     A=ATAN(H,B)
     H=0.5*LOG((X2**2+Z2**2)/(X1**2+Z1**2))
     EA(J)=EA(J)+P(I)*(A*S(I)-H*C(I))
     EB(J)=EB(J)+P(I)*(H*S(I)+A*C(I))
     END    END
     DO I=1 TO V
     DH=(PX*EA(I)+PZ*EB(I))*AL
     DZ=(PX*EB(I)-PZ*EA(I))
     AN(I)=(PXE*DH+PZE*DZ)
     END
     END NGAM
/*   ************************************************************   */
     END L1
    END MXO1IIB
*
/L.SYSLIB  DD  DSNAME=SYS1.PL1LIB,DISP=SHR
/  DD  DSNAME=SYS2.LOAD.SSP,DISP=SHR
/  DD  DSNAME=SYS1.FORTLIB,DISP=SHR
/G.SAVE  DD DSNAME=&RED,UNIT=2314,VOLUME=SER=UNE999,                  C
/             DISP=(NEW,DELETE),SPACE=(CYL,10),                       C
/             DCB=(RECFM=VT,LRECL=1600,DSORG=PS)
/G.SYSIN   DD  *
*
```

APPENDIX 3

THE COMPUTER PROGRAMME REGLLSQ

This programme uses a least squares technique to fit a straight line (Y = MX+C) to a series of specified data points (x, y). For each data point a print out is given of the original value, the computed regional value and the residual difference. The programme has been written in PL/1 for use on the N.U.M.A.C. I.B.M. 360/67. The programme provides a quantitative method for subtracting a linear regional trend from total field magnetic observations. The procedure is mainly intended for use with marine profile data extending over hundreds of kilometres.

Notes on data format

Data input points are labelled L1, L2, L3, L4 in the programme 'print-out'.

L1:

N = total number of data points.

NO = total number of sections for the profile, normally set = 1 unless variable XSTEP (see L2, L3) required for different sections.

L2:

DATA = data control trigger,

If DATA = 0 then go to L3.

If DATA = 1 read x - co-ordinates (X) for magnetic field values (N values).

L3:

Generation of magnetic field point x - co-ordinates for regular spaced data.

XO = x - co-ordinate for first field-point value.

STA = array of numbers (dimension NO, see L1) specifying the final field-point at the end of each profile section.

XSTEP = array of numbers (dimension NO) specifying the x - increment for each section of the profile.

L4:

ANOM = array of total field values (dimension N).

Appendix 3. Programme Print Out

```
PLOEL  JOB  (0107,69,,2),DGPLOEL.M.HUTTON,MSGLEVEL=1,CLASS=A
     EXEC NPL1FCLG
SYSIN  DD  *
 NEGLLSQ: PROCEDURE OPTIONS (MAIN)
  ********************************************************************  */
                                                                          */
  ********************************************************************  */
                                                                          */
  THIS  PROGRAMME  USES A LEAST.SQUARES  TECHNIQUE  TO  FIT  A          */
  STRAIGHT  LINE (Y=MX+C) TO A SERIES  OF  SPECIFIED  DATA              */
  POINTS (X,Y).  **  FOR  EACH  DATA  POINT  A  PRINT  OUT  IS         */
  GIVEN  OF  THE  ORIGINAL  VALUE, THE  COMPUTED  REGIONAL  VALUE       */
  AND  THE  RESIDUAL  DIFFERENCE.                                       */
  ********************************************************************  */
                                                                          */
  ********************************************************************  */
           ***  PARAMETER  DEFINITIONS  ***                             */
  N= TOTAL  NO.  OF  DATA  POINTS                                       */
  NO= TOTAL  NO. OF SECTIONS  FOR  THE  PROFILE.  *  SET=1               */
  UNLESS VARIABLE  XSTEP  REQUIRED  FOR  DIFFERENT  SECTIONS.           */
  DATA= PROGRAMME  CONTROL  TRIGGER.                                    */
  STA= ARRAY  OF  NOS.  SPECIFYING  THE  FINAL  DATA  POINT  AT         */
  THE  END  OF  EACH  PROFILE  SECTION.                                 */
  XSTEP= ARRAY  OF  NOS.  SPECIFYING  THE  X-INCREMENT  FOR             */
 'EACH  PROFILE  SECTION.                                               */
  XO= INITIAL  X CO.ORDINATE, REQUIRED  FOR  XSTEP  OPTION              */
  ANOM= ARRAY STORING  Y  CO-ORDINATE  VALUES                           */
  X    = ARRAY STORING  X  CO-ORDINATE  VALUES                          */
  ********************************************************************  */
                                                                          */
  ********************************************************************  */
  DECLARE (EPS,R,RESID,DATA,XO)
1: GET LIST (N,NO)
  M=2  IW=1   EPS=0.0001
A: BEGIN
  DECLARE (A(M,N),(S,IPIV) (M),AUX(2*M),(ANOM,AC,X) (N))
2: GET LIST (DATA)
  IF DATA=0 THEN GO TO L3
  GET LIST (X)
  GO TO L4
3: GET LIST (XO)
  X(1)=XO
  DECLARE (STA,XSTEP) (NO)
  GET LIST (STA,XSTEP)
  DO I=1 TO NO
  IF I>1 THEN DO J=(STA(I-1)+1) TO STA(I)
  X(J)=X(J-1)+XSTEP(I)
  END
  ELSE DO J=2 TO STA(I)
  X(J)=X(J-1)+XSTEP(I)
  END   END
4: GET LIST (ANOM)
  ********************************************************************  */
```

```
/*                                                                    */
/*   ****************************************************************   */
     A(1,*)=1
     A(2,*)=X
     AC=ANOM
     CALL LLSQ(A(1,1),ANOM(1),N,M,IW,S(1),IPIV(1),EPS,IER,AUX(1))
     PUT PAGE LIST(IER)
     PUT EDIT ('DISTANCE','TOTAL INTENSITY','REGIONAL','RESIDUAL')
     (SKIP(2),X(7),A,X(3),A,X(3),A,X(4),A)
     DO I=1 TO N
     R=S(1)+S(2)*X(I)
     RESID=AC(I)-R
     PUT EDIT ((I),X(1),AC(I),R,RESID) (SKIP,F(4),X(3),F(8,3),X(7),
     F(7,1),X(8),F(7,1),X(4),F(7,1))
     END
     PUT EDIT ('REGIONAL AT FALSE ORIGIN=',S(1)) (SKIP(3),A,F(8,1))
     PUT EDIT ('REGIONAL GRADIENT ALONG X AXIS=',S(2)) (SKIP,A,
     F(11,6))
     END LA
 /*  ****************************************************************   */
     END REGLLSQ
*
/L.SYSLIB  DD  DSNAME=SYS1.PL1LIB,DISP=SHR
/  DD  DSNAME=SYS2.LOAD.SSP,DISP=SHR
/  DD  DSNAME=SYS1.FORTLIB,DISP=SHR
/G.SYSIN   DD   *
*
```

APPENDIX 4

THE COMPUTER PROGRAMME FLT

This programme uses a least squares technique to fit five terms of a simple fourier series ..... (AO, A1 sin (THETA), A2 cos (THETA), A3 sin (2*THETA), A4 cos (2*THETA)), to a series of specified data points (x, y). For each data point a print-out is given of the original value, the computed trend and the residual difference. The programme has been written in PL/1 for use on the N.U.M.A.C. I.B.M. 360/67. The programme provides a quantitative method for removing certain long wavelength components from reduced magnetic anomaly profiles. This filtering procedure attempts to provide a form of correction for errors of observations, of quite small amplitude but long wavelength within the reduced magnetic anomaly values, such as may be caused by the diurnal variation. The programme is mainly intended for use in conjunction with the computer programme REGLLSQ (Appendix 3), prior to application of the programmes MXOCEAN III (A) or (B) (Appendices 1 & 2).

Notes on data format

Data input points are labelled L1, L2, L3, L4 in the programme 'print-out'.

L1:

N = total number of data points.

NO = total number of sections for the profile, normally set = 1 unless variable XSTEP (see L2, L3) required for different sections.

DIS = total length of profile.

L2:

DATA = data control trigger,

If DATA = 0 then go to L3.

If DATA = 1 read x - co-ordinates (XS) for magnetic anomaly values (N values).

L3:

Generation of magnetic anomaly field point x - co-ordinates for regular spaced data.

XO = x - co-ordinate for first magnetic anomaly value.

STA = array of numbers (dimension NO, see L1) specifying the final field-point at the end of each profile section.

XSTEP = array of numbers (dimension NO) specifying the x - increment for each section of the profile.

L4:

ANOM = array of magnetic anomaly values (dimension N).

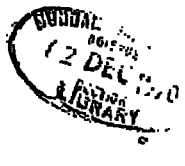

Appendix 4. Programme Print Out

```
//DGPIOMAR JOB (0701,69,,2),DGPIOMAR.M.HUTTON,MSGLEVEL=1,CLASS=A
//     EXEC NPL1FCLG
//SYSIN DD *
FLT  PROCEDURE OPTIONS (MAIN)
 /*************************************************************  */
                                                                  */
 /*************************************************************  */
                                                                  */
 THIS  PROGRAMME  USES A LEAST.SQUARES  TECHNIQUE  TO FIT  FIVE   */
 LOW  ORDER  TERMS  OF  A  SIMPLE  FOURIER  SERIES...(A0, A1SIN   */
 (THETA), A2COS(THETA), A3SIN(2*THETA), A4COS(2*THETA)... TO  A   */
 SERIES  OF  SPECIFIED  DATA  POINTS (X,Y). **  FOR  EACH  DATA   */
 POINT  A  PRINT 'OUT  IS GIVEN  OF THE  ORIGINAL  VALUE, THE     */
 COMPUTED  TREND  AND  THE  RESIDUAL  DIFFERENCE                  */
 /*************************************************************  */
                                                                  */
 /*************************************************************  */
          ***  PARAMETER  DEFINITIONS  ***                        */
 N= TOTAL  NO.  OF  DATA  POINTS.                                 */
 NO= TOTAL  NO.  OF  SECTIONS  FOR  THE  PROFILE. **  SET=1       */
 UNLESS  VARIABLE  XSTEP  REQUIRED  FOR  DIFFERENT  SECTIONS.     */
 DIS= TOTAL  LENGTH  OF  PROFILE                                  */
 DATA= PROGRAMME  CONTROL  TRIGGER                                */
 XO= INITIAL  X. CO.ORDINATE,  REQUIRED  FOR  XSTEP  OPTION.      */
 STA= ARRAY  OF  NOS.  SPECIFYING  THE  FINAL  DATA  POINT       */
 AT  THE 'END  OF  EACH  PROFILE  SECTION.                        */
 XSTEP= ARRAY  OF  NOS.  SPECIFYING  THE  X-INCREMENT  FOR        */
 EACH  PROFILE  SECTION.                                          */
 ANOM= ARRAY  STORING  Y  CO.ORDINATE  VALUES                     */
 XS  = ARRAY  STORING  X  CO.ORDINATE  VALUES                     */
                                                                  */
 /*************************************************************  */
                                                                  */
 DECLARE (REG,RES,W,X,XO,X1,X2,X3,X4,DIS)
1:GET LIST (N,NO,DIS)
A:BEGIN
 DECLARE (ANOM(N),XS(N),A(5,5),Y(5))
2:GET LIST (DATA)
 IF DATA=0 THEN GO TO L3
 GET LIST (XS)
 GO TO L4
3:GET LIST (XO)
 XS(1)=XO
 DECLARE (STA,XSTEP) (NO)
 GET LIST (STA,XSTEP)
 DO I=1 TO NO
 IF I>1 THEN DO J=(STA(I-1)+1) TO STA(I)
 XS(J)=XS(J-1)+XSTEP(I)
 END
 ELSE DO J=2 TO STA(I)
 XS(J)=XS(J-1)+XSTEP(I)
 END   END
4:GET LIST (ANOM)
 A=0   Y=0
 W=(3.14159665/DIS)
 DO J=1 TO N
 X=XS(J)*W
 X1=SIN(X)
 X2=COS(X)
 X3=SIN(2*X)
 X4=COS(2*X)
```

```
A(1,1)=A(1,1)+1
A(1,2)=A(1,2)+X1
A(1,3)=A(1,3)+X2
A(1,4)=A(1,4)+X3
A(1,5)=A(1,5)+X4
A(2,1)=A(2,1)+X1
A(2,2)=A(2,2)+((X1)**2)
A(2,3)=A(2,3)+(X1*X2)
A(2,4)=A(2,4)+(X1*X3)
A(2,5)=A(2,5)+(X1*X4)
A(3,1)=A(3,1)+X2
A(3,2)=A(3,2)+(X2*X1)
A(3,3)=A(3,3)+((X2)**2)
A(3,4)=A(3,4)+(X2*X3)
A(3,5)=A(3,5)+(X2*X4)
A(4,1)=A(4,1)+X3
A(4,2)=A(4,2)+(X3*X1)
A(4,3)=A(4,3)+(X3*X2)
A(4,4)=A(4,4)+((X3)**2)
A(4,5)=A(4,5)+(X3*X4)
A(5,1)=A(5,1)+X4
A(5,2)=A(5,2)+(X4*X1)
A(5,3)=A(5,3)+(X4*X2)
A(5,4)=A(5,4)+(X4*X3)
A(5,5)=A(5,5)+((X4)**2)
Y(1)=Y(1)+ANOM(J)
Y(2)=Y(2)+((ANOM(J)*X1))
Y(3)=Y(3)+((ANOM(J)*X2))
Y(4)=Y(4)+((ANOM(J)*X3))
Y(5)=Y(5)+((ANOM(J)*X4))
END
PUT PAGE DATA (A)
PUT SKIP DATA (Y)
L=5
CALL SIMQ(A(1,1),Y(1),L,KS)
PUT PAGE LIST (KS)
PUT SKIP DATA (Y)
PUT PAGE EDIT ('DISTANCE','ANOMALY','FILTERED COMPONENT',
'RESIDUAL') (X(7),A,X(4),A,X(3),A,X(4),A)
DO J=1 TO N
X=XS(J)*W
X1=SIN(X)
X2=COS(X)
X3=SIN(2*X)
X4=COS(2*X)
REG=Y(1)+(Y(2)*X1)+(Y(3)*X2)+(Y(4)*X3)+(Y(5)*X4)
RES=ANOM(J)-REG
PUT EDIT (J,XS(J),ANOM(J),REG,RES) (SKIP,F(4),X(4),F(7,3),X(4),
F(7,1),X(11),F(7,0),X(7),F(7,1))
END
END LA
*********************************************************************  */
END FLT

SYSLIB  DD  DSNAME=SYS1.PL1LIB,DISP=SHR
DD  DSNAME=SYS2.LOAD.SSP,DISP=SHR
DD  DSNAME=SYS1.FORTLIB,DISP=SHR
SYSIN  DD  *
```

APPENDIX 5

THE COMPUTER PROGRAMME DISAZ

This programme computes the true distance and azimuth on the spheroid between two given points of latitude and longitude. The procedure employed is based on the formulation given in the Admiralty Manual of Hydrographic Surveying, Vol. 1, 1965. The figure of the earth is taken from that given by Hayford (1910). For each pair of fixes (A-B) considered, the programme prints out the original values, the azimuth and the intervening distance. The programme will compute successive and cumulative distances for an undimensioned sequence of fixes along a particular course. The programme has been written in PL/1 for use on the N.U.M.A.C. I.B.M. 360/67.

Notes on data format

The successive data input point is labelled LA in the programme 'print-out'. The first fix is read in two lines before this point in an unlabelled statement that is executed once.

ALATD, ALATM = (A) latitude degrees & minutes.

ALOND, ALONM = (A) longitude degrees & minutes.

LA:

BLATD, BLATM = (B) latitude degrees & minutes.

BLOND, BLONM = (B) longitude degrees & minutes.

General Notes

(a) The computed distance is in kilometres.

(b) The azimuth is computed as a back bearing from B to A ($\pm 180^{\circ}$).

(c) Sign convention +N, +E.

Appendix 5. Programme Print Out

```
//LON   JOB  (3701,69),OGPIOHM.HUTTON,MSGLEVEL=1,CLASS=A
      EXEC PL1FCLG
//SYSIN   DD   *
 DISAZ: PROCEDURE OPTIONS (MAIN)
  ************************************************************** */
                                                                  */
  ************************************************************** */
  THIS  PROGRAMME  COMPUTES  THE  SPHERICAL  DISTANCE  AND       */
  AZIMUTH  BETWEEN  TWO  GIVEN  POINTS  OF  LATITUDE  AND        */
  LONGITUDE.  * * *  ELLIPSOID CONSTANTS  ARE  ADOPTED  FROM     */
  THE  INTERNATIONAL  FORMULA , INTERNATIONAL  UNION  OF  GEODESY */
  AND  GEOPHSICS   1924 .                                        */
  THE  PROCEDURE  EMPLOYED  IS  BASED  ON  THE  FORMULATION      */
  GIVEN  IN  THE  ADMIRALTY  MANUAL  OF  HYROGRAPHIC  SURVEYING  */
   VOL  1.  1965 .                                               */
                                                                 */
  ************************************************************** */
                                                                 */
  ************************************************************** */
  ON ENDFILE(SYSIN) GO TO LB
  DECLARE (AB,ALAT,ALON,ALATD,ALATM,ALOND,ALONM,AZ,BLAT,BLON,BLATD,
  BLATM,BLOND,BLONM,CA,CHORD,DIS,GB,P,R,SA,TD,UA,UB,V,XA,XB,YA,YB,
  ZA,ZB)
  PUT PAGE EDIT ('A LAT.','A LONG.','B LAT.','B LONG.','AZIMUTH',
  'XSTEP','DISTANCE') (SKIP,X(8),A,X(4),A,X(7),A,X(4),A,X(5),A,X(5),
  A,X(5),A)
  TD=0   N=0
  GET LIST (ALATD,ALATM,ALOND,ALONM)
  ALON=(ALOND+(ALONM/60))
  ALAT=(ALATD+(ALATM/60))
A:GET LIST (BLATD,BLATM,BLOND,BLONM)
  BLAT=(BLATD+(BLATM/60))
  BLON=(BLOND+(BLONM/60))
  UA=ATAN(0.996633*TAND(ALAT))
  UB=ATAN(0.996633*TAND(BLAT))
  GB=((0.99327733*TAN(UB))/TAN(UA))+((0.00672267)*COS(UA))/COS(UB)
  AZ=ATAND((SIND(ALON-BLON)),(SIND(ALAT)*(COSD(ALON-BLON)-(GB))))
  SA=SIND(AZ)   CA=COSD(AZ)
  XA=(6378388)*COS(UA)*COSD(ALON)
  YA=(6378388)*COS(UA)*SIND(ALON)
  ZA=(6356912)*SIN(UA)
  XB=(6378388)*COS(UB)*COSD(BLON)
  YB=(6378388)*COS(UB)*SIND(BLON)
  ZB=(6356912)*SIN(UB)
  CHORD=SQRT((XA-XB)**2+(YA-YB)**2+(ZA-ZB)**2)
  AB=SIND((ALAT+BLAT)/2)
  V=(6378388)/SQRT(1-(0.00672267)*(AB**2))
  P=((V)*(1-0.0672267))/(1-(0.00672267)*(AB**2))
  R=((P)*(V))/(P*(SA**2)+V*(CA**2))
  DIS=(((CHORD)**3)/(24*((R)**2)))+(3*((CHORD)**5))/(640*((R)**4))
  DIS=DIS+CHORD
  DIS=DIS/1000
  TD=TD+DIS
  N=N+1
  PUT EDIT (N,ALAT,ALON,BLAT,BLON,AZ,DIS,TD) (SKIP(2),F(4),X(4),
  F(7,3),X(4),F(8,3),X(3),F(7,3),X(4),F(8,3),X(7),F(6,1),X(4),
  F(7,3),X(4),F(8,3))
  ALAT=BLAT    ALON=BLON
  GO TO LA
LB:END DISAZ

//SYSIN  DD  *
```

APPENDIX 6

```
/*************************************************************  */
/*                  THE COMPUTER SUBROUTINE SLAB                */
/*************************************************************  */
/*                                                               */
/* THIS  PROCEDURE  COMPUTES  THE  MAGNETIC  ANOMALY, AT  FIELD  */
/* POINTS (XS,ZS) , CAUSED  BY  A  HORIZONTAL  SEMI-INFINITE     */
/* SLAB  HAVING  A  VERTICAL  END  FACE                          */
/*              PARAMETER  DEFINITIONS                           */
/*                                                               */
/* XA= X CO-ORDINATE  OF  VERTICAL  SLAB  FACE.                  */
/* ZAT= Z CO-ORDINATE  OF  UPPER  SURFACE  OF  SLAB.             */
/* ZAB= Z CO-ORDINATE  OF  LOWER  SURFACE  OF  SLAB.             */
/* AN = MAGNETIC  ANOMALY  AT  FIELD.POINT (XS,ZS).              */
/* SBETA =)                                                      */
/* CBETA =) GLOBAL  PARAMETERS  USED  IN  MAIN  PROGRAMMES       */
/* A     =) MXOCEAN III (A) & (B) .  REF. APPENDICES (1 AND 2).  */
/* XS    =)                                                      */
/* ZS    =)                                                      */
/*                                                               */
/*************************************************************  */
/*                                                               */
/*************************************************************  */
                                                                 */
SLAB: PROCEDURE(XA,ZAT,ZAB,AN)
      DECLARE (XA,ZAT,ZAB,AN,DZB,DZT,DX,R1,R2,Q1,Q2,Q3,Q4)
      DZB=(ZAB-ZS)      DZT=(ZAT-ZS)      DX=(XA-XS)
      R1=(DZT*DZT)+(DX*DX)      R2=(DZB*DZB)+(DX*DX)
      Q1=(DX/DZT)       Q2=(DX/DZB)
      Q3=(Q2-Q1)        Q4=(1+Q1*Q2)
      AN=(SBETA*(0.5)*LOG(R2/R1)-CBETA*ATAN(Q3,Q4))
      AN=AN*A
      END SLAB
                                                                 */
                                                                 */
/*************************************************************  */
/*************************************************************  */
```

General Notes

This subroutine was written for use within the main programme MXOCEAN III (A) (Appendix 1). Formulae were derived by differentiating the corresponding gravity formula for a semi-infinite slab and using Poisson's relationship between gravity and magnetic potential (after Bott 1969b). The procedure was used to provide a correction for the effect of magnetic material located just beyond the survey line. The magnetic layer was then formed from a sequence of model blocks as before, except that a semi-infinite slab was incorporated at each end. Solution problems were encountered when dealing with an infinite horizontal magnetic layer (section 2.3.3) and ill-conditioning of the matrix equation occurred in a number of other situations. The procedure may be more applicable for a simple magnetic layer incorporating few model blocks.